

Determining the Effectiveness of Oleophobic Gaskets

Final Report



Team Number: 1

Submission Date: 04-08-16

Submitted To: Dr. Gupta, Dr. Shih

Faculty Advisor: Dr. Oates

Authors: Heather Davidson (hld12), David Dawson (dpd13), Aruoture Egoh (aje15f), Daniel Elliott (dse13), Norris McMahon (nfm11b), Erik Spilling (eds11b)

Table of Contents

Table of Figures	i
Table of Tables	iii
ACKNOWLEDGEMENTS	iv
ABSTRACT	v
1. Introduction	1
2. Project Definition	2
2.1 Background Research	2
2.2 Need Statement	3
2.3 Goal Statement and Objectives	4
3. Design and Analysis	5
3.1 Project Constraints	5
3.2 Design Specifications.....	5
3.3 Performance Specifications	6
3.4 Functional Analysis	6
3.4.1 Ideal Gas Law	6
3.5 House of Quality	7
3.6 Concept Generation	8
3.6.1 Concept #1	9
3.6.2 Concept #2	9
3.6.3 Concept #3	10
3.6.4 Concept #4	10
3.6.5 Concept #5	11
3.7 Evaluation of Concepts	11

3.8 Detailed Evaluation of Concept Five	13
3.9 Failure Modes and Effect Analysis	14
3.10 Analysis of Design	15
3.10.1 Pressure Distribution Analysis	15
3.10.2 Flange Thickness Calculations	16
3.11 Final Design	18
3.11.1 Concept Design Optimization	19
3.11.2 Bolt Load Measurement	20
3.11.3 Hardware Selection	21
3.12 Design for Manufacturing	23
3.12.1 Sub-Assembly Fabrication	23
3.12.2 Assembly of Test Rig	24
3.12.3 Manufacturing of Oleophobic Gaskets	26
3.12.4 Assembly Time	26
3.12.5 Future Design Optimization	27
3.13 Design for Reliability	28
3.14 Design for Economics	29
4. Design of Experimentation	30
4.1 Test Rig Component Testing	30
4.2 Functional Diagram	31
4.3 Operation Instructions	32
4.4 Troubleshooting	34
4.5 Regular Maintenance	35
5. Results	37
5.1 Conventional Gasket Testing	37

5.2 Non-Conventional Gasket Testing.....	38
5.3 Final Leak Rate Testing.....	39
5.4 Post-Test Gasket State	44
6. Project Management.....	45
6.1 Resource Allocation.....	46
6.2 Schedule/Deliverables.....	47
6.3 Risk Assessment and Reliability	47
6.4 Procurement	48
6.5 Communications	50
7. Environmental, Safety, and Ethics	51
8. Conclusion.....	52
References	53
Appendix A	54
Appendix B	56
Appendix C	65
Appendix D.....	67
Appendix E	68
Appendix F	69
Appendix G.....	71
Appendix H.....	72
Biography.....	73

Table of Figures

Figure 1. Nonoleophobic (left) vs. oleophobic (right).....	2
Figure 2. Constructed HOQ using sponsor information	8
Figure 3. Concept #1 and Concept #2 cross section.....	9
Figure 4. Concept #3 cross section	10
Figure 5. Concept #4 cross section	10
Figure 6. Concept #5 cross section	11
Figure 7. Pugh decision matrix for test rig decision	12
Figure 8. CAD model of test rig Concept #5	13
Figure 9. Cross sectional view of the test rig.....	14
Figure 10. One-quarter of the test rig.....	16
Figure 11. Gasket clamping pressure distribution based on analysis results	16
Figure 12. Top view of removable bottom flange	17
Figure 13. CAD model of the final design for the test rig	18
Figure 14. Modified bolt with strain guage	20
Figure 15. Short RTD probe	21
Figure 16. Pressure transducer	22
Figure 17. Air Valve Stem.....	22
Figure 18. Ball Valve.....	22
Figure 19. Straval 1/8" Rva 05-01T Pressure Relief Valve.....	23
Figure 20. Exploded view of Top Assembly	24
Figure 21. Exploded view of the final assembly for the test rig.....	25
Figure 22. Pie chart showing distribution of funds.....	29
Figure 23. Top flange and bottom flange surface roughness.....	30

Figure 24. Function Diagram of Project	31
Figure 25. Test rig positioned on hot plate during testing	34
Figure 26. Paper gaskets before and after application of oleophobic solution	37
Figure 27. Rubber coated metal gaskets before and after applicatoin of oleophobic solution	37
Figure 28. High density felt after oil has been poured onto it	38
Figure 29. High density felt impregenated with oleophobic solution.....	38
Figure 30.High density felt coated with oleophobic spray	38
Figure 31. Woven fabric before and after application of impregantor solution	39
Figure 32. Results of room temperature test at 0.5 MPa	39
Figure 33. Results of room temperature test at 2 MPa	40
Figure 34. Results of room temperature test at 10 MPa	40
Figure 35. Results of elevated temperature test at 0.5 MPa.....	41
Figure 36. Results of elevated temperature test at 2 MPa.....	41
Figure 37. Results of elevated temperature test at 10 MPa.....	42
Figure 38. Oleophobic spray removal due to abrasion	44
Figure 39. Impregnated paper gasket stuck to top flange	44

Table of Tables

Table 1. Project Objectives	4
Table 2. Design Specifications	6
Table 3. Failure Modes and Effect Analysis.....	15
Table 4. Assembly Time for Test Rig.....	27
Table 5. Final Leakage over Two Hours	43
Table 6. Budget.....	48
Table 7. Purchased Items	49

ACKNOWLEDGEMENTS

Thank you to Parker Harwood, our Cummins Inc. liaison, for providing guidance and support throughout the project as well as gasket materials for the team to use for baseline testing. Additionally, the team would like to thank Dr. Gupta and Dr. Shih for their oversight of the project and providing instruction to the team. Finally, the team would like to thank many faculty members, including Dr. Oates, Dr. Kumar, Dr. Hollis, Dr. Hrudu, Dr. Wang, and Dr. Van Sciver, for being a source of knowledge and expertise in their chosen disciplines. Their advice and contribution has immeasurably enhanced the team's experience and taught valuable skills to the team members.

ABSTRACT

The goal of this Cummins Inc. sponsored project was to determine the effectiveness of oleophobic gaskets compared to standard nonoleophobic gaskets. This objective was completed by utilizing on market oleophobic sealing solutions on current gasket materials, as well as non-traditional gasket materials and then testing these products in an experimental test rig, which was designed and constructed by the team. The effectiveness of the oleophobic gaskets was assessed by comparing the respective leak rates of each gasket type under several conditions, including two variable temperatures and three variable clamping pressures, to that of baseline nonoleophobic gasket leak rates. The team has performed research on types of oleophobic solutions and have investigated which of these solutions are potential candidates to create an oleophobic gasket. The test rig was designed and built by the team so that it could test gaskets with oil at room temperature and at an elevated engine-like temperature while under a constant low internal pressure of 2.5 psi with variable gasket clamping pressure. Multiple concepts were generated and then evaluated using a Pugh Matrix. Once the final concept was chosen, in-depth analysis was performed on various components in hopes of reducing and mitigating any sort of failure. After constructing the final and optimized test rig design, testing was performed on all of the gasket specimens. The final conclusions were that the impregnated paper gaskets were not more effective, the sprayed rubber coated metal (RCM) gaskets were more effective, the Teflon gaskets performed well but were very expensive, and finally the unique felt gasket failed completely.

1 Introduction

Cummins Inc. proposed a project to determine the effectiveness of oleophobic gaskets to reduce the measured leak rate at low pressure, large joints on engines compared to the current gaskets used on engines. Oleophobic items are items which repel oil by having a lower surface energy than the oil. A gasket is an item which is placed between two flanges to form a seal, which is meant to prevent oils from leaking to the opposite side of the flange. The theory behind the project was that if the gasket could repel the oil, it would be less likely that oil will be capable of leaking past the gasket.

In order to determine the effectiveness of oleophobic gaskets, the design team needed to determine what products on the market could be used to give a gasket oleophobic properties, create oleophobic gaskets using these products and nontraditional gasket materials, as well as design and build a test rig which measured the leak rate of a gasket at various temperatures and clamping pressures. The test rig was capable of testing oil temperatures that ranged from 22 to 120°C and inducing an internal pressure of less than or equal to 2.5 psi. Once the design and construction of the test rig was completed, tests were performed on oleophobic and standard gaskets using the test rig and the results were compared to determine their effectiveness.

2 Project Definition

2.1 Background Research

Gaskets are used for different applications to prevent leakage of fluids at a joint, typically flanged bolted joints. These gaskets are usually metallic, polymeric, or paper materials, and they are expected to function effectively when subjected to various pressures and temperatures [1]. Gaskets are more likely to fail under adverse conditions, such as at higher internal pressures, higher temperatures, and poor flange surface conditions. The failure of gaskets can also be dependent on the size of the gasket, as larger gaskets have more potential leak paths. This project team was saddled with the task of determining if the use of an oleophobic gasket would prevent or reduce the effect of a gasket failure, while still having the reliability and durability of standard gaskets. The gasket performance was tested with the use of a test rig, which was the second responsibility of the team.

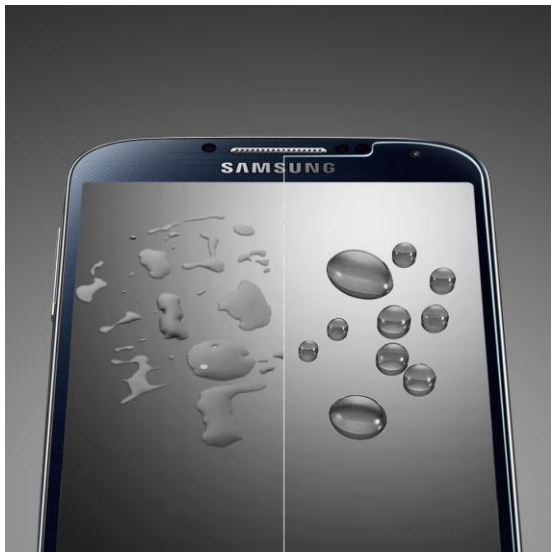


Figure 1. Nonoleophobic (left) vs. oleophobic (right)

To have oleophobic properties means a material will have a tendency to repel oil from its surface which can be seen in Figure 1 [2]. Oleophobicity is reliant upon the concept of surface energy, which is the excess energy on the surface of a bulk material [3]. Therefore, oleophobic materials must have a lower surface energy than oil.

This project was a first for FAMU-FSU senior design, meaning it was not a continuation of a previous project. Also, Cummins Inc. had not performed research or tests of their own, meaning that this senior design team was the first group to work on this topic. Previous works related to this project involving oleophobic coatings are found on various items such as phones and clothing. Additionally, oleophobic impregnators are used as a tile and grout sealer. These sealants are not intended to prevent oil leakage. All of the aforementioned oleophobic solutions aim to simply repel oil from a surface, allowing the surface to maintain a clean finish. The design team found no existing work involving the use of oleophobic sealing solutions on gaskets.

In his paper, Lakshmi discusses how to lower the surface energy of a material through the application of a fluoropolymer [4]. This is relevant to the project as fluoropolymers are typically found in oleophobic sealing solutions, confirming the feasibility of on market sealing solutions.

There are four main types of gaskets used on engines to create seals: paper gaskets, FIPG gaskets, molded elastomer gaskets, and rubber coated metal (RCM) gaskets. Paper gaskets are composed of 90% fibers and 10% elastomeric binder [1]. These gaskets are widely used because of how cost effective the production process is for them; however, they are subject to many failure modes such as weeping oil through the paper and deforming over time. FIPG gaskets are gaskets that are applied to flanges in a liquid state and cure to create a seal. FIPG gaskets rely on adhesion to the flange surface to prevent leakage rather than pressure, as the other gaskets do. Rubber coated metal gaskets are composed of a metal core, which is coated with a thin layer of rubber, typically 25-75 μm thick [1]. Rubber coated metal gaskets are typically used in high temperature applications. The final type of gasket, molded elastomer gaskets, are gaskets which are composed of elastomers which were molded into a particular shape for usage. An example of a molded elastomer gasket is an o-ring. These gaskets typically display the best sealing characteristics of the four types of gaskets.

2.2 Need Statement

Cummins Inc., the largest diesel engine manufacturer in the world, wished to investigate if introducing an oleophobic substance to gaskets would decrease the amount of oil leakage experienced at various joints on their engines. The scope of the investigation was to research different types of oleophobic products, the different application procedures for these products, and which materials was compatible with these products. The contact joints that Cummins Inc. was most interested in are larger, low pressure flange joints. Examples of such a joint is the joint between the engine block and the oil pan. In such a joint, the oil is at a low pressure, but there is a large exposed gasket length for potential leaks to occur at. These leaks can lead to excessive engine wear and possible catastrophic failure. Currently gaskets prevent oil leakage solely through contact pressures between the gasket and the flange surfaces, which create a seal. The purpose of this project was to determine if using an oleophobic gasket would reduce the amount of oil leakage compared to current gaskets used by Cummins Inc.

Need Statement:

“Gaskets used at large joints where the oil is at low pressure leak more oil than desired.”

2.3 Goal Statement and Objectives

Goal Statement: “Determine the effectiveness of oleophobic gaskets through the use of a test rig designed by the team.”

Table 1. Project Objectives

Objective Number	Objective
1	Research what causes items to become oleophobic.
2	Create oleophobic gaskets using on market products.
3	Create oleophobic gaskets using non-conventional gasket materials.
4	Design and build the test rig to be capable of varying clamping pressure and temperature.
5	Test oleophobic gaskets and currently used gaskets for leak rate and compare results.

3 Design and Analysis

3.1 Project Constraints

Multiple constraints associated with this project were adhered to in order to determine the effectiveness of the gaskets. There are several categories for the constraints, and they are as follows:

Gaskets

- A unique oleophobic gasket must be tested using non-conventional gasket materials. This means that any form of rubber was not used in the creation of this gasket.

Time Constraint

- The test rig construction was completed within one month prior to the end of the semester, allowing time for gasket testing.
- The leak rate test results were completed by the end of Spring 2016 semester.

Testing Constraints

- Cummins Inc. required that the design team use two types of standard gaskets as a baseline test to compare to the oleophobic gaskets. These two standard gasket types were paper gaskets and rubber coated metal gaskets.
- Cummins Inc. asked that the design team not test at internal pressures greater than 2.5 psi. The reasoning behind this was to accurately simulate the pressure present within an oil pan of an engine and to reduce the risk of injury during testing.

3.2 Design Specifications

Measurable design specifications important to this design included test rig dimensions, internal stress bearing capacity of the test rig, flange dimensions, clamping pressure needed for the bolts on the flanges, as well as flange surface roughness as shown in Table 2. Some materials were considered for the design through preliminary research. For example, the test rig could have been made from an aluminum alloy or a steel alloy. The thickness of the test rig wall was not critical since the pressure difference between the inside and outside of the test rig was nearly negligible. The minimum thickness of the bottom flange was determined to be 4.94 mm as calculated in Appendix A.

Table 2. Design Specifications

Design Specifications	Required Value
Test Rig Dimensions	Inner Diameter (ID): < 55 mm
Test Rig Stress Capacity	Minimum thickness of bottom flange: 4.94 mm
Flange Dimensions	Inner Diameter (ID): < 55 mm Minimum Outer Diameter (OD): 140 mm
Clamping Pressure	Minimum of 0.5 MPa according to Cummins standards. Maximum of 10 MPa according to Cummins standards.
Flange Surface Roughness	Maximum 3.2 microns RA.

3.3 Performance Specifications

The gasket sits between the flanges of the test rig, providing adequate sealing and minimal leak rate during testing, thus simulating an actual bolted joint on an engine. The operational temperature of the test rig was between 22-120° C with ± 2° C accuracy, and the internal oil pressure ranged from 0 to 2.5 psi with ± 0.01 psi accuracy. The pressure transducer provided the necessary resolution as it was used to measure the leak rate, which was a relatively small value. The test rig was heated through an electric hot plate, which displayed the external temperature on its digital display. This heating arrangement induced elevated temperature within the oil, which was measured via an RTD (Resistance Temperature Detector) sensor within the test rig.

3.4 Functional Analysis

3.4.1 Ideal Gas Law

In order to calculate the leak rate from the test rig, the Ideal Gas Law was used. The Ideal Gas Law is shown in Equation 1.

$$PV = nRT \quad (1)$$

In Equation 1, P is the pressure of the gas which in this case is the air, V is the volume of the air, n is the number of moles of air, R is the universal gas constant, and T is the temperature of the air. During the testing of the gaskets within the test rig, the temperature (T) of the air within the test rig was maintained at a constant temperature. Also, the number of moles (n) of air within the test rig remained constant since air did not leak out of the test rig. In addition, the value of the gas

constant (R) remained constant since it is a constant value by definition. Therefore, the entire right side of the Ideal Gas Law in Equation 1 remained constant throughout the tests. As a result of this, the Ideal Gas Law was reduced to enable the calculation of the final volume of air in the pressure vessel (V_2) since the values of the initial internal pressure of the air (P_1), the initial volume of air (V_1), and the final pressure (P_2) were known. The pressure values were recorded using a pressure transducer, and the initial volume of air was known based on the known volume of the test rig as well as the volume of oil which was inserted into the test rig. The reduced version of the Ideal Gas Law is shown in Equation 2.

$$P_1V_1 = P_2V_2 \quad (2)$$

Following the calculation of the volume of air in the test rig at the end of the test (V_2), the difference between the initial volume of the air and the final volume of air equaled the change in volume of oil within the test rig. This volume, when divided by the total time of the test, gave the oil leak rate. This oil leak rate is a result of the oil which leaked past the tested gasket, thus giving a quantifiable number to the effectiveness of the gasket.

3.5 House of Quality

After first speaking with the sponsor and defining their requirements, a diagram known as a House of Quality (HOQ) was constructed (Figure 2). This diagram relates the sponsor's requirements with various engineering characteristics. For instance, there is a strong correlation between the requirement of comparable performance and the characteristic gasket leak rate. Additionally, the diagram also depicts the relationship between any two engineering characteristics. This is illustrated in the top triangle of the "house." There is a strong positive correlation between the cost and the test rig pressure. To simulate higher pressures in the test rig, a more complex design is required and this will require money thus increasing the cost. Through this diagram, the number one engineering characteristic identified was the gasket leak rate. The HOQ was used by the team to meet the customer requirements through prioritizing the corresponding engineering characteristics when deciding between concepts.

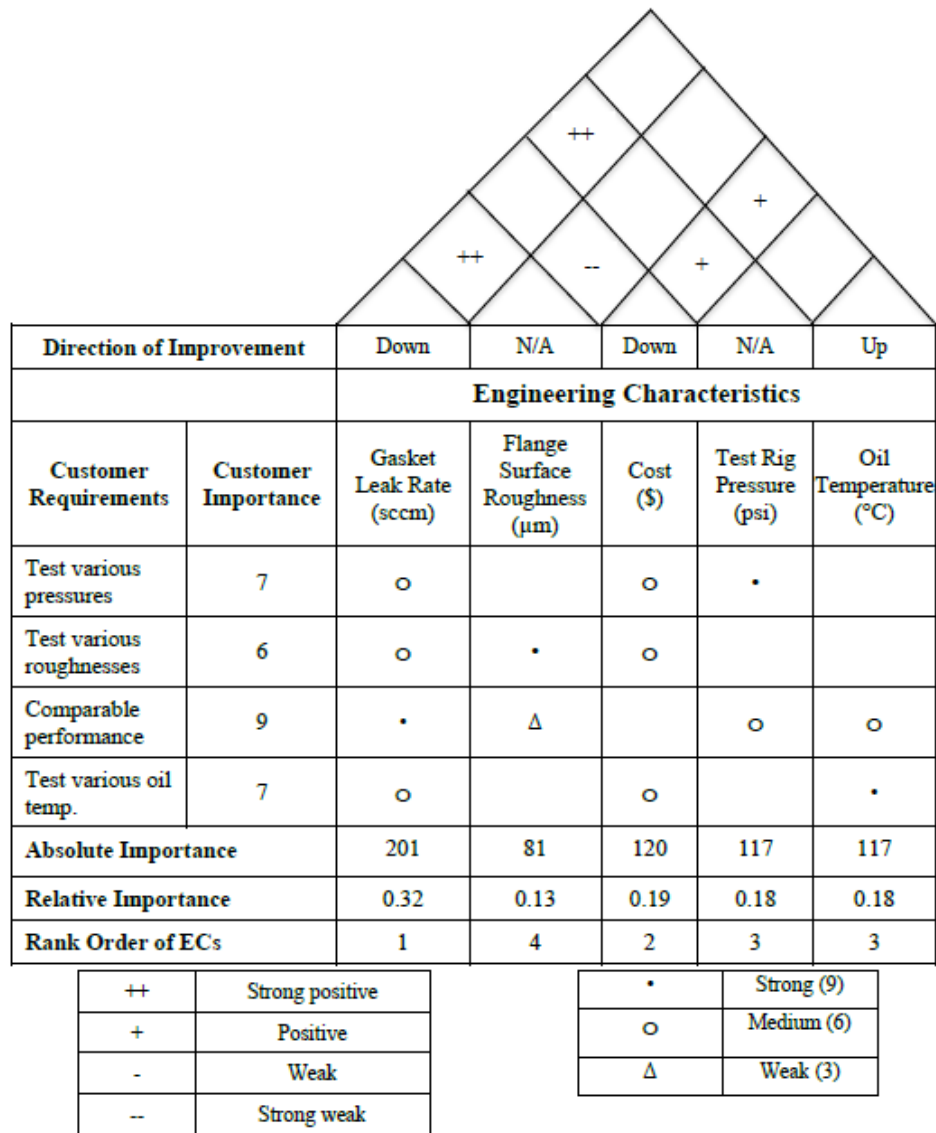


Figure 2. Constructed HOQ using sponsor information

3.6 Concept Generation

In order to design and build the most efficient and accurate test rig, the design team generated a total of five concepts. Each concept contained the same base requirements, as explained in the product specifications. All five concepts had a cylindrical shaped pressure vessel capable of withstanding the 2.5 psi internal pressure induced upon it, and each concept contained two flanges which would compress a flat gasket. In addition to the flanges, each test rig concept contained four bolts which are oriented 90 degrees apart from one another. These bolts were to serve two purposes

for the test rig concepts: create a clamping load on the flanges and simply align the two test rig “halves.” If the bolts are used to create the clamping load, then they will keep the test rig component aligned. Another feature of all five concepts is the elevation of the fasteners (nuts and/or bolts) from the bottom surface of the test rig. The design team had decided upon using a hot plate as the heat source for the test rig; therefore, it was necessary to elevate the fasteners off the bottom surface to prevent the heating of them directly. If the fasteners were heated directly, it is more likely that there could be a load relaxation in the bolted flange caused by thermal expansion of the bolts.

3.6.1 Concept #1

With the goal in mind to create a test rig which can interchange at least one the flange that is in contact with the gasket, the team generated Concept #1, which is shown in Figure 3. Concept #1 utilizes removable flanges which slide onto and off of the upper and lower bodies of the test rig, thus allowing the flanges to be changed while maintaining the repeated use of the main components of the test rig, such as any sensors. The upper and lower flanges shown in Figure 3 are removable. The lower body of the test rig is identical to the upper body in terms of geometric measurements, and thus fasteners are elevated off the bottom surface of the test rig as desired.

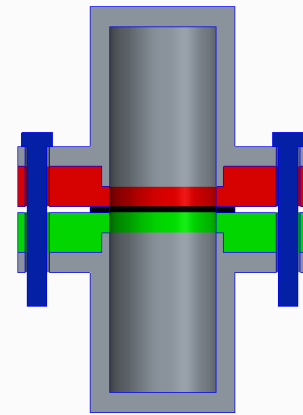


Figure 3. Concept #1 and Concept #2 cross section

3.6.2 Concept #2

The second concept the team generated is very similar to Concept #1 in appearance, thus Figure 3 is also a good representation of Concept #2. The feature which distinguishes Concept #2 from Concept #1 is the means of adding/removing the removable flanges. Instead of sliding on and off, as in Concept #1, the flanges in Concept #2 will have internal threading which will allow the flanges to screw onto the test rig body components. Obviously, this will also require that the test rig body components have external threading to create the interface with the flanges. In order to reduce the leak paths which are associated with straight threads, Concept #2 utilizes tapered threads which will create an air tight seal between the test rig and the flanges. Therefore, it is anticipated that Concept #2 would contain less unwanted leak paths, however lacks the easy of assembly and durability of Concept #1

3.6.3 Concept #3

Concept #3 takes a different approach to incorporating a means to interchange at least one flange which is in contact with the gasket as seen in Figure 4. Instead of having removable flanges, Concept #3 would instead have several different lower test rig bodies which would be interchanged based on the experimental trial. The lower test rig body would contain the flange that is in contact with the gasket, thus reducing the leak path introduced by having a removable flange. The upper body of the test rig would also have the flange incorporated into it as a solid body, since only one flange needs to be interchangeable based on the sponsor requirements. In order to keep the fasteners elevated off the bottom surface of the test rig, the lower body pieces will have a bowl shape. Thus, the bottom of the lower body remains as the lowest surface of the test rig.

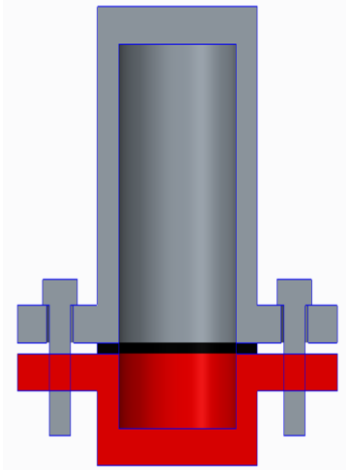


Figure 4. Concept #3 cross section

3.6.4 Concept #4

Concept #4 again utilized the idea of having several different test rig lower bodies rather than removable flanges. However, Concept #4 took a different approach to keeping the fasteners off the lowest surface of the test rig. The bowl-shaped test rig lower body in Concept #3 requires fabrication in order to create the bowl. As an attempt to reduce the amount of fabrication, the team set out on creating a concept which utilized a flat plate as the lower body/flange. Therefore, as shown in Figure 5, Concept #4 uses a flat plate instead of a bowl shaped lower body. In order to prevent the fasteners from being the lowest surface on the test rig, the bottom plate would be threaded for the bolts.

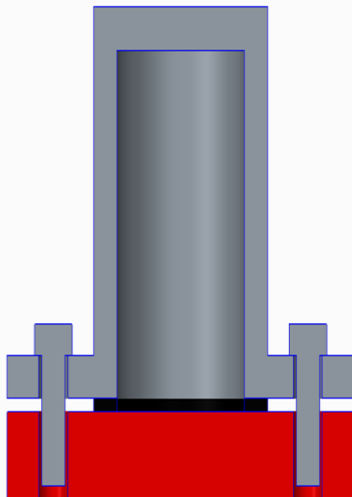


Figure 5. Concept #4 cross section

By threading the lower body directly, as long as the bolts used were not long enough to protrude from the lower body, the bolt would not contact the heat source. However, this will require that the lower body be thicker than otherwise necessary. Also, the possibility of thermal expansion of the bolt is still a risk since the bolt is in direct contact with the threaded component on the heat source (the lower body). Therefore,

Concept #4 would be easier to manufacture, but may not offer the best performance in terms of functionality.

3.6.5 Concept #5

With Concept #5, the design team wanted to use a flat plate for the lower body/flange, but offer a different method to prevent the fasteners from being the lowest surface on the test rig. As it can be seen in Figure 6, Concept #5 uses a thinner flat plate for the lower body/flange. This plate would be changed and replaced with a different plate based on the experimental trial being performed. Nuts will be used to secure the bolts in Concept #5, therefore the lower body/flange will not be threaded as it is in Concept #4. In order to prevent the fasteners from being the lowest surface of the test rig, an additional spacer will be placed below the lower body/flange. This spacer will be of the same material as the rest of the test rig, therefore will have the same thermal conductivity as the lower body/flange. The spacer would not be permanently secured to the lower body/flange, therefore the same spacer could be used for every lower body/flange used in testing. This spacer would sit directly on the heat source, thus elevating the fasteners. Concept #5 allows for fast and simple fabrication, as well as preventing the thermal expansion of the fasteners.

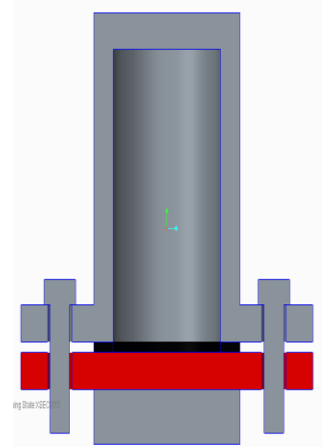


Figure 6. Concept #5 cross section

3.7 Evaluation of Concepts

The technique chosen to evaluate these five concepts was in the form of a Pugh matrix (Figure 7). On the left hand side, there are different categories such as number of leak paths, ease of assembly, and machinability assigned to each concept. These categories were then assigned a weighting factor which was dependent upon their importance. The weighting factors of all of the categories summed up to one. Therefore, the categories of greater importance were assigned higher weighting values. For instance, number of leak paths was weighted the highest at 0.25 because this was the main method of determining the effectiveness of oleophobic gaskets, whereas cost was weighted the lowest at 0.05 since additional funding can be obtained if needed. This means the team was more concerned with a test rig that will not confound the results with potential leak paths than with the cost of manufacturing it.

This Pugh matrix allowed for evaluation of different concepts in relation to a baseline concept. The first concept was set as the baseline with zeros in all of the categories. All of the other concepts were evaluated in relation to whether it was an improvement or degradation of concept one. A score of one or two denotes improvement, while negative one or negative two denotes degradation. A score of zero means neither improvement nor degradation.

All team members participated by completing their own Pugh matrix and the results were averaged together as shown in Figure 7 below. The results of the Pugh matrix identified concept five as the winning one. This concept won due to the very high scores in categories: number of leak paths, machinability, and cost. Concept Five simplifies the bottom flange down to a single sheet of material that does not require embedded threading or extra material as a buffer for the bolt lengths.

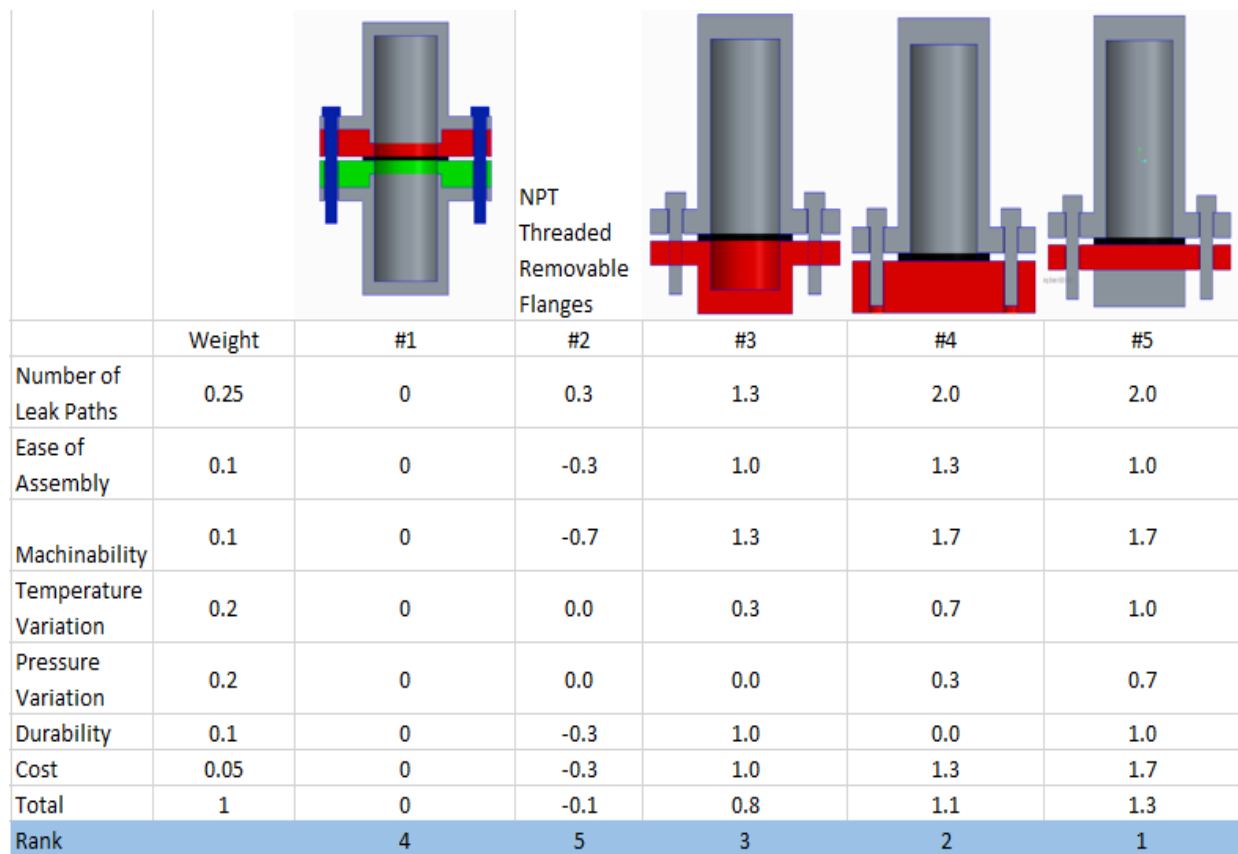


Figure 7. Pugh decision matrix for test rig decision

3.8 Detailed Evaluation of Concept Five

After selecting Concept #5 as the winning concept for the test rig, the design team began to lay out where the hardware items would be located. Figure 8 shows a CAD model of the more detailed

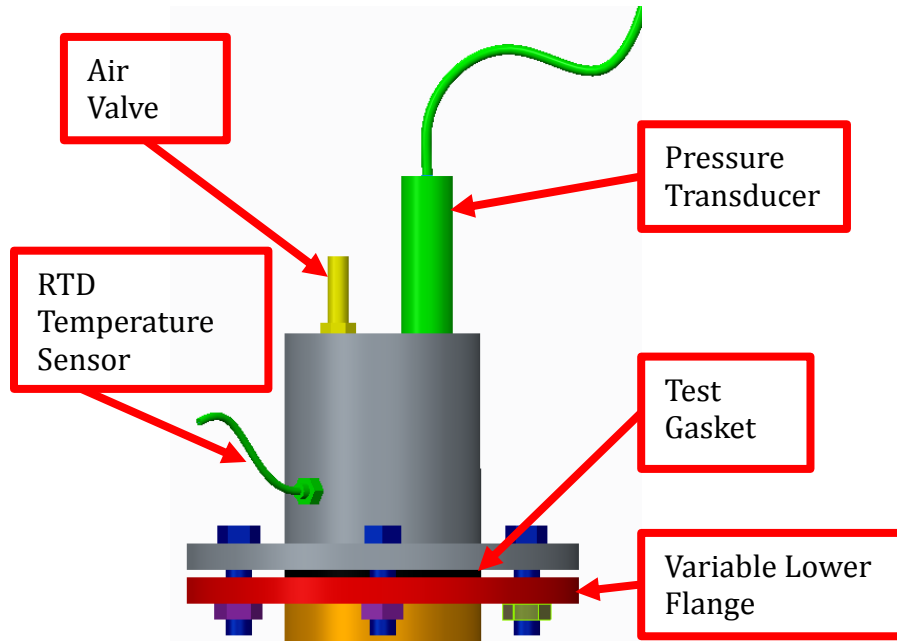


Figure 8. CAD model of test rig Concept #5 with the additional hardware components required for testing purposes

layout of the test rig. The hardware includes items such as the pressure transducer, air inlet valve, and the RTD temperature sensor. This hardware was what the team initially determined was needed in the test rig. The layout of the hardware in Figure 8 was dependent on the bolts that were used to create a clamping pressure on the gasket. As shown in Figure 8, all of the hardware items were located on the upper body of the test rig. This allowed for the hardware to be installed only once except for the removal of the pressure transducer after each testing session to avoid oil from coming in contact with it when draining out the oil. If the hardware were installed in the lower flange, then the hardware items would need to be removed and re-installed any time the lower flange was swapped for testing conditions. Not only does having all the hardware located on the upper body make the testing process more time efficient, but it also minimized the likelihood of a leak occurring at any of the hardware interfaces. All of the hardware except the pressure transducer has NPT threading, which creates a tight seal by causing yielding in the materials when tightened. Therefore, NPT threads are not durable to repeated installation and removal.

As shown in Figure 8, the pressure transducer and the air inlet valve are located on the top surface of the test rig. This allows both of these hardware components to be open to the air cavity which is present above the oil level. Figure 9 shows the approximate oil level location for the test rig. With both of these items being exposed to the air, it minimizes the likelihood of oil entering either of these components and fouling them. The pressure transducer needs to be exposed to the air in order to measure the air pressure, which is used in the Ideal Gas Law calculations. The RTD sensor is located below the oil level, as shown in Figure 9. This allows for the oil temperature to be measured rather than the air temperature.

The purpose of measuring the oil temperature is to know the state of the oil during the test. For example, the oil will become less viscous at elevated temperatures, and therefore more likely to leak.

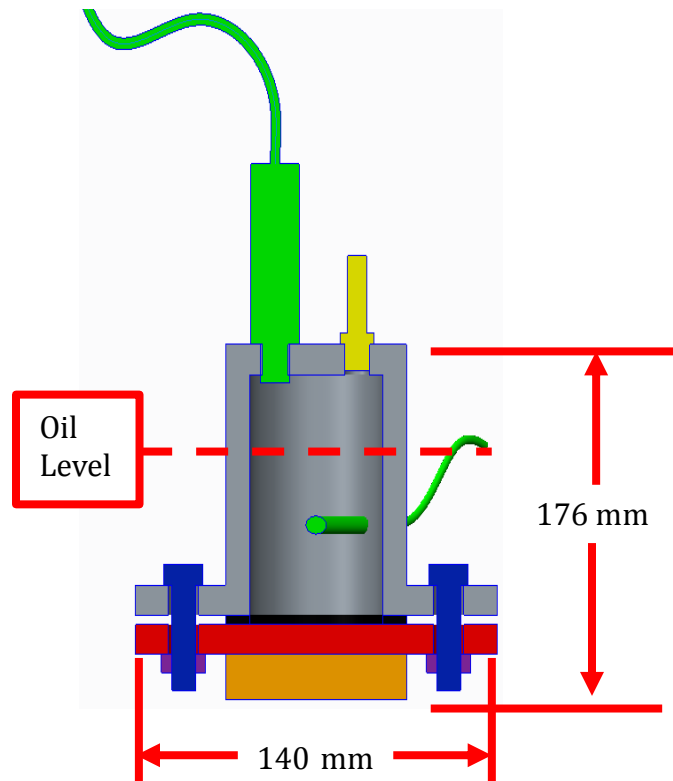


Figure 9. Cross sectional view of the test rig, which shows the oil level relative to the hardware components

3.9 Failure Modes and Effect Analysis

In order to minimize and prevent failures of the test rig, a Failure Modes and Effect Analysis (FMEA) was constructed, as shown in Table 3. Each component in the test rig was evaluated in Table 3 to determine the methods in which the component could fail during testing. Each failure mode had its own cause and effect along with their probability and severity respectively. For example, a failure mode for the sensors is “inaccuracy”, shown in the bottom row of Table 3. This failure mode had a cause of “improper selection” of the sensors and had a low probability of 1, since the team selected a sensor based on the known test conditions.

Table 3. Failure Modes and Effect Analysis

Component	Mode Of Failure	Cause	Probability	Effect	Severity	Suggested Action
Flanges	Bending	Over Loaded Bolts	4	Increase in leak rate	2	Monitor bolt load
	Surface Roughness	Machining Flaw	2			Follow machining standards
Gasket	Blowout	Material selection	1	Safety hazard	5	Material testing
	Oil leak	Improper materials	4	Increase in leak rate	4	Material testing
		Leak paths	6		2	Design selection
Pressure Vessel	Crack/ break	Material selection	1	Gasket blowout	6	Factor of Safety
		Tolerances	2			
Sensors	Overload	Improper selection	1	Inaccurate results	6	Consult sensor data sheet
	Accuracy					

Ranking Scale: 1-6; 1 = Low 6 = High

This was followed by the effect of “improper selection” which was “inaccurate results” with a high severity of 6, since the entire design project focused on producing accurate results for analysis. In order to ensure the failure modes’ probabilities of occurring are minimized, the FMEA table was iterated to ensure that the “suggested action” for each mode of failure of each component would decrease or eliminate the “cause” and therefore the “effect” of said failure. Analysis of the design was then performed to minimize several of these modes of failure.

3.10 Analysis of Design

3.10.1 Pressure Distribution Analysis

In order to test that the use of four bolts would cause the clamping pressure on the gasket to not dip below the desired pressure, a simulation was created within Creo Parametric 2.0 to analyze the contact pressure on the gasket face. In order to improve the “run-time” of the analysis, the test rig was divided into four pieces. Analysis was done for one-quarter of the test rig, with the bolts being

located at the cut interfaces. Figure 10 displays the CAD model used in the analysis. During the simulations, the bolt load which was applied was equal to the axial force found during the torque

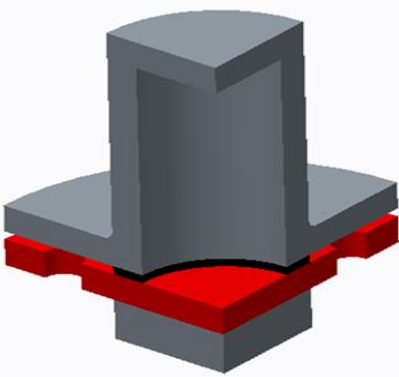


Figure 10. One quarter of the test rig, which was used for analysis

calculations for desired pressures. For example, for the desired clamping pressure of 10 MPa, the applied axial forces in the analysis was 5.01 kN. Figure 11 displays the results of the analysis for a desired clamping load of 10 MPa. The results of the analysis shows that between the bolts, there is no portion of the gasket which will experience less than 10 MPa of pressure all the way across the gasket face. Based on this result, the use of four bolts was confirmed to be a suitable amount of bolts for the design.

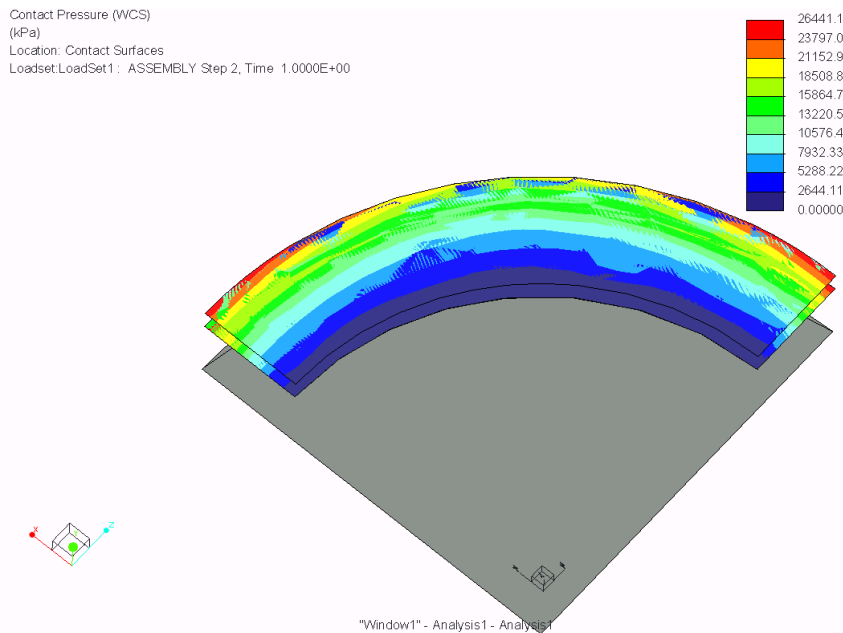


Figure 11. Gasket clamping pressure distribution based on analysis results

3.10.2 Flange Thickness Calculations

To ensure that the bottom removable flange would pose no threat of suddenly failing under the various pressures present during experimentation, a minimum thickness analysis was performed. Both A36 Steel and Aluminum 6061 were analyzed; however, A36 Steel was chosen as it was determined to be the more inexpensive of the two minimum thicknesses calculated. This analysis was broken up into two different regions. The bottom flange is subject to the internal pressure of

the vessel as well as the clamping pressure from the bolts. The internal pressure is felt on a center circular portion of the flange. The maximum internal pressure that will be felt is 2.5 psi. This center disc extends out to the inner radius of the vessel (50 mm). A visual of this can be viewed below in Figure 12.

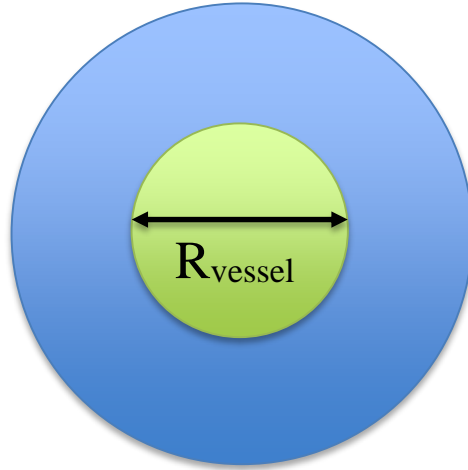


Figure 12. Top view of removable bottom flange

The second region is the outer ring of the bottom flange that is affected solely by the clamping pressure of the four bolts, which is a maximum of 10 MPa. The final and simplified equation that was used to calculate the minimum thickness of these two portions is dependent upon a pressure differential (ΔP), Poisson's ratio (ν), failure strength (σ_f), radius (R), density (ρ), area (A), and a constant (C) which is determined based upon whether the region is clamped ($C=1$) or simply supported ($C=3$). The equation is as follows

$$t_{min} = \frac{\sqrt{\frac{3\pi^2 R^6 \Delta P (C+\nu)}{8}} \left(\frac{\rho}{\sqrt{\sigma_f}} \right)}{\rho * A} \quad (3)$$

Using Eq. 3, the A36 Steel minimum thickness required for the middle circular portion was calculated to be 0.31 mm, while the outer ring minimum thickness was calculated to be 4.94 mm. These calculations can be found in Appendix A. The large difference in thicknesses is due to the significant difference in the pressure differential term. To make the machining process easier, the minimum bottom flange thickness was decided to be the larger of the two thicknesses as this

accounts for both thickness requirements. Following this logic, the bottom flange's overall minimum thickness was determined to be 4.94 mm.

3.11 Final Design

After completing the FMEA and the appropriate analysis, the team was able to revise the selected design concept to create the final design for the test rig. Figure 13 shows the CAD model for the final design. In this final design, the team selected the optimum location for all of the hardware components.

The oil valve, which will be used to add and remove the oil, is located at the top face of the test rig. It is also offset from the center of the top face, which will allow for easier removal of the oil. Also on the top face of the test rig is the pressure relief valve. The pressure transducer and air valve are both on the cylindrical wall towards the top of the test rig. This location exposes those items to the air cavity above the oil, but also places them far from the oil valve. This minimizes the likelihood of oil getting inside of these hardware items during the process of adding or removing oil. The RTD sensor is still on the cylindrical wall of the test rig, but is located below the oil level. It is also below the pressure transducer and the air valve, which was done so that as many wires as possible would originate from a similar location, making the usage of the test rig have a cleaner appearance. This also makes it easier to set up the electrical connections on the test rig during testing. A removable flange was still incorporated in the final design because the team wanted to test a scenario in which no gasket is used, but an oleophobic

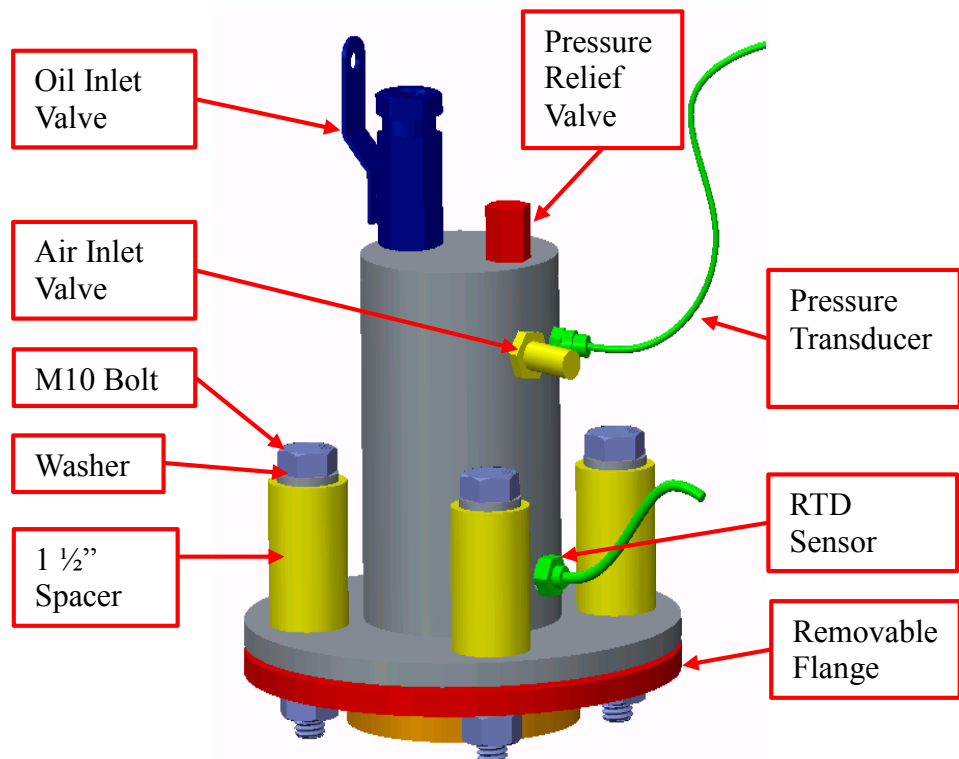


Figure 13. CAD model of the final design for the test rig.

test rig. This location exposes those items to the air cavity above the oil, but also places them far from the oil valve. This minimizes the likelihood of oil getting inside of these hardware items during the process of adding or removing oil. The RTD sensor is still on the cylindrical wall of the test rig, but is located below the oil level. It is also below the pressure transducer and the air valve, which was done so that as many wires as possible would originate from a similar location, making the usage of the test rig have a cleaner appearance. This also makes it easier to set up the electrical connections on the test rig during testing. A removable flange was still incorporated in the final design because the team wanted to test a scenario in which no gasket is used, but an oleophobic

solution is applied directly to the lower flange face. Thus, two lower flanges were still required. The CAD drawing for the final design can be found in Appendix B. These are the drawings that were used by the machine shop to fabricate the test rig.

3.11.1 Concept Design Optimization

The final design of the test rig took into account all of the analysis results to create the optimum design. For example, the calculated required flange thickness was found to be 4.94 mm. However, the thread engagement length for many of the hardware components were recommended to be approximately 0.25 inches. Therefore, the team decided to purchase A36 steel with a 0.25 inch thickness for the test rig. This thickness is uniform throughout the test rig, meaning that both the flanges as well as the cylindrical walls are composed of steel at this thickness. This not only provided a margin of safety in our design, with our selected thickness being 31% thicker than required, but also reduced the machining time required to fabricate the test rig. So not only was the material thickness chosen as the optimum thickness based on analysis requirements, but also in terms of being the optimum thickness to reduce the fabrication time in the machine shop. If the team had chosen a thinner thickness for the cylindrical walls, then additional items would have been required to be welded onto the test rig to provide adequate thread engagement for the hardware.

Another item of the test rig that was optimized was the selection of four bolts. For sealing the test rig, any number of bolts could have been selected. However, the team wanted the design to simulate an actual seal on an engine in the most realistic way possible. To simulate an actual seal, the pattern formed by connecting the bolts should follow the path of the gasket. With a circular design having been specified by the sponsor, the test rig would only create a circular bolt pattern if many bolts were used. However, the use of many bolts would no longer allow for a realistic pressure drop on the gasket faces between bolts, since the bolts would be placed too closely together. The design team determined that the use of four bolts provided an adequate compromise to meet both of these requirements. Four bolts is better at following the gasket path than the use of two or three bolts, but still provides adequate bolt spacing to allow for a realistic pressure prop on the gasket face. Thus, a four bolt pattern was chosen as the optimum design. Also, M10 bolts were specified as the bolt to use because they can easily handle the required load for proper sealing and are similar to the bolt sizes used on an engine.

3.11.2 Bolt Load Measurement

One of the test parameters that the team needed be capable of varying was the clamping pressure on the gasket. In order to vary this pressure, the team needed a method of controlling the bolt load applied by the bolts used to clamp the two flanges together. One method to control the bolt load was to use a torque wrench with a predefined torque setting. Based on the coefficient of friction for the bolt, a theoretical torque value can be calculated to provide the desired bolt load. Since the clamp load was applied through the use of bolts, the relationship between the applied torque (T) (measured via a torque wrench) and clamping force (F) was determined. Equation 4 shows the relationship between the applied torque to a bolt and the axial force it applied [5].

$$T = cdF \quad (4)$$

The nominal major bolt diameter is defined by d , and the coefficient of friction of the material is shown as the variable c . For testing, the induced clamping pressure over the gasket will be varied from 0.5 –10 MPa. The relationship between total bolt force (F), gasket area (A), and clamping pressure (P) is shown in Equation 5. Thus, the team could relate the desired clamping pressure to an applied torque value on the bolts. This can be found in Appendix C.

$$P = \frac{F}{A} \quad (5)$$

However, it is not possible to measure the exact coefficient of friction for each bolt. The standard friction coefficient for a steel bolt is 0.2, but this can vary by as much as 30% from bolt to bolt [6]. Therefore, this method of controlling the bolt load would put the clamping pressure on the gasket in the approximate range desired, but it would not be a precise value. Because of this potential error, the team decided to use an alternative method for controlling the bolt loads.

Load cells are devices that are capable of measuring the force being applied to them through the use of strain gauges within them. The team investigated purchasing load cells, however the cost of just the load cells would equal the budget for the entire project. Cummins Inc. then



Figure 14. Modified bolt with strain gauge.

offered to provide the team with strain gauges that could be machined onto the bolts themselves. Cummins Inc. has the capabilities at their facilities to machine bolts and apply sheet resistive type strain gauges to the modified bolts. Figure 14 shows what the modified bolts look like with a strain gauge applied to them. Therefore, the senior design team provided bolts to Cummins Inc., and Cummins Inc. made the necessary modifications to the bolts and sent them back to the senior design team. With strain gauges applied to the bolts, Cummins Inc. created a calibration curve for each bolt. Using an MTS machine to apply a tensile load to each bolt, the output microstrain value of the strain gauges were calibrated to the known applied load. Using this calibration, the team was able to tighten these modified bolts on the test rig and knew the exact bolt load value based on the output of the strain gauges. This method of measuring the bolt load was very precise as well as a cost effective solution to measuring the bolt load. Using these bolts, the clamping pressure on the gasket was known and was easily repeatable from test to test.

3.11.3 Hardware Selection

As shown in Figure 13, there are multiple pieces of hardware being utilized in this test rig. In order to select the hardware with a correct resolution, a range of detection and an accuracy was targeted. As stated previously, the temperature sensor reads the oil temperature and is not used in later calculations; therefore, its accuracy is not as important as the accuracy of the pressure which is

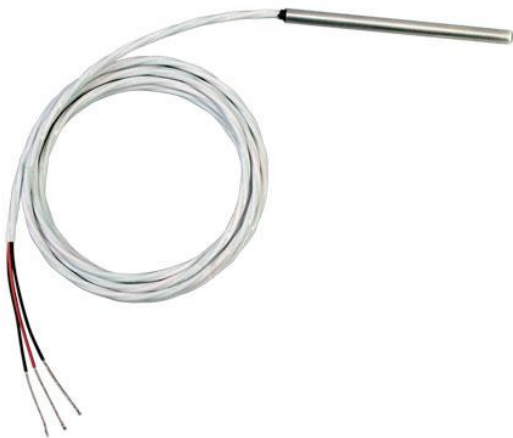


Figure 15. Short RTD probe [7]

used in future calculations. The temperature sensor must be able to read the range between 22-120° C with $\pm 2^\circ$ C accuracy. This accuracy was selected by the team as appropriate for the variable. Using this information, an RTD (Omega PR-20 series), seen in Figure 15, was chosen as the best fit and most inexpensive sensor that meets the requirements. This RTD is smaller than a typical laboratory RTD as it must fit inside of the test rig fully submerged in the oil. It will be fitted into the side of the test rig using a compression fitting.

The pressure sensor is much more important to the experiment and is required to read a range between 0-2.5 psi with a minimum of ± 0.01 psi accuracy. Additionally, it must function at the elevated temperatures mentioned above. Given these requirements, a pressure transducer (Kulite XT-123B-190-G) was chosen as the best fit, which can be seen in Figure 16. This pressure transducer is a gage sensor which will require an amplifier to read its 100 mV output range. The



Figure 16. Pressure transducer [8]

amplifier used for the senior design team's testing was provided by Dr. Rajan Kumar. The output from the amplifier was sent to the DAQ (Data Acquisition) system set up in the laboratory. The pressure transducer can measure up to 5 psi with an accuracy of ± 0.005 psi, which is better than the minimum accuracy required.

The other pieces of hardware on the test rig include the air inlet valve, the oil inlet valve, and the pressure relief valve. The air inlet valve will be a very basic stem (Figure 17) that can be fitted with a tap connected to compressed air which will pressurize the air cavity above the oil. This valve stem can be imagined as the air valve stem on a traditional bicycle tire.



Figure 17. Air valve stem [9]

The air is pumped in and can be released by pressing on the center of the valve stem. The oil inlet



Figure 18. Ball Valve [10]

valve will be a ball valve, as shown in Figure 18, which creates an air-tight seal. To fill the test rig with oil, the ball valve is opened by turning the valve handle, and a funnel can be used to pass the oil through it. During testing, the valve will be sealed shut which will eliminate the possibility of oil and air leaking past the valve. After each test, the valve can be opened and the test rig can be drained. The team selected an appropriate ball

valve to use for the test rig. The ball valve selected is a compact high pressure ball valve, which has a total length of 1.875 inches and a male thread of 1/8" NPT. This small size allows for the ball valve to claim minimal space on the test rig, thus leaving room for the other hardware.

The design team decided to use a pressure relief valve on the test rig for two purposes: as a method to control the initial 2.5 psi internal pressure, and to prevent the pressure transducer from being damaged from over-pressurizing it. Therefore, the design team specified a pressure relief valve, the Straval 1/8" Rva05-01T. Figure 19 is an image of the pressure relief valve ordered.



Figure 19. Straval 1/8" Rva05-01T pressure relief valve [11]

3.12 Design for Manufacturing

For the fabrication of the test rig, machining occurred in two locations. The machining and fabrication of the steel components, such as the flanges, was completed at the FAMU-FSU College of Engineering Machine Shop because the use of the water jet was needed. The only component not fabricated at the FAMU-FSU College of Engineering Machine Shop was the strain gauge bolts. These bolts were machined at a Cummins Inc. facility in Columbus, Indiana. Cummins Inc. had the experience and capabilities to modify a standard M10 bolt in order to incorporate strain gauges; therefore, it was decided it would be best to allow Cummins Inc. to prepare the bolts. Full CAD drawings are shown in Appendix B, where details such as dimensions, materials, and tap sizes can be found. The drawings in Appendix B also state all the part names, as well as the quantity in which they are needed in the test rig. Also, Appendix D contains a detailed "Design for Manufacturing, Reliability, and Economics" report.

3.12.1 Sub-Assembly Fabrication

Before assembly of the test rig could occur, the Top Assembly sub-assembly needed to be fabricated. The Top Assembly consists of the following parts: Top Flange, Top Tube, and Top Cap. These parts were welded together using stainless steel weld, and the welds were done as full beads in order to create an air tight joint between the parts. In Figure 20, the Top Assembly is shown in its exploded view in order to show how the components mate together prior to welding. After the welding was completed, the Oil Inlet Valve, Pressure Relief Valve, Air Inlet Valve, and the RTD sensor with its compression fitting were assembled to the Top Assembly. Each of these parts had NPT threads in order to create an air tight seal; therefore, it was required to apply significant torque to each part while installing in order to distort the threads as desired. As an

additional form of sealing, PTFE Teflon tape was wrapped around the threads of the parts before they were installed into the Top Assembly. This serves as an additional seal in order to ensure there is no gap between threads. The rest of the parts for the test rig do not require sub-assembly, and therefore are included in the final assembly stage.

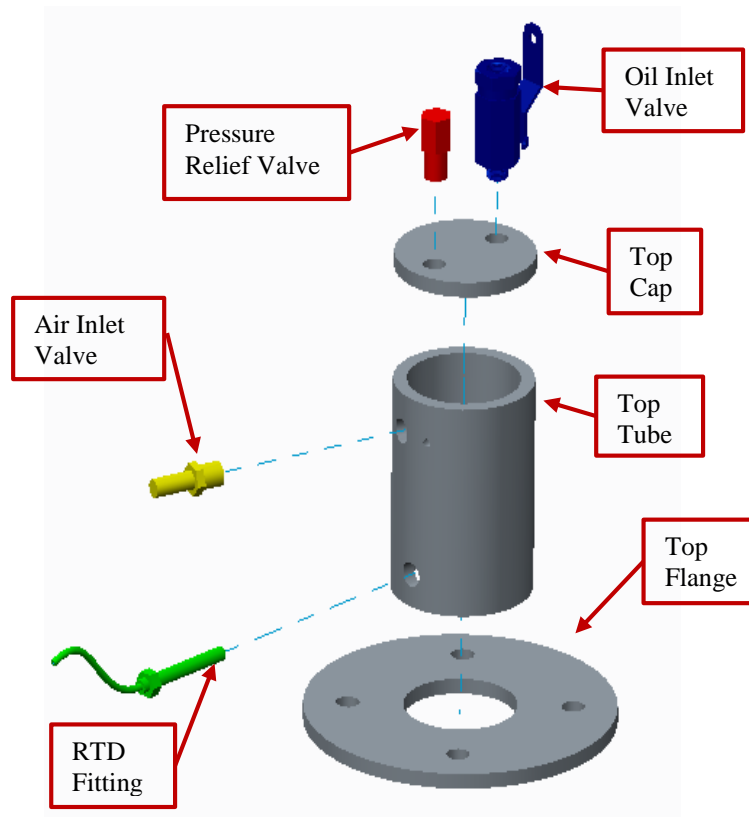


Figure 20. Exploded view of the Top Assembly

3.12.2 Assembly of Test Rig

After completing the Top Assembly sub-assembly, the remaining components could be assembled to the test rig. This assembly process occurs before every use of the test rig, meaning that this assembly is done before every gasket test. Figure 21 shows the final assembly exploded view for the test rig.

The first step of the assembly is to place the Bottom Flange on top of the Spacer. If the test being performed is a high heat test, then the Spacer should be placed on top of the cool hot plate prior to placing the Bottom Flange onto it. Once the Bottom Flange is in position, the next step is to place the gasket onto the Bottom Flange. The tabs which were welded onto the Bottom Flange serve as a method of centering the gasket. So while assembling the gasket to the Bottom Flange, the tabs on the Bottom Flange were always placed within the inner diameter of the gasket.

With the gasket in position, the Top Assembly was then lowered onto the gasket. While lowering the Top Assembly, care was taken to ensure the bolt thru holes from the Top Assembly and the Bottom Flange were aligned along their respective center axes. This removes the need to adjust the alignment after the Top Assembly is fully lowered, since adjustments after that point can cause damage to the gasket.

The next step in the assembly was to install the Bolt Spacers, Bolts, Washers, and Nuts. The arrangement of these parts can be found in Figure 21. For the purpose of conducting an experiment/test on a gasket, the nuts are not torqued down immediately. Since the bolts are strain gauged, it is important to collect the unstrained microstrain value. This is used to calibrate each bolt prior to applying a load. After the unstrained microstrain value was recorded, the bolts were tightened to the desired bolt load value. During the tightening process, the bolts were gradually loaded while alternating between sides of the test rig in order to ensure even loading on the gasket.

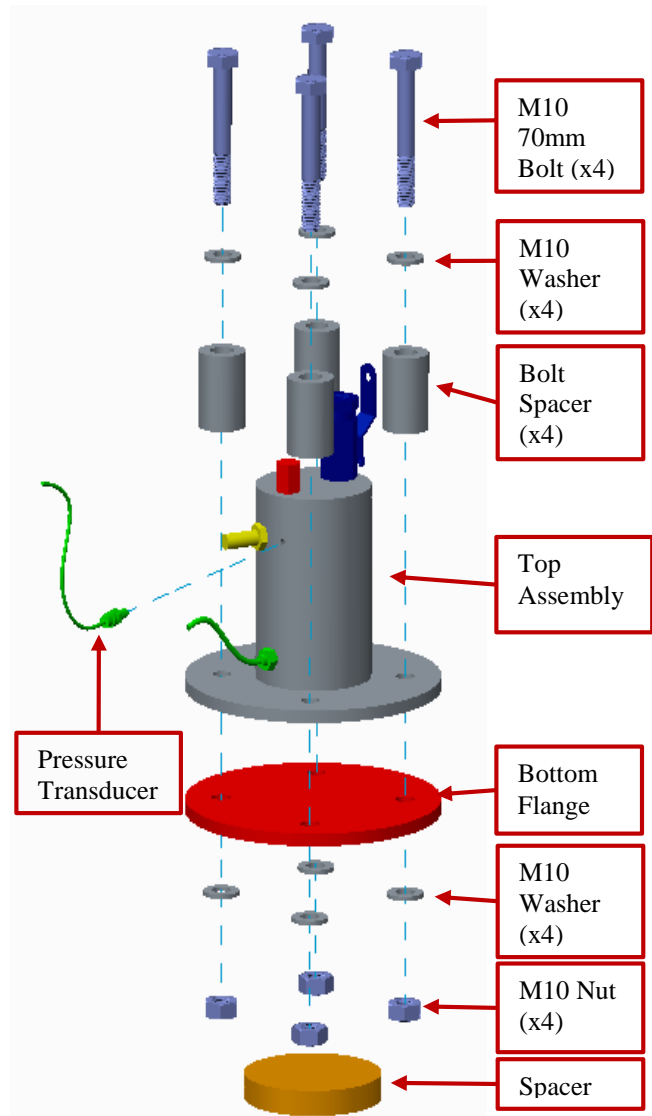


Figure 21. Exploded view of the final assembly for the test rig.

With the Bolts installed, the final step in the assembly of the Test Rig was to install the Pressure Transducer. This is done after oil is added to the test rig. That process is part of the testing procedure, and not the assembly of the test rig. The Pressure Transducer is installed into the Top Assembly section of the test rig using an 8 mm wrench.

3.12.3 Manufacturing of Oleophobic Gaskets

Oleophobic gaskets were also manufactured by the team. There were two different solutions chosen to make gaskets oleophobic; Staingaurd WB Impregnator and Ultra-EverDry Spray. For the Impregnator, the manufacturing process consists of dipping the gaskets into a bath of the solution and then allowing it to dry for 24 hours. For the Spray, the manufacturing process consists of applying two different coats via an aerosol spray. The first coat is an adhesive layer, which must be allowed to dry for 1 hour before application of the second coat. The second coat is the oleophobic solution, and it must be allowed to dry for 2 hours after application.

The gaskets which were manufactured were impregnated paper gaskets, sprayed Rubber Coated Metal (RCM) gaskets, and impregnated and sprayed combination felt gaskets. The oleophobic paper and RCM gaskets were made by applying the solutions to standard paper and RCM gaskets which were provided by Cummins Inc. The felt gasket was first cut to size from a sheet of high density felt and then had the oleophobic solutions applied. The total time to create the gaskets, including the 24 hour dry time, was 25 hours.

3.12.4 Assembly Time

The assembly of our test rig occurred over a period of about 2 months. However, this is not reflective of how long the actual assembly time is. The reason that the assembly process took a month to complete was because the strain gauged bolts provided by Cummins Inc. arrived much later than scheduled. Table 4 shows the timeline of the assembly process of the test rig in both the actual dates, as well as the physical number of hours to perform the task. The majority of the assembly time was from the fabrication process in the COE Machine Shop, where the cutting and welding of the Top Assembly was done. The rest of the assembly process was just installing threaded components, so the assembly time in terms of hours was relatively short.

Table 4. Assembly Time for Test Rig

Assembly Task	Time Span to complete	Duration (hours)
Fabrication in COE Machine Shop	1/11/2016 - 1/20/2016	5
Installation of Oil Inlet Valve, Air Inlet Valve, and Pressure Relief Valve	1/21/2016	1
Installation of RTD sensor	3/1/2015	0.25
Final Mock Up Assembly	3/1/2015	0.5
Total Assembly Time	1/11/2016 - 3/1/2016	6.75

3.12.5 Future Design Optimization

During the design process of the test rig, the team made a strong effort to keep the design as simple as possible. Therefore, it would be very difficult to reduce the number of components of the system. Every component on the system serves an important role. For example, all items on the Top Assembly, such as the Oil Inlet Valve, Air Valve, etc. were needed for the functionality of the test rig. Even items such as the Bolt Spacer were required for functional usage, since Cummins, Inc. required that the strain gauged bolts have at least two inches of length between the bolt head and the first engaged thread.

However, there could be an added component to the test rig which the team did not anticipate needing. This component is an additional RTD sensor in the air cavity. During testing, it was discovered that the air temperature does not reach equilibrium as quickly as the oil, and thus the air temperature continued to increase even after the RTD sensor in the oil displayed a stabilized condition. With the addition of an RTD sensor in the air cavity, the air temperature could be measured as well to ensure that there isn't a temperature fluctuation in the air. The team discovered this air temperature fluctuation during testing, because a pressure increase was recorded instead of a pressure decrease. The only source of a pressure increase would be the air temperature changed.

3.13 Design for Reliability

In order to ensure consistent results when testing gaskets, various methods of design analysis were completed before the final prototype was constructed, including a Failure Modes and Effects Analysis (FMEA), a Finite Element Analysis (FEA) of the contact pressure, a surface roughness measurement, and a minimum material thickness analysis.

The first analysis conducted was FMEA on the test rig (Table 3). Each part of the test rig was analyzed to determine the most likely methods of failure. In order to reduce or eliminate the possibility of these failure modes, the last column of the table recommends an action.

The second analysis conducted on the prototype was FEA on the gasket pressure, shown in Figure 11. This shows the pressure distribution along the gasket face due to a 10MPa clamping pressure. The FEA results proved that the use of four bolts was sufficient because the gasket face had the desired clamping load and showed no leak paths as a result of the design.

Another analysis completed was the measurement of the flange surface roughness using a Coherix ShaPix S150 sensor. Initially, the average surface roughness values found were higher than the 3.2 micron RA maximum Cummins Inc. had set for the test rig; however, this was mitigated by sending the flanges back to the machine shop in order to decrease the surface roughness.

The final analysis conducted was to verify that the thickness of the material being used for the test rig was thick enough to prevent any yielding or failure under pressurized and loaded conditions. This analysis considered the maximum internal stress of the test rig of 2.5 psig and the maximum clamping bolt pressure of 10 MPa. The result of the analysis was that the minimum thickness of the test rig was 4.94 mm, and therefore the team selected 6.35 mm material to provide a factor of safety.

In addition to the above analyses, the reliability of the test rig could be improved with some additional long-term design problem mitigations. The provided raw strain gauge wires protruding from the bolts machined by Cummins Inc. would not be sustainable long-term because of their susceptibility to breakage with a small application of force to the connection. This weakness could be corrected through the use of a protective casing to ensure the protection of the connections.

This design could be reliable for hundreds of tests because of the careful analyses conducted on each aspect of the test rig, as well as the simplicity of the design. One source of reliability concern

would be damage to the flange surfaces after repeated use, such as scratches. This damage could be easily remedied with a simple finishing pass or some other method of machining the flange to produce a surface roughness within the defined machining standards.

3.14 Design for Economics

The budget given for this project was \$2,000 through the Aero Propulsion, Mechatronics and Energy (AME) Center. This budget was used to acquire all of the materials that were needed for application and testing for determining the effectiveness of oleophobic gaskets. Even after calculating for the maximum prices, the total estimated cost only came out to \$1,850, which left a remainder of \$150 in case of an emergency.

The test rig sensors cost \$704.00 and the test rig materials cost \$218.41. The oleophobic solution cost \$70.00, whereas the teflon gaskets cost \$170.00. The rest of the money spent was used for anything needed for the testing process which totaled \$73.42. The pie chart in Figure 22 shows the percentage breakdown of the different budget categories.

After extensive research, a similar test rig made by the German company Amtec was found; however, this test rig is not for sale [12]. It measures bolt load and leak rate but does not measure temperature. Also, for the leak rate to be calculated correctly, the test rig must be placed in a vacuum chamber and the leak is measured using a helium mass spectrometer, which would be much more expensive than our test rig design.

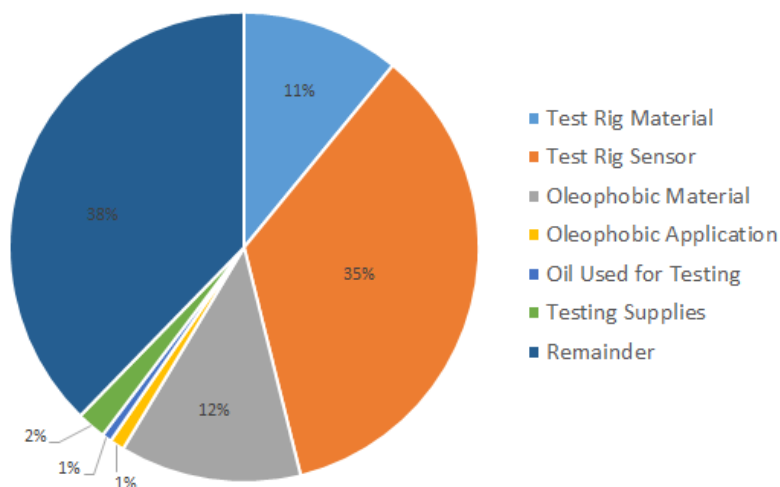


Figure 22. Pie chart showing distribution of funds

4 Design of Experimentation

4.1 Test Rig Component Testing

Each individual electronic and mechanical component was instrumental in the data acquisition process. If one of them was not installed correctly, there was a chance that the data collected could be skewed. The Omega RTD sensor was calibrated by using a bucket of ice water and the temperature of the air to make sure that temperature readings were accurate. The Kulite pressure transducer was calibrated at the Aero-Propulsion Mechatronics and Energy (AME) building using their equipment by accurately testing it at various known pressures. Thus the pressure transducer's ability to monitor an internal pressure of 2.5 psi and adjust as air exited the cavity was verified.

Another item of the test rig that needed to be tested and verified was the surface roughness of the

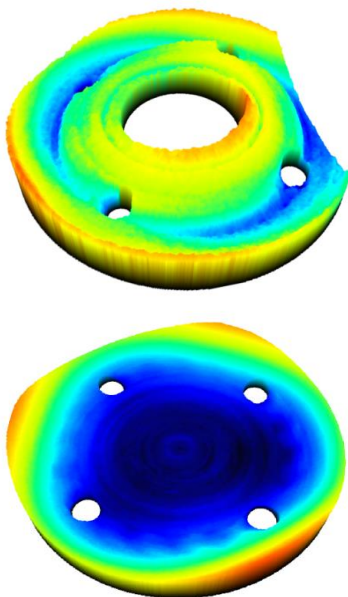


Figure 23. Top Flange (2.90 micron RA) and Bottom Flange (2.03 micron RA)

top and bottom flanges. Cummins Inc. specified that the flanges needed to have a surface roughness of 3.2 microns RA or smoother in order to simulate an engine flange. In order to measure the surface roughness of the flanges, the team used a Coherix ShaPix S150 sensor, which was available at High Performance Materials Institute (HPMI). This machine records the valleys and peaks of the entire flange in an x-y origin system, therefore the surface roughness could be extracted from the measurement. After the team received the flanges from the COE machine shop, the top and bottom flanges were found to be above the 3.2 micron RA specifications. This issue was resolved by sending the flanges back to the machine shop for additional finishing passes to improve the surface finish of the parts seen in Figure 23.

The strain gauge bolts that were used for monitoring clamping load had to be calibrated before each test. The bolts were positioned with one washer below the head of the bolt, a spacer above the two flanges and a washer and nut loosely tightened below the flanges but not quite touching the bottom flange as to accurately measure an unloaded bolt load strain. Once these were recorded, the bolts were torqued down so that the new loaded bolt load strain could be obtained. As a test to

prove that the strain gauge bolts output an accurate bolt load value, the team also compared the strain gauge output to the expected output based on an applied torque on the bolt. When a bolt was torqued to 95 inch pounds, which would correspond to a 5.01 kN bolt load based on ideal calculations, the strain gauge measured a bolt load of 5.5 kN. Since it was known that the torque wrench method would have an error of up to 30%, the team determined that the strain gauge bolts did in fact measure the bolt load accurately since it was similar to the value expected based on the torque input.

Once all of the other components had been properly calibrated and installed, the testing of the air inlet and pressure release valves ensued. The air inlet and pressure relief valves were tested by running the data acquisition software, then pumping in air via the air inlet valve. The air inlet valve functioned properly to add air into the test rig, which was verified when the pressure relief valve opened up at an internal pressure of 2.5 psi. Therefore, both the air inlet valve and pressure relief valve functioned properly.

4.2 Functional Diagram

Figure 24 shows the functional diagram of the test set up. The gasket material to be tested was placed in between the flanges of the test rig, and then the strain gauged bolts were torqued down

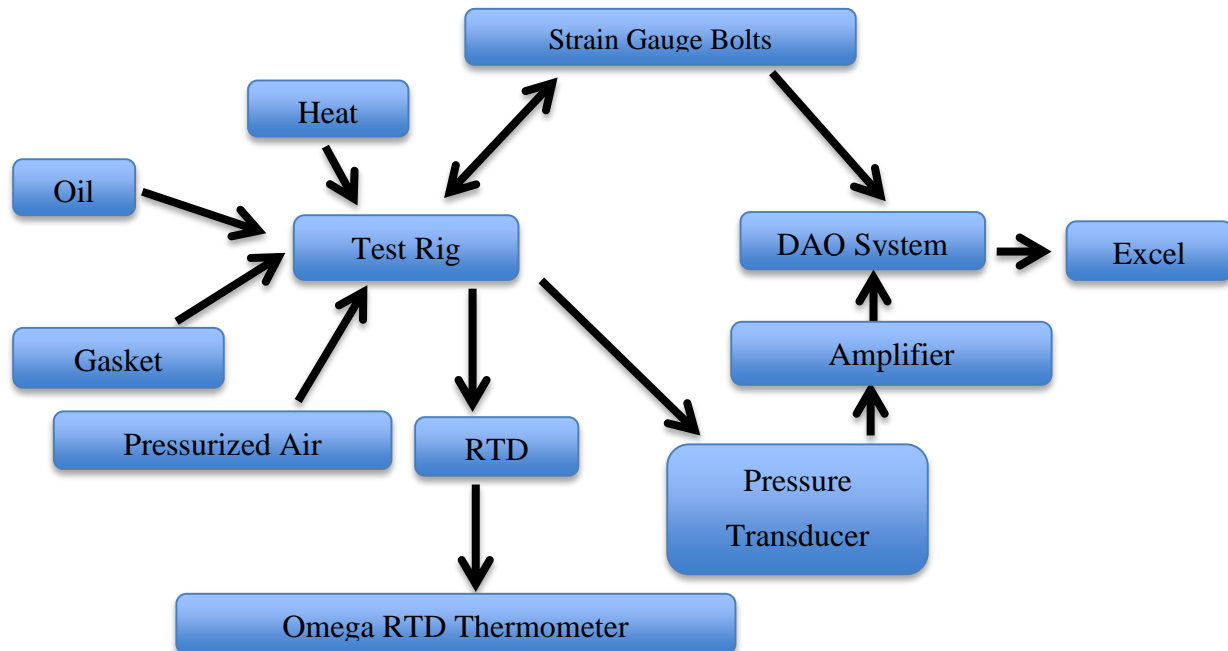


Figure 24. Functional Diagram of Project

to the desired clamping load. The desired clamping load for the experimental set-up was obtained through the use of the strain gauges that were connected to the DAQ system. Oil was poured into the test rig through the oil valve and pressurized air (2.5 psig) was induced into system. For elevated temperature testing, the test rig was heated to a desired temperature, which was monitored by the RTD sensor which was connected to the omega RTD thermometer. The pressure transducer which was connected to the DAQ system through the amplifier to record the internal pressure during each test. In Appendix E, the complete “Operation Manual” can be found.

4.3 Operation Instructions

This test rig is designed to measure the leak rate of various circular gaskets with an inner diameter of 55 mm and an outer diameter of 75 mm. The internal pressure can only be set to 2.5 psi or less; however, the temperature is variable, as well as the bolt clamping loads. The following instructions refer to testing procedures:

1. Turn on power to the signal box for the pressure transducer. Let it warm up and stabilize while the test is being set up.
2. Place selected gasket in the center of the bottom flange. Four small weld marks have been placed radially out from the center of the flange. All four welds should be inside the gasket inner radius, which will ensure the gasket does not move out of place during set up.
3. Carefully set the top flange on top of the bottom flange. Make sure the four bolt holes in the top flange match with the bolt holes in the bottom flange.
4. Place a washer and spacer around each bolt and then place all of the bolts in the bolt holes. Write the number of each bolt with a permanent marker on its washer. This is important as each bolt has a different calibration curve provided by Cummins Inc.
5. Loosely tighten a washer and a nut onto the end of each bolt. Do not let the washer and nut touch the bottom flange.
6. Connect two bolts that are physically across from one another on the test rig to the DAQ system. Plug in their respective power sources. Be careful to not tangle or break any wires.
7. Open the DAQ two channel VI in Labview. Keep all inputs at their default values, except for the sampling rate which should be set to 20,000 Hz. Set the file path to the desired location and name the file accordingly.
8. Run the VI from the front panel. Locate and open the output file with Excel. There should be two columns of many data points which correspond to many samples of the unstrained voltage of each bolt.
9. For each bolt, take an average of all of its unstrained voltage data points. Record the two average unstrained voltage values in Excel. It is common for these values to differ.

10. Begin tightening down these two bolts to the specified clamping load either through two wrenches or a torque wrench, depending upon how much torque needs to be applied.
11. Run the VI from the front panel once again at the same conditions as step six. Repeat the process of accessing the file in Excel and finding one average value.
12. Using the respective Cummins Inc. calibration curves and standard formulas for strain gauges, an excel file was set up such that the only required values to calculate the bolt loads are the average unstrained and average strained voltage values from each bolt. Place the experimentally determined average values in this Excel sheet.
13. Adjust the tightness of the bolt until the desired bolt load is met.
14. Repeat steps 6-13 for the other two bolts.
15. Carefully measure 75 milliliters of Shell Rotella T 15W-40 diesel oil and pour into the test rig via the oil inlet valve on the top of the test rig (a small funnel is recommended).
16. Connect RTD to an instrument that will read out the temperature on a digital screen. This data does not need to be recorded.
17. For room temperature tests, skip steps 18-22.
18. For elevated temperature tests, set hot plate to 500°C. Place the test rig on the hot plate on top of a metal spacer. This spacer is to ensure the bolts are not touching the hot plate.
19. Continuously monitor the temperature of the oil from the instrument digital screen. When it reaches approximately 100°C, change hot plate to about 345°C.
20. Wait for the oil temperature to stabilize around 119°C-120°C. Carefully close oil inlet valve using proper heat protectant gloves.
21. Every few minutes, pop open oil inlet valve to relieve pressure and then close again.
22. After about 15 minutes at a steady temperature, relieve pressure one last time.
23. Close oil inlet valve.
24. Tighten pressure transducer into the appropriate hole in the test rig using an 8 mm wrench. Be careful to not tangle or break any wires.
25. Open the DAQ one channel VI in Labview. Change the sampling rate to 100 Hz, the timeout to 7,200 seconds, and samples per channel to 720,000. These are the settings for a two hour run time test. All tests are run for two hours. Set the file path to the desired location and name the file accordingly.
26. Connect the pressure transducer to the DAQ system.
27. Start running the VI from the front panel.
28. Unscrew cap off of air inlet valve and begin pumping air into the test rig via a bike pump. Stop pumping when the pressure safety valve pops open, which should occur at 2.5 psi. Replace cap back onto air inlet valve.
29. Let the test run for the entire two hours. Have at least one person present in the room at all times.
30. Access the output file as previously described.
31. Input experimental data into an Excel file that is already set up to convert the change in the pressure of the air to an oil leak rate.

32. For hot tests, allow entire test rig to cool down before handling.
33. Remove pressure transducer.
34. Carefully open the oil inlet valve and tilt the test rig to slowly drain most of the oil out making sure to not allow the oil to enter the pressure relief valve. Dispose of the oil.
35. Loosen the bolts and open the test rig up.
36. Document the state of the gasket and dispose of it.
37. Wipe down the bottom and the top flange with paper towels, as well as carefully cleaning inside of the test rig.
38. Return the test rig back to its original condition and begin testing again.

An actual setup of the final test rig can be seen below in Figure 25. This figure was taken during an elevated temperature test experiment. All components that were listed above in the functional diagram in Figure 24 can be seen in Figure 25.

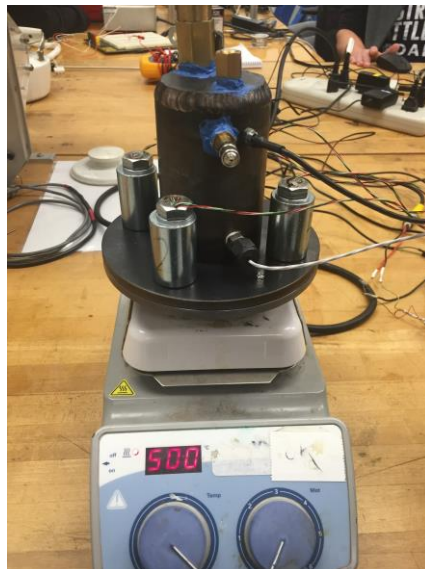


Figure 25. Test rig positioned on the hot plate during testing.

4.4 Troubleshooting

Rarely do experiments ever happen without some error or unexpected occurrence. Thus, there were a few problems throughout the duration of the experimentation. The first and most common problem was the breaking of strain gauge bolt wires. The wires on the strain gauges are very thin and fragile. Making too fast or strong of movements with them would cause them to break connection. This was noticed either visually or when there was a zero voltage return on Labview. The wires could be repaired using a soldering iron and shrinkwrap.

Another noticeable occurrence throughout the experiment was having oil come out of the pressure relief valve. When the pressurized air was inserted into the test rig, remaining oil from previous experiments that had gotten into the valve would shoot out. This could possibly affect the internal pressure for the next experiments. The best way to mitigate this is to remove the oil very slowly from the test rig and to be very careful when cleaning the inside of the test rig for the next experiment.

Fluctuating internal temperature was also an issue. The hot plate heats the spacers, the spacers heat the test rig, and the test rig heats the oil. So we had to gauge the internal temperature by changing the external applied temperature from the hot plate. When the temperature is fluctuating, the best way to mitigate that was to allow the temperature to equalize for a longer time. Once the temperature remained constant for 30 minutes, then experimentation should begin.

The last noticeable occurrence was when we tested a sprayed rubber coated metal gasket with high heat. After the experiment, the RCM gasket had partially melted onto the flange. To fix the partially melted gasket, place the flange back on the hot plate so the gasket will warm up and be easier to remove. The melting was a result of the oleophobic solution, not the test rig. However, in the event that tested gaskets do melt, re-heating the flange allows the gasket to be removed.

4.5 Regular Maintenance

There was only minimal regular maintenance to be done throughout the course of this experimentation process because the test rig was designed to be as simple as possible. One part of the maintenance was using the RTV Silicone to ensure no air leaks were present so that the test rig would remain pressurized. While the RTV Silicone is not required since NPT threading was used to prevent air leaks, the RTV Silicone can be added as an additional safe guard to prevent air leakage.

The second part of the maintenance plan, and most common, was to remove residual oil that was in the test rig between each experiment. Once a majority of the oil was poured out of the test rig and it was disassembled, the inside of the upper cavity and the bottom flange had to be cleaned every time. Depending on the amount of leakage for the test, sometimes the bolts, spacers, washers, and nuts had to be cleaned off if oil ended up reaching them.

The last part of the routine maintenance was to check the integrity of all the components of the test rig and fix any issues. The only noticeable component that had to be repaired was the o-ring on the pressure transducer. Due to the continuous high heat in addition to repeated loading, the o-ring on the pressure transducer sheared and had to be replaced with the back-up o-ring that was supplied.

5 Results

5.1 Conventional Gasket Testing

Cummins Inc. has provided the team with two types of their standard gaskets commonly used on regions of their engines that experience low pressure failure. The gaskets provided were rubber coated metal gaskets and paper gaskets. The spray-on oleophobic solution that the team obtained is Ultra-Ever Dry and is applied using Ever Dry Sprayers provided from UltraTech International. First, each of the paper and rubber coated metal gaskets were tested by dropping an oil droplet onto the gasket before any oleophobic solution was applied. Seen in Figures 26 and 27, these

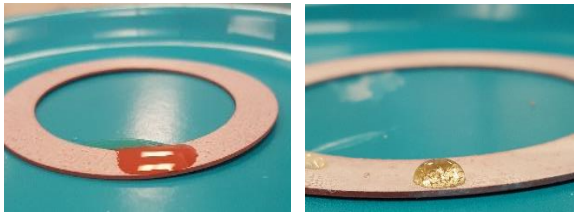


Figure 26. Paper gaskets before and after application of oleophobic solution.

results are provided, as well as the results after they had the Ultra-Ever Dry solution applied to them. The Ultra-Ever Dry must be applied in two stages. The first stage is an adhesive layer and must cure for an hour after being applied. After that hour has

passed, the top layer which contains the oleophobic properties is applied and must dry overnight.

In the before photos, the oil droplets on the paper gasket and rubber coated metal gasket are flat and spread out across their respective surfaces.

Once applied with the oleophobic solution, the paper and rubber coated metal gaskets' contact angles increased significantly, which formed an oil bead in one concise location. This result demonstrated that the spray-on oleophobic solution was successful at transforming the standard gasket materials into an oleophobic gasket.



Figure 27. Rubber coated metal gaskets before and after application of oleophobic solution.

5.2 Non-Conventional Gasket Testing

The team obtained non-conventional gasket material samples from McMaster-Carr. These samples included a high density felt (Figures 28, 29 and 30), and a woven fabric as seen in Figure 31. The team also received samples of an impregnator solution, Stainguard WB-50. The application procedure of the impregnator solution is to coat the material's surface using a brush, or allow the material to soak in the impregnator solution and then dry overnight. First, the felt and woven fabric were tested using no solution. As seen in Figures 28 and 31, the oil soaked completely through both materials and no oil beaded up on the surface. Two samples of the high density fabric were then applied with the impregnator and spray.



Figure 28. High density felt after oil has been poured onto it.

The two images in Figure 29 show the high density fabric applied with an oleophobic impregnator.

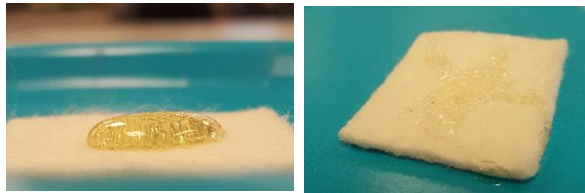


Figure 29. High density felt impregnated with oleophobic solution before and after oil has been poured off of it.

A high contact angle has been generated as no solution penetrated the material. There is a small film of excess oil that can still be seen on the surface after the oil was attempted to be removed by tilting the felt at an inclined angle. This is a drastic improvement from having the oil soak completely through the material. The two images

in Figure 30 show the high density felt applied with the oleophobic spray. The spray created a contact angle even larger than the contact angle generated by the impregnator solution. When the felt sample that had the spray-on solution was inclined to remove the oil, only a few small droplets remained on the surface. The team believed they could reduce the amount of oil left on top of both the impregnator and spray solution by testing and finding the best methods of application for both solutions. These results suggested that the oleophobic solutions are capable of making non-

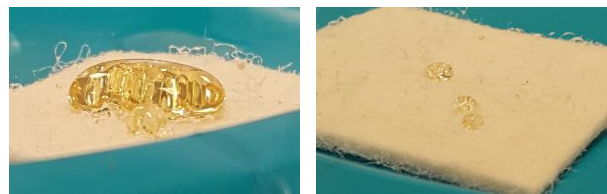


Figure 30. High density felt coated with oleophobic spray before and after oil has been poured off of it.

conventional gasket materials oleophobic. Therefore, the team created gaskets out of the high density felt material and used them in the test rig during gasket testing.

The before and after photos of the woven fabric can be seen in Figure 31. Similar to the high density felt, oil soaked directly through the woven fabric. The photo on the right in Figure 31 shows oil beaded up on the surface. This might be the most

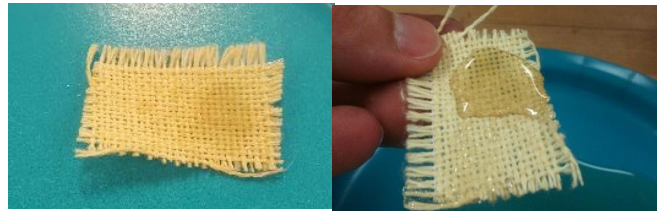


Figure 31. Woven fabric before and after application of impregnator solution.

impressive result from our initial testing because there are holes in the fabric where the oil could not pass through due to the impregnator solution. The impregnator soaked into the material and created a barrier in which the oil could not pass through. This is a good sign for the actual testing in the spring semester because it showed that materials with no oil repellent properties could be effective sealing solutions when applied with the correct chemical substance.

5.3 Final Leak Rate Testing

After performing one trial of each test, the data was collected and analyzed in a couple of different forms. To begin, the results were displayed in the form of a graph which demonstrates the relationship between the amount of oil leaked and time.

These plots can very easily be used to draw conclusions about the effectiveness of each gasket, as it is simple to compare one plot to another since all the gaskets were under the same conditions. The first set of graphs discussed are the room temperature (22°C) tests. Figure 32 is a room temperature test at the lowest

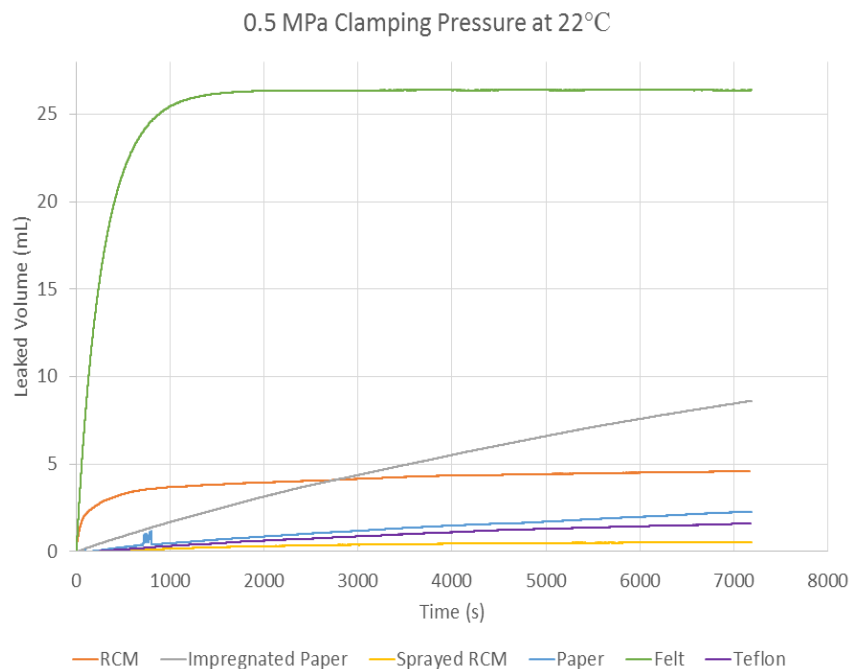


Figure 32. Results of room temperature test at 0.5 MPa

clamping pressure of 0.5 MPa. It is clear that the felt gasket failed completely by leaking over one third of the initial oil amount (75 mL). The felt gasket was a unique gasket designed by the team, which was impregnated and sprayed with oleophobic solutions. Since the solid felt gasket failed, the woven fabric gasket was eliminated from testing. An interesting find in this plot is the fact that the impregnated paper, which theoretically should leak less, leaked more than the normal paper

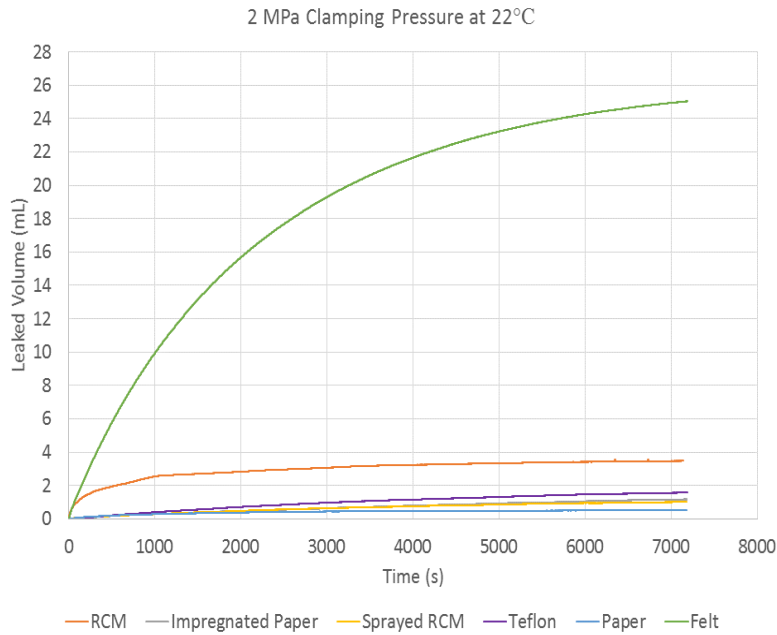


Figure 33. Results of room temperature test at 2 MPa

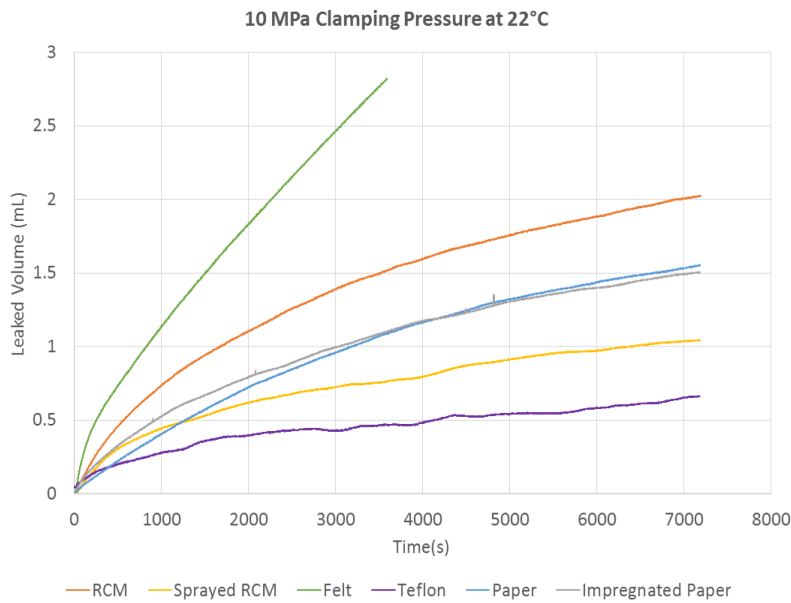


Figure 34. Results of room temperature test at 10 MPa

gasket. On the other hand, the sprayed RCM appeared to leak much less than the normal RCM, suggesting a preliminary positive result of the oleophobic spray solution on RCM gaskets. In relation to the others, Teflon gaskets performed very well at sealing the two flanges without any solution, as they are naturally oleophobic.

Figure 33 and Figure 34 are the other two room temperature tests at 2 MPa and 10 MPa, respectively. In both cases, the felt gasket failed again. The data for the felt gasket at the 10 MPa pressure was purposefully cut short due to its previous failures. The impregnated paper gasket leaked more at 2 MPa clamping pressure and leaked about the same as the normal paper gasket at 10 MPa clamping pressure, proving its failure as a viable

oleophobic gasket. However, the sprayed RCM gaskets continued to prove their success by leaking less than the normal RCM gaskets in both tests. Teflon gaskets performed well, as was expected according to the first room temperature test.

The next three graphs discussed are the hot temperature (120°C) tests. These results are much

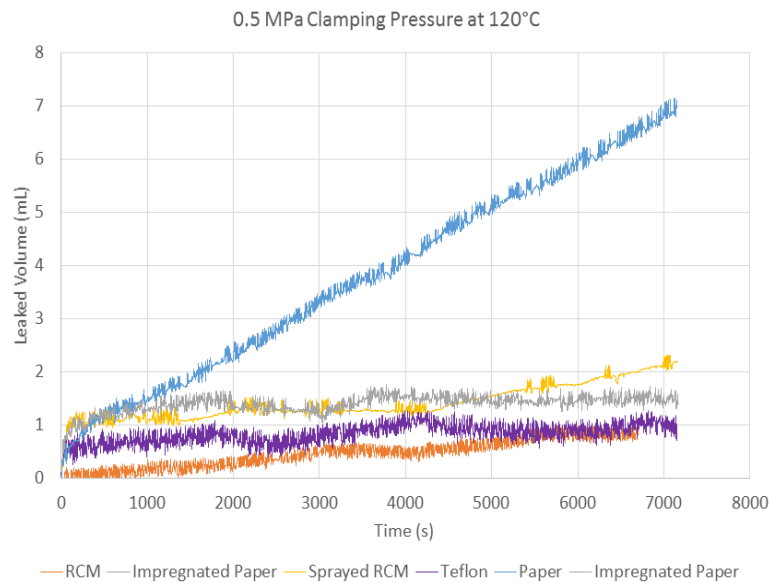


Figure 35. Results of elevated temperature test at 0.5 MPa

noisier than the previous plots as the pressure transducer did not perform as well as expected at high temperatures. It would naturally fluctuate during the test by about 0.1-0.5°C even after slowly coming to a heated temperature over the course of two hours. Thus it is difficult to conclude a change in air pressure during these tests is solely due to an oil leak. This fluctuating temperature violates the modified ideal gas law which assumes the temperature of the oil and air remain constant. In Figure 35, the paper gasket leaked the most out of all the gaskets. This is a case where the impregnated paper gasket performed better than the normal paper gasket. Another unexpected result in this test includes the normal RCM gasket leaking less than the sprayed RCM gasket. This could be indicative of the effectiveness of the oleophobic spray at an elevated temperature or it could be bad data due to the difficulty in running elevated temperature tests. The Teflon gasket continued to be a reliable and

reliable and

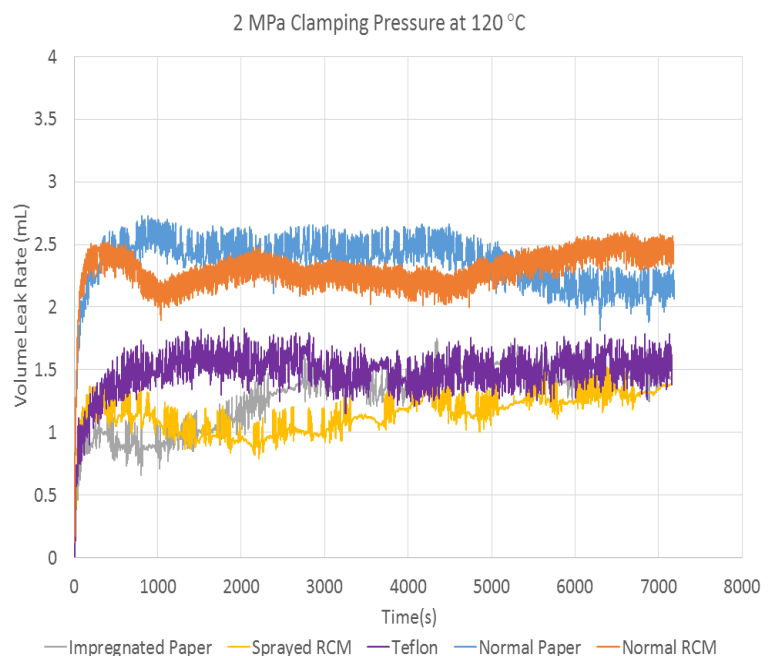


Figure 36. Results of elevated temperature test at 2 MPa

effective gasket. In Figure 36, the impregnated paper gasket leaked less than the normal paper gasket, and the sprayed RCM gasket leaked less than the normal RCM gasket. This test was a success for both oleophobic traditional gaskets. The Teflon gasket's performance is squarely in the middle of the other gaskets, leaking approximately 1.5 mL of oil.

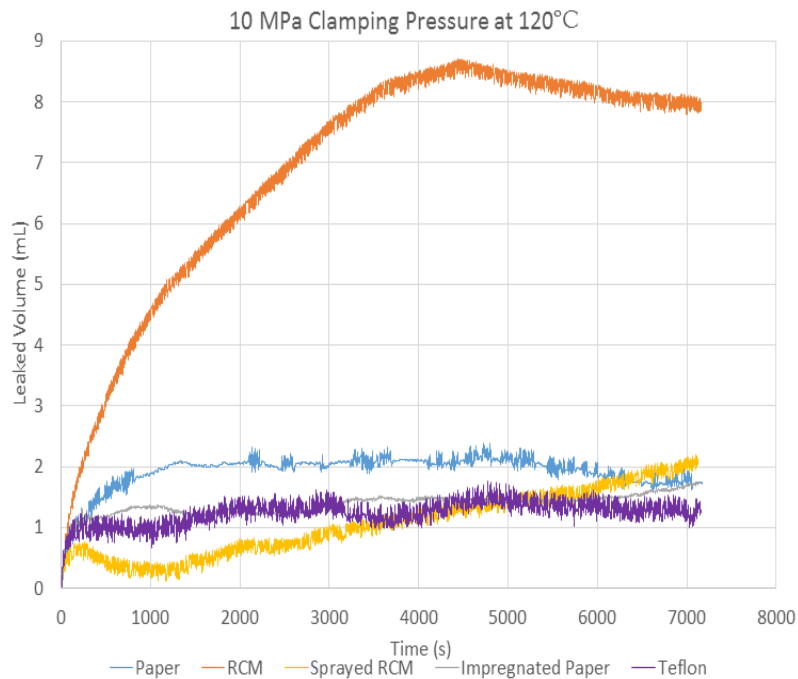


Figure 37. Results of elevated temperature test at 10 MPa

allowing it to conform to the flange shape. Due to their unpredictability, impregnated paper gaskets cannot be considered a viable and acceptable gasket choice. In this test, the sprayed RCM gasket performed much more effectively than the normal RCM gasket. Overall, the sprayed RCM gaskets proved to be a success for almost every single test. The Teflon gasket performance again sits in the middle of the other gaskets' performances, meaning it may not work as well at an elevated temperature. An additional deterrent is the cost of the Teflon gaskets.

Furthermore, just the final values of the total amount of oil leaked in milliliters during the two-hour test was compiled into Table 5. Felt gaskets were not tested under elevated temperature conditions due to their complete failure at room temperature. Ordinarily, as the clamping pressure of the gasket increases, the amount of oil leaked should decrease. However, this was not always the case. This could be due to a couple different reasons: the fluctuating temperature issue discussed above in the case of the elevated temperature tests or potential damage to the flange. The

Finally, Figure 37 indicates the impregnated paper gasket again performed better at sealing than the normal paper gasket. All of the elevated temperature tests proved the success of the impregnated paper gasket, whereas all of the room temperature tests proved the failure of them. The team's theory behind the success at high temperatures is that the heat reduces the stiffness of the impregnated gasket, thus

lower clamping pressure tests were performed first and a few issues arose with removing some of the gaskets after testing had been completed. On a few occasions, the gasket actually adhered so severely that the team had to scrape away at the gasket, meaning the flange sustained a couple scratches and shallow cuts. These could potentially cause the higher clamping pressure tests to leak more oil than the lower temperature test, thus explaining the higher than expected leak rates at the 10 MPa clamping loads. However, this does not mean the testing was unsuccessful at the 10 MPa clamping load. Since all the gaskets were exposed to the same damaged flange, the effectiveness of the gaskets were still tested under consistent conditions throughout the clamping load. Moreover, some of the values in Table 5 appear to be very apparent outliers and could be tested again, if time permitted, to ensure accurate and repeatable results.

Table 5. Final Leakage Over 2 Hours

Material	Temperature (°C)	Leakage (mL)		
		0.5MPa	2MPa	10MPa
Paper	22	2.28	0.48	1.55
	120	7.12	2.03	1.73
Impregnated Paper	22	8.62	1.18	1.50
	120	1.56	1.46	1.74
RCM	22	4.62	3.48	2.02
	120	0.93	2.31	7.81
Sprayed RCM	22	0.50	1.00	1.05
	120	2.16	1.39	2.05
Teflon	22	1.64	1.58	0.66
	120	1.07	1.45	1.22
Felt	22	26.35	25.03	2.83 (1 hr)

5.4 Post-Test Gasket State

Not only is the quantitative data important, but the qualitative data also provided clues to how well these gaskets would perform in an actual engine. Most of the room temperature tests did not damage the integrity of the gaskets, whether they had an oleophobic solution on them or not. They

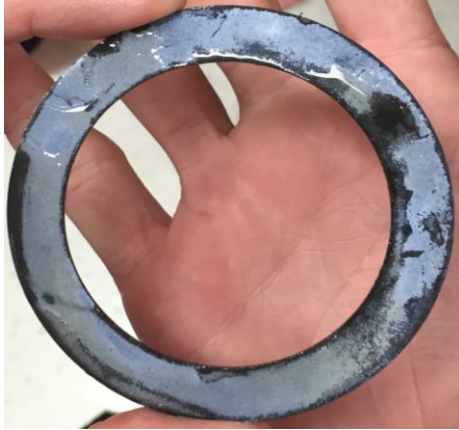


Figure 38. Oleophobic spray removal due to abrasion

were usually easy to remove; however, it is important to note that the oleophobic spray solution did not stay in place if any sort of abrasion was encountered. Just placing the two flanges together and putting the bolts through the holes could be enough to start rubbing the solution off of the RCM gaskets. In Figure 38, it is clear that after performing the test, the white spray film is removed in random areas of the gasket. This is a longevity issue that should be investigated as a next step. Additionally, the team ran into some issues

with removing gaskets after an elevated temperature test was performed. The oleophobic solutions appear to become sticky and adhesive when heated up. Even though these solutions were rated for high temperatures, the compression of the gaskets in addition to the heat became a major issue when attempting to remove them. In Figure 39, an impregnated paper gasket was nearly permanently sealed onto the bottom flange. The team had to resort to means of scraping away at it layer by layer, which ended up damaging the surface roughness of the bottom flange. It was difficult to tell how well the impregnated solution remained within the paper gasket after testing, as the solution altered the entire appearance of the paper

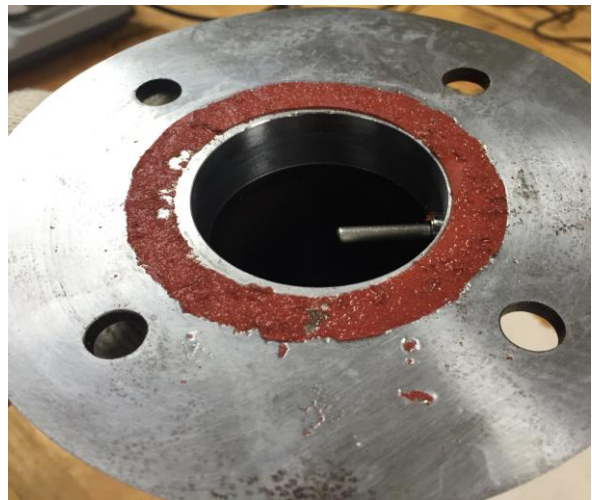


Figure 39. Impregnated paper gasket stuck to top flange

gasket which made it impossible to see a difference. At times, the sprayed RCM gaskets were difficult to remove at elevated temperature tests; however, the process of detaching them was much easier. If a sprayed RCM gasket became stuck, the flange was just placed back on the hot plate which immediately loosened up the gasket.

6 Project Management

The first major objective of the project that was completed was to determine what options are currently on market to make gaskets oleophobic. In order to determine which options were available, the team researched the market using the internet, and by contacting suppliers to get professional feedback. Once current market items were determined, they were evaluated by the team for practicality, performance, and environmental applications. The team then selected the suitable method(s) to make an oleophobic gasket and procured these “on market” products. Using these products, the team created the oleophobic gaskets, which were leak rate tested.

The other major objective of the project was to design and build a test rig which was capable of measuring the leak rate of gaskets. The team held discussions with the sponsor to determine if there are any company standards for test purposes, such as leak path length, standard diameters, pressure ranges, and availability of current gaskets used by the sponsor. Using this information, the required size of the system was determined and the test rig was designed. The physical designing of the test rig utilized CAD software for visual purposes as well as part drawings, and any mathematical calculations were done using Mathcad in order to ensure accuracy.

Testing was performed on the oleophobic gaskets using the test rig built by the team. The leak rate test results for the oleophobic gaskets were compared to standard gaskets, which allowed the team to draw conclusions on the effectiveness of an oleophobic gasket. The tests were performed using different clamping pressures and temperatures within the test rig, which provided more data to compare with standard gaskets.

In order to prevent exceeding the \$2,000 budget, price was weighed in every decision to make sure the team made the best decisions between performance and costs. Items which were used in the building of the test rig were quoted to ensure the lowest possible price was obtained, thus using the team’s budget efficiently. In order to keep the project on schedule, a Gantt chart was created (Appendix F). The Gantt chart was continuously updated by the team as the project advanced, allowing for proper planning if the project deviated from the original schedule.

6.1 Resource Allocation

The background research phase was completed as an entire team, where individual team members were assigned small topics to research and share with the team. Heather Davidson and Norris McMahon researched the science behind oleophobicity, while Daniel Elliott researched common causes for gasket failures. Erik Spilling researched into what types of oleophobic spray coatings are currently available on market, and David Dawson researched if a product could be used to impregnate a material to create oleophobic characteristics for the material. The team also investigated temperature and pressure measurement devices, as well as bolt load and its effect on clamping force. The entire team contributed to the background research phase of the project.

The senior design team decided to divide into sub-teams so that the necessary effort could be applied to both the oleophobic gasket aspect of the project, as well as the design and fabrication of the test rig, simultaneously.

- Gasket Team:
 - This sub team consists of Norris McMahon, David Dawson, and Aruoture Egoh. The gasket team was responsible for continued research into what process and products can be used to create an oleophobic gasket. Once the gasket team identified the available oleophobic solutions on market, they were responsible for selecting the solutions for the team to purchase and test. The gasket team was responsible for creating the oleophobic gaskets. They were also responsible for providing the gasket needs to Cummins Inc., so that Cummins Inc. can provide the necessary gaskets for testing.
- Test Rig Design Team:
 - The test rig design team consists of Erik Spilling, Heather Davidson, and Daniel Elliott. The test rig team was responsible for generating concepts for the test rig, performing the calculations to determine the design details for the test rig (such as wall thickness, bolt loads, etc.), creating the CAD models and drawings, material selection, and creating a list of raw material quantities which would need to be purchased. The test rig design team worked as a group to complete all of the aforementioned tasks, since the team believes a group effort yields the best design.

The raw materials for the test rig were machined by the COE machine shop in January, but the assembly of the test rig was completed by the entire team. The sensors were set up and calibrated at AME Center by David Dawson with help from John Strike.

The testing process was performed by the entire team as well. Since a large number of tests were performed, the team completed testing in smaller groups. The data was compiled and processed by Erik Spilling, whereas the set up and cleaning of the test rig was done by other team members. These initial tests were done together to create a step by step testing process that the entire group understood. Then, testing was broken into smaller groups so that the entire team did not need to be present for every single test run. The smaller groups were at least three people. This allowed someone to stabilize the test rig while someone else tightened the bolts to the correct strain. While, the third person handled the computer and data conversion. This allowed the test set up and clean up to go quickly and smoothly.

The team web page was designed by Heather Davidson. The team utilized the advice and resources provided by Ryan Kopinsky in order to best design the team web page.

6.2 Schedule/Deliverables

A schedule of the team's project plan for the entire year can be found in a Gantt chart (Appendix F). This Gantt chart encompasses critical tasks were identified by their duration in the time schedule. For example, part acquisition was a very critical task as it was expected to take the longest, and the project could not precede without the completion of it.

6.3 Risk Assessment and Reliability

After analyzing the risks that could occur during this project, a new set of testing procedures was created focusing on safety. When creating oleophobic gaskets, the team wore gloves, long-sleeved shirts, long pants, closed toe shoes, eye protection, and masks at all times. The test rig was built by the FAMU/FSU machine shop safely and efficiently. When conducting the leak tests, the test rig was placed into a plastic container. Anyone handling or monitoring a short distance away from the test rig wore heavy clothing which didn't reveal skin, closed toe shoes, a mask with eye and face protection, and heavy gloves.

When examining the possible reliability issues for this project, it was found that there are two potential areas of concern: data collection and the test rig structure. Both of these issues have been noted, and the correct procedures have been created to make sure that neither will be a problem during testing. To make sure the data is collected correctly and identically each time, the team used strain gauges to record the load on the bolts. The team also consulted Dr. Rajan Kumar on which pressure transducer and RTD probe to fit the constraints given to us by our sponsor.

The other goal was to create a test rig which would be able to handle the temperature, pressure, and bolt load. To make sure that there would be no problem with failures in the test rig, the minimum thickness for the metal was calculated, and A36 steel was chosen. This material with a thickness of 0.25 inch will allow us to operate the test rig with no concern of failure.

6.4 Procurement

Parts ordering has been completed. David Dawson was responsible for maintaining the team budget, and thus was also responsible for the parts ordering. The sub teams provided David with a list of the desired raw materials, and David checked to make sure that the parts or materials could be purchased within the team's budget, and made the purchases.

The budget given for this project was \$2,000 through the Aero Propulsion, Mechatronics and Energy Center. This budget was used to acquire all of the materials that were needed for application and testing for determining the effectiveness of oleophobic gaskets. The values shown in Table 6 are the maximum estimated values for each item needed and were calculated by researching into potential products. Even after calculating for the maximum prices, the total cost only came out to \$1,850, which left a remainder of \$150 in case of an emergency.

Table 6. Budget

Item	Maximum Estimated Amount
Test Rig Raw Materials	\$150.00
Test Rig Sensors	\$1,000.00
Gasket Materials	\$150.00
Oleophobic Solutions	\$300.00
Oleophobic Material	\$200.00
Oils Used for Testing	\$50.00
Total	\$1,850.00

In Table 7, all of the purchased items are shown with quantity and price. It is also organized by which category that item fits into within the budget. As it can be seen, the team is under the estimated cost for each of the budget sub groups.

Table 7. Purchased Items

Budget Category	Item	Quantity	Cost
Test Rig Material	M8 Class 10.9 Cap Screw	1(Pack of 25)	\$7.91
Test Rig Material	M8 General Purpose Steel Washer	1 (Pack of 100)	\$6.09
Test Rig Material	M8 Class 10 Steel Nut	1 (Pack of 100)	\$10.48
Test Rig Material	M10 General Purpose zinc plated steel washer	1 (Pack of 100)	\$4.36
Test Rig Material	M10 Class 8 Zinc Plated Steel Hex Nut	1 (Pack of 100)	\$10.48
Test Rig Material	Zinc-Plated Steel Unthreaded Spacer	4	\$55.32
Test Rig Material	M10x1.5 70mm long class 8.8 cap screw	1 (Pack of 10)	\$8.58
Test Rig Material	Pressure Relief Valve	1	\$48.00
Test Rig Material	Compact High-Pressure Brass Ball Valve	1	\$11.34
Test Rig Material	Brass Air Fill Valve Straight	1	\$4.40
Test Rig Material	1ft x 1ft x ¼ in Thick A36 Steel Plate	1	\$15.41
Test Rig Material	1ftLong 2-1/2 OD x 2 ID Round Steel Tube	1	\$36.04
Test Rig Material	Total		\$218.41
Test Rig Sensors	Short RTD Probe	1	\$66.00
Test Rig Sensors	Compression Fitting	1	\$20.00
Test Rig Sensor	Pressure Transducer	1	\$618.00
Test Rig Sensor	Total		\$704.00
Oleophobic Material	Teflon Gaskets	20	\$170.00
Oleophobic Material	Oleophobic Impregnator	1(Gallon)	\$80.00
Oleophobic Material	Total		\$250.00
Oleophobic Application	Spray Gun	1	\$19.99
Oil Used for Testing	T Triple Protection CJ-4 15W-40 Motor Oil	1 (Gallon)	\$13.44
Testing Supplies	Torque Wrench	1	\$39.99
Purchased	Total		\$1,245.83

6.5 Communications

The senior design team made an effort from the start of the project to minimize any communication problems through several means. To eliminate any communication issues within the team, a group chat was made which was connected to everyone's phone. With this group chat, any inter-team questions could be asked and answered in the quickest time possible. The senior design team also held weekly meetings with the Cummins Inc. liaison, Parker Harwood, where the team provided a powerpoint presentation to him containing information on tasks that had been completed and the necessary next steps. This allowed the senior design team to make any changes that the sponsor wanted immediately, which saved time for the senior design team. If the weekly meetings weren't held, there would have been several cases of the team investing a week or two on a task that the sponsor no longer required. To stay in communication with our advisor, the senior design team would typically communicate via email, or set up appointments to meet in his office for advice. As a result of these communication measures taken, the team never had any major communications problems. Inter-team questions were always resolved quickly, and the sponsor was always in the loop regarding the progress of the project.

7 Environmental, Safety, and Ethics

The assigned project was more of research oriented and not actually building a mass production item. Thus, environmental consideration was not focused on the production process, but rather the environmental impacts of our testing process. For example, the testing of the gasket was completed using oil. To ensure that the used oil did not harm the environment, it was recycled at a recycling center after testing was completed. Also, any leftover chemical solutions were disposed at a proper disposal site.

Safety was an influential factor during the design of the test rig and the testing of the gaskets. When designing the test rig, the stability and rigidity of the fixture was taken into consideration, not only for performance reasons, but also for the safety of the team. The test rig was built using A36 steel with uniform thickness of 0.25 inch to provide a safety factor in the design. This was to prevent any form of sudden failure during testing. When creating the various oleophobic gaskets, team members wore personal protective equipment (gloves, shoes, eye goggles, and masks) at all times. When conducting the leak tests, the test rig was placed in a plastic container. In addition, FMEA was carried out on the selected design concept of the test rig in order to locate possible failures modes in the final design, and how to best prevent the failure.

Ethics was also considered when designing the test rig. The team built the test rig based on an original design and the analysis done by the team. The design was developed solely by the team, thus using only the team's intellectual property. The team followed engineering ethics during the project, ensuring that safety was a major focus, and that all designs generated were the intellectual property of the team.

8 Conclusion

The main purpose of this project was to determine if the development and implementation of oleophobic gaskets would be useful in practical applications. The team was saddled with responsibility of designing and building a test rig which could test standard and non standard gasket materials with and without oleophobic solutions. This was achieved by researching oleophobic solutions and selecting the best ones to apply to gaskets. The team carried out preliminary testing on the conventional and non-conventional gaskets to ensure the feasibility of the final testing. These oleophobic gaskets were compared to baseline model tests using engine oil at a constant pressure of 2.5 psi. The test rig was designed to handle an internal pressure of 2.5 psi, a temperature range between 22 and 120°C, and also clamping pressures between 0.5 and 10 MPa. The results from this experiment provided a better understanding if oleophobic gaskets were effective in terms of practicality, performance, and applicability.

The computation of the leak rate after performing the various tests proved that the high density felt was not a viable gasket material and the impregnated paper was not feasible at room temperature but performed better at elevated temperature. The sprayed RCM gasket material proved viable as it produced a lower leak rate than the standard RCM gasket, suggesting a positive result of a sprayed oleophobic solution on a gasket material. The Teflon gaskets, which are naturally oleophobic, demonstrated a reduced leak rate but they are relatively expensive.

Future recommendations to continue this project for coming years would mostly be in the selection and testing of more non-conventional gasket materials. Another future recommendation would be to research more oleophobic solutions as well as an enhanced quality control after coating the gaskets with oleophobic solutions.

References

- [1] "Gasket Materials and Selection." Gasket Materials and Selection. Web. 25 Sept. 2015.
- [2] "Spigen." Galaxy S4 Screen Protector Glass Nano Slim Premium Tempered Glass-Oleophobic Coating. Web. 25 Sept. 2015.
- [3] "Surface Energy and Wetting." Surface Energy and Wetting. Web. 25 Sept. 2015.
- [4] "Fabrication of Superhydrophobic and Oleophobic Sol-gel Nanocomposite Coating." Fabrication of Superhydrophobic and Oleophobic Sol-gel Nanocomposite Coating. Web. 25 Sept. 2015.
- [5] "Torque." Engineers Edge. Web. 28 Oct. 2015
- [6] "Tightening Torque." *Field Guide to Optomechanical Design and Analysis* (2012): Web.
- [7] "Short RTD Probe." *Short RTD Probe*. Web. 30 Oct. 2015.
- [8] "PX409 Series High Accuracy Pressure Transducers Now with 0.05% Accuracy and 0.03% Linearity Options." *High Accuracy Pressure Transducers*. Web. 30 Oct. 2015.
- [9] "Valve, Air Tank Filler." *Cdi Control Devices TV12*. Web. 30 Oct. 2015.
- [10] "Ball Valve" *McMaster-Carr*. Web. 30 Oct. 2015.
- [11] "RVA-05 Stainless Steel Economy Atmospheric Discharge Relief Valve." Stainless Steel Economy Atmospheric Discharge Relief Valve. Web. 08 Apr. 2016.
- [12] "Leakage Test Rig." Gasket Test Rig for Leakage Testing. Web. 01 Apr. 2016.

Appendix A

$$\sigma_{\text{clamping}} := 10\text{MPa}$$

$$\sigma_{\text{vessel}} := 2.5\text{psi} = 0.017\text{MPa}$$

$$\text{ID} := 50\text{mm}$$

$$\text{OD} := 150\text{mm}$$

$$D_{\text{gasket}} := 75\text{mm}$$

$$A_{\text{vessel}} := \pi \cdot \left(\frac{\text{ID}}{2}\right)^2 = 2.376 \times 10^{-3} \cdot \text{m}^2$$

A36 Steel

$$\nu_{\text{steel}} := 0.26$$

$$A_{\text{flange}} := \pi \cdot \left[\left(\frac{\text{OD}}{2}\right)^2 - \left(\frac{\text{ID}}{2}\right)^2 \right] = 0.015 \text{m}^2$$

$$\sigma_{\text{failuresteel}} := 322.5\text{MPa}$$

$$\text{density}_{\text{steel}} := 7.85 \cdot 10^6 \frac{\text{gm}}{\text{m}^3}$$

$$P_{\text{atm}} := 14.696\text{psi} = 0.101\text{MPa}$$

$$\Delta P_{\text{vessel}} := P_{\text{atm}} - \sigma_{\text{vessel}} = 0.084\text{MPa}$$

$$\Delta P_{\text{flange}} := \sigma_{\text{clamping}} - (P_{\text{atm}}) = 9.899\text{MPa}$$

A36 Steel

$$m_{\text{vesselsteel}} := \left[\frac{3 \cdot (1 + \nu_{\text{steel}}) \cdot \Delta P_{\text{vessel}} \cdot \left(\frac{\text{ID}}{2}\right)^6 \cdot \pi^2}{8} \right]^{\frac{1}{2}} \cdot \left[\frac{\text{density}_{\text{steel}}}{\left(\sigma_{\text{failuresteel}}\right)^{\frac{1}{2}}} \right] = 5.693 \times 10^{-3} \text{ kg}$$

$$m_{\text{vesselsteel}} = 5.693 \times 10^{-3} \text{ kg}$$

$$t_{\text{vesselsteel}} := \frac{m_{\text{vesselsteel}}}{\text{density}_{\text{steel}} \cdot A_{\text{vessel}}}$$

$$t_{\text{vesselsteel}} = 0.305 \cdot \text{mm}$$

$$\sigma_{\text{failuresteel}} = \frac{3 \cdot (3 + \nu_{\text{steel}}) \cdot \Delta P_{\text{flange}}}{8 \cdot t_{\text{flange}}^2}$$

$$m_{\text{flangesteel}} = \text{density}_{\text{steel}} \cdot A_{\text{flange}} \cdot t_{\text{flangesteel}}$$

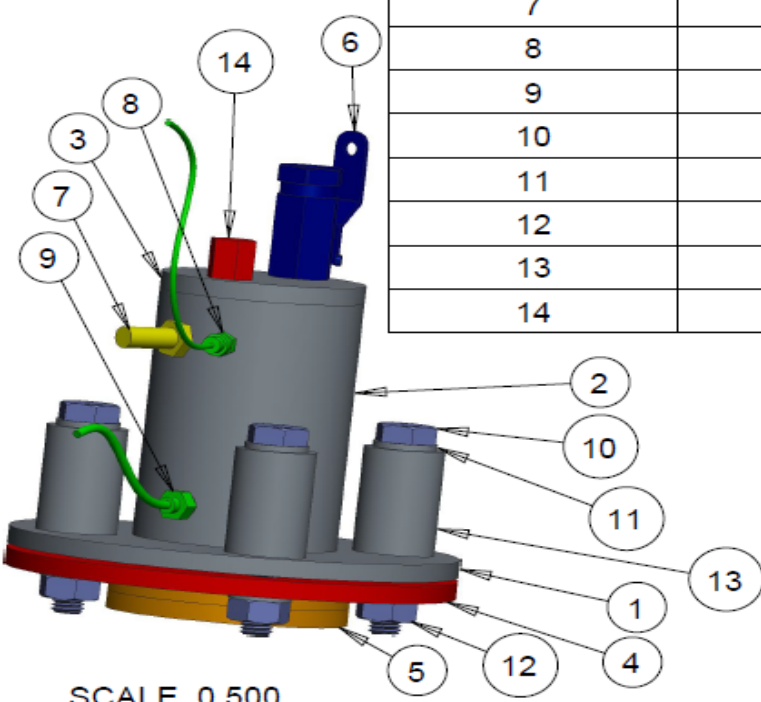
$$m_{\text{flangesteel}} := \left[\frac{3 \cdot (3 + \nu_{\text{steel}}) \cdot \Delta P_{\text{flange}} \cdot \left[\left(\frac{D_{\text{gasket}}}{2}\right)^2 - \left(\frac{\text{ID}}{2}\right)^2 \right] \cdot \pi^2}{8} \right]^{\frac{1}{2}} \cdot \left[\frac{\text{density}_{\text{steel}}}{\left(\sigma_{\text{failuresteel}}\right)^{\frac{1}{2}}} \right] \cdot \left[\left(\frac{\text{OD}}{2}\right)^2 - \left(\frac{\text{ID}}{2}\right)^2 \right] = 0.593 \text{ kg}$$

$$m_{\text{flangesteel}} = 0.593 \text{ kg}$$

$$t_{\text{flangesteel}} := \frac{m_{\text{flangesteel}}}{\text{density}_{\text{steel}} \cdot A_{\text{flange}}}$$

$$t_{\text{flangesteel}} = 4.939 \cdot \text{mm}$$

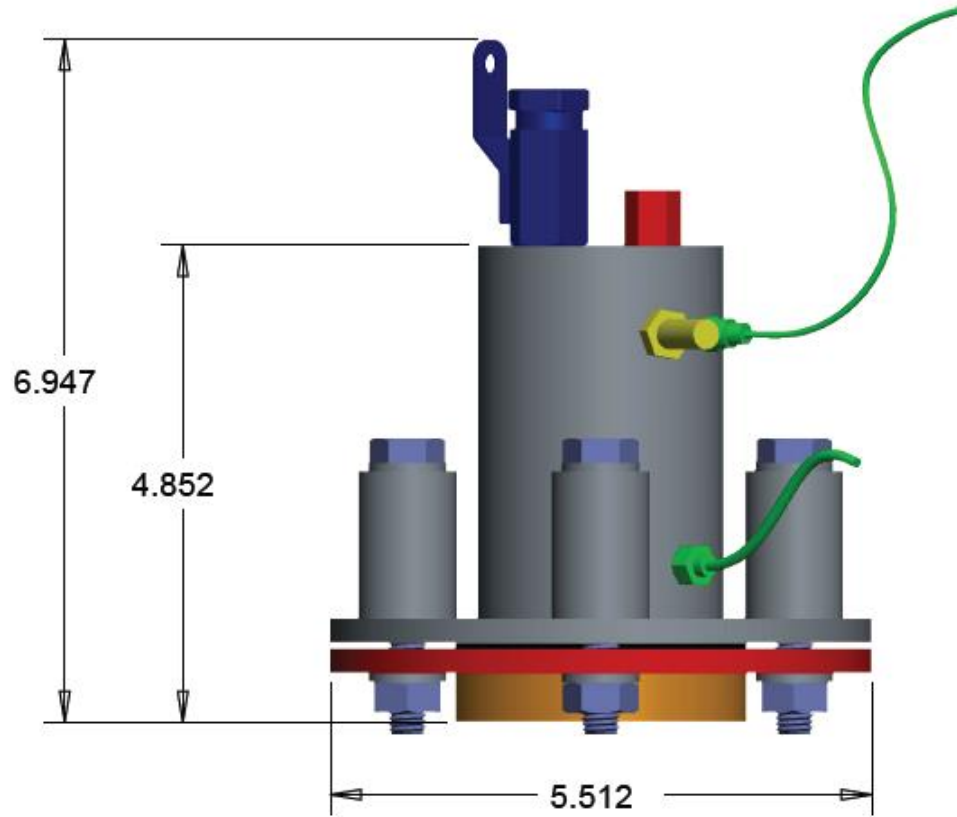
Appendix B



Part Number	Part Name	Quantity	Material
1	Top Flange	1	A36 Steel
2	Top Tube	1	A36 Steel
3	Top Cap	1	A36 Steel
4	Bottom Flange	1	A36 Steel
5	Spacer	2	A36 Steel
6	Oil Valve	1	Bronze
7	Air Valve	1	Bronze
8	Pressure Transducer	1	Steel
9	RTD Sensor	1	Steel
10	M10x1.5 70mm Bolt	4	Steel
11	M10 Washer	8	Steel
12	M10x1.5 Nut	4	Steel
13	Bolt Spacer	4	Steel
14	Pressure Relief Valve	1	Brass

Project Name		Part Name	
Team 1		BOM	
Drawn By		Part Number	
Erik Spilling		NA	
Date	Revision	Sheet Number	
11/13/2015	0	1	

SCALE 0.500



SCALE 0.600

Project Name		Part Name	
Team 1		Assembly	
Drawn By		Part Number	
Erik Spilling		NA	
Date	Revision	Sheet Number	
11/13/2015	0	2	

Part Number	Part Name	Quantity	Material
1	Top Flange	1	A36 Steel
2	Top Tube	1	A36 Steel
3	Top Cap	1	A36 Steel

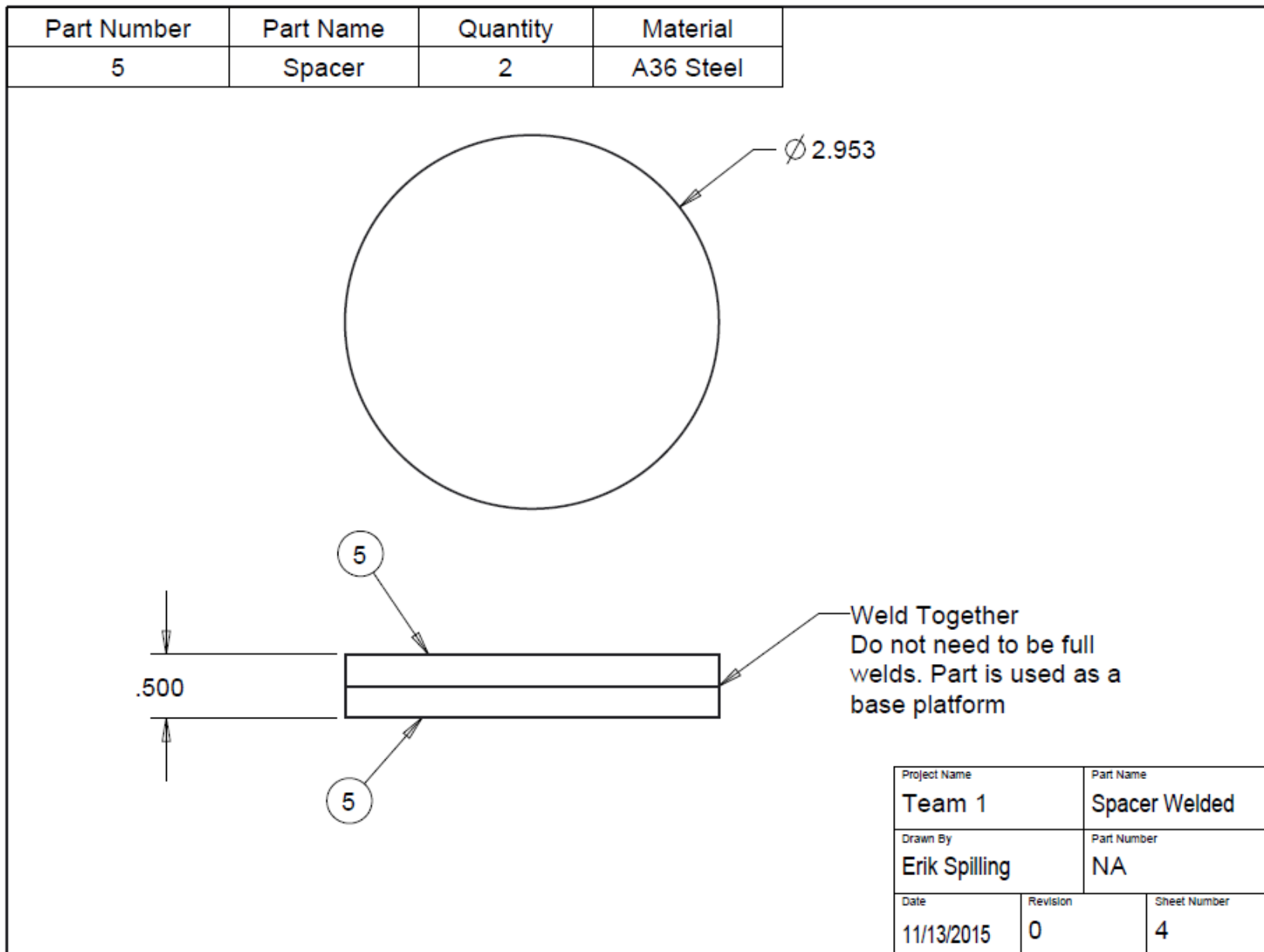
Orient the top cap so that one of the tapped holes in the cap is in line with the lower tapped hole on the tube

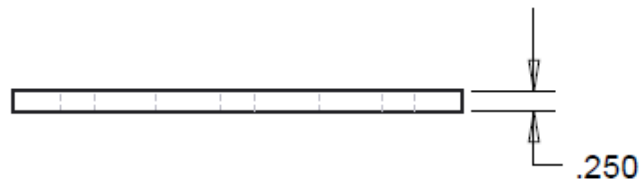
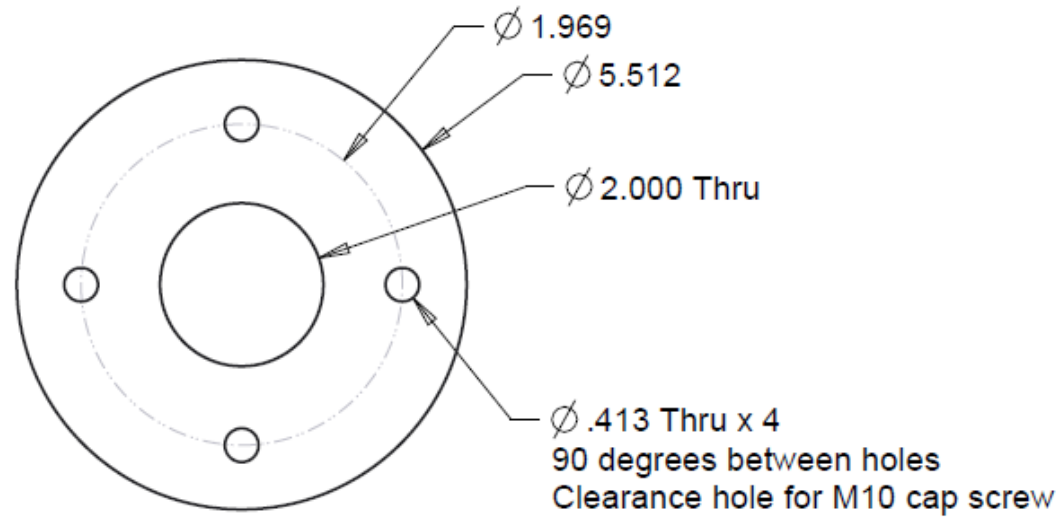
Weld all the way around
Must be air/water tight

Weld all the way around
Must be air/water tight

Project Name		Part Name	
Team 1		Top Assembly	
Drawn By		Part Number	
Erik Spilling		NA	
Date	Revision	Sheet Number	
11/13/2015	0	3	

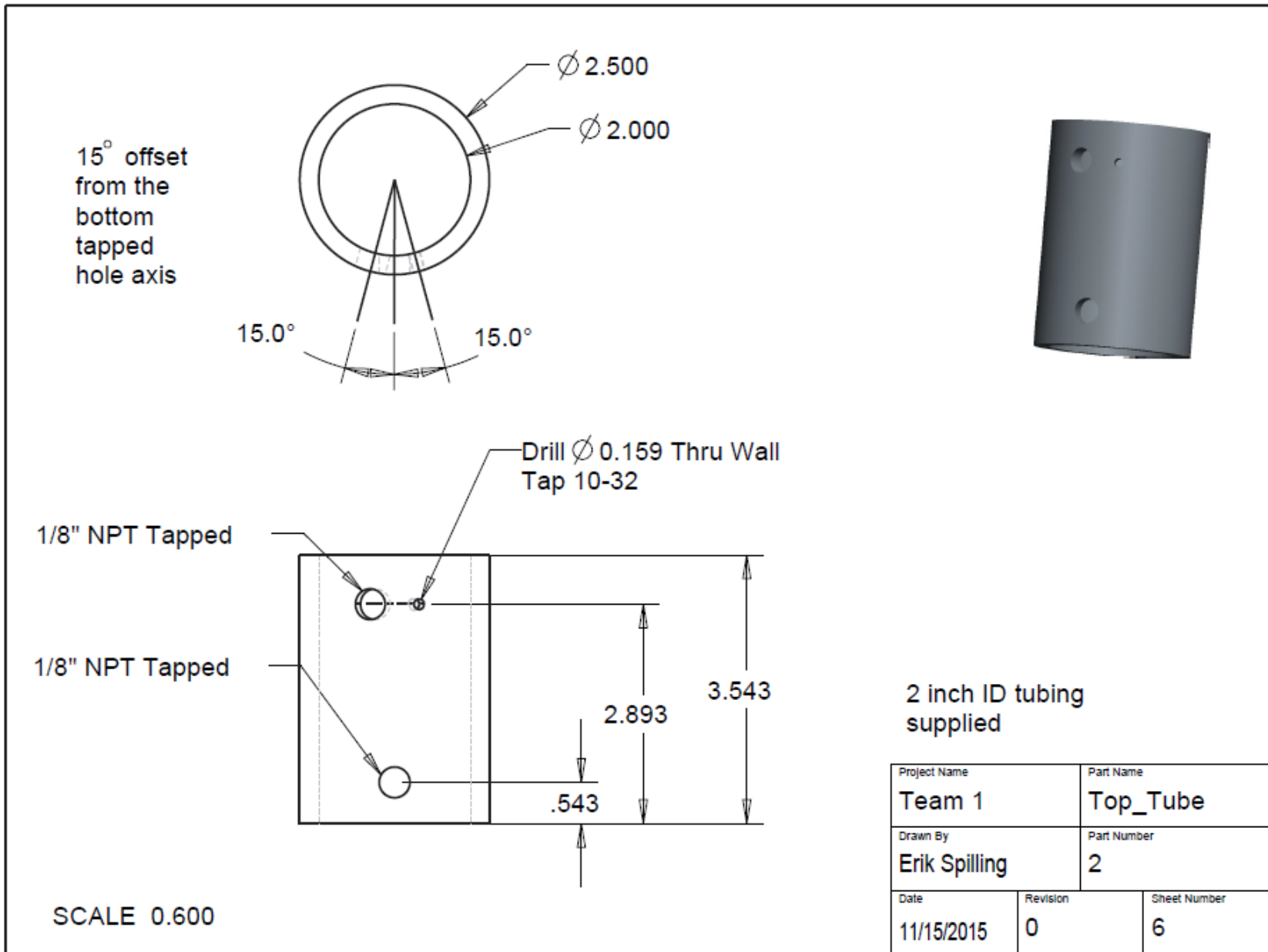
SCALE 0.500

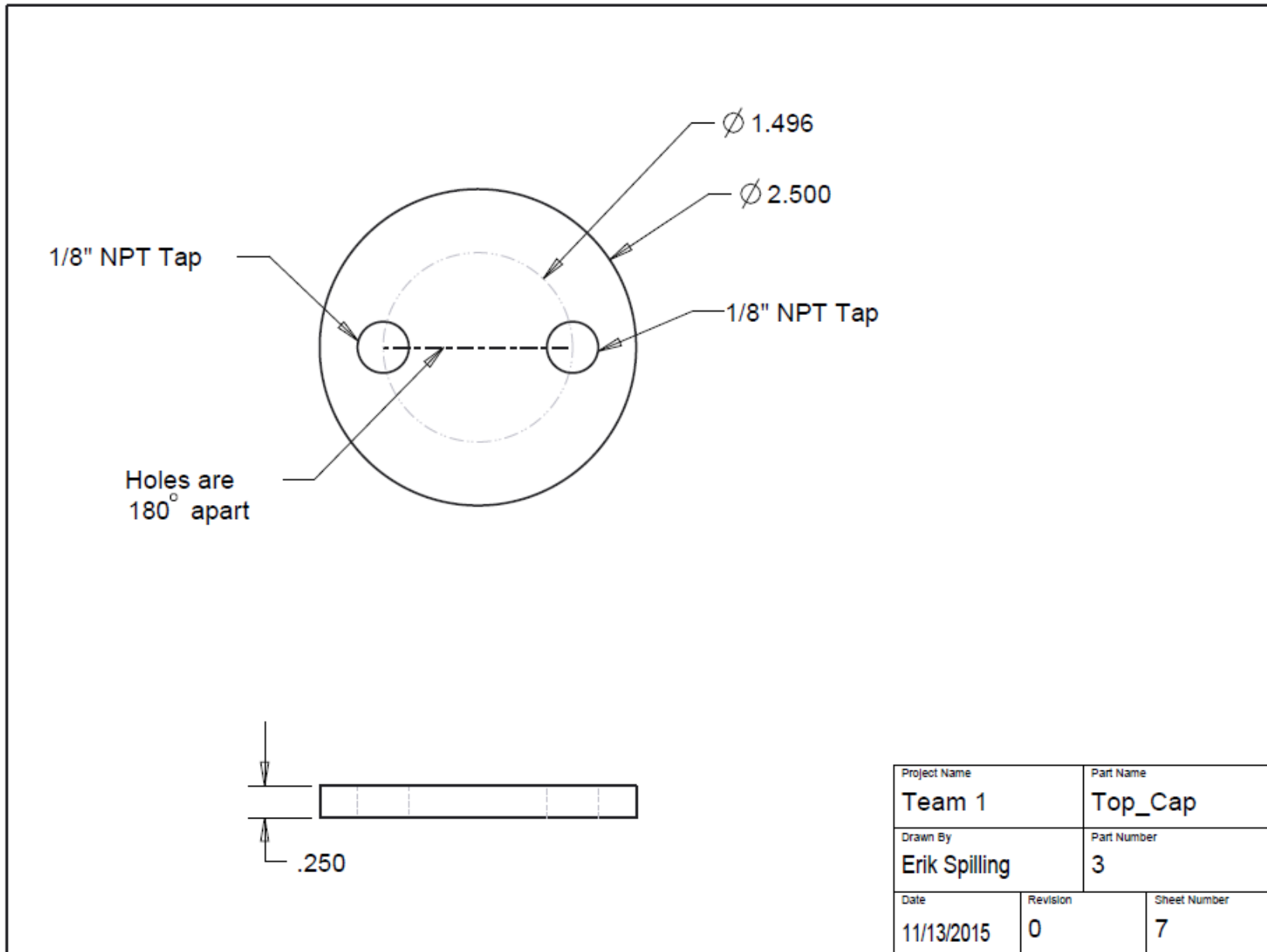


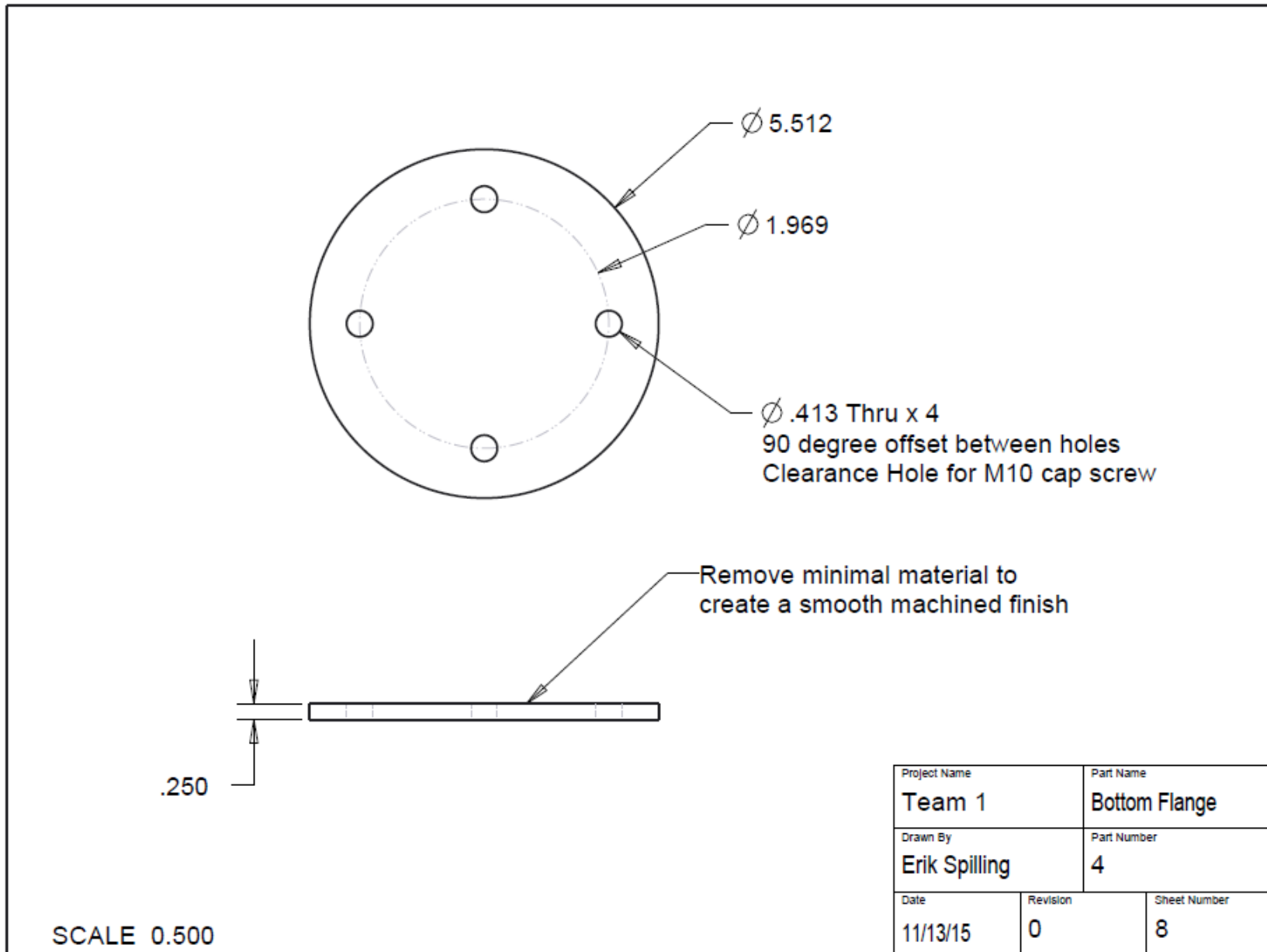


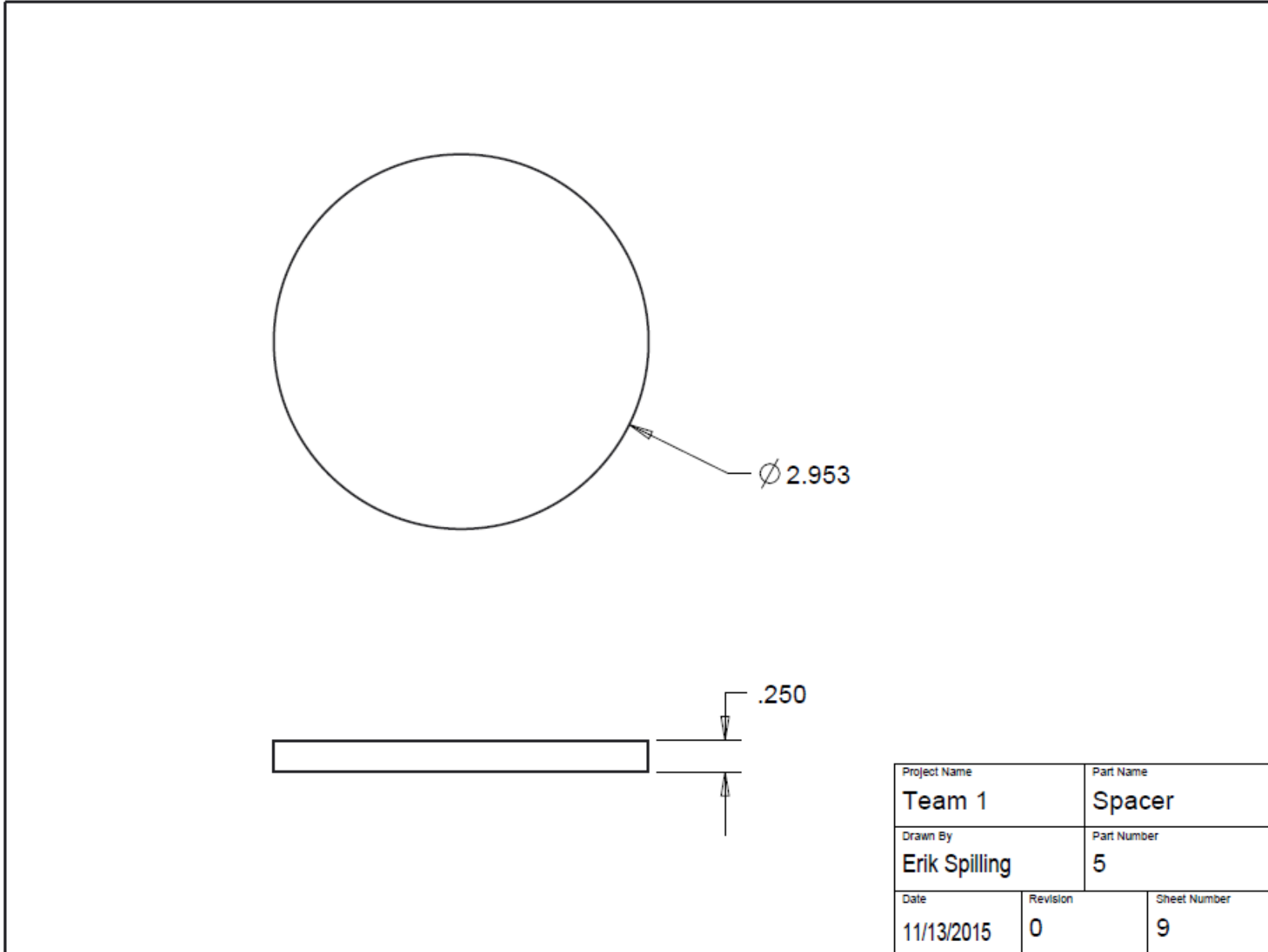
SCALE 0.500

Project Name		Part Name	
Team 1		Top Flange	
Drawn By		Part Number	
Erik Spilling		1	
Date	Revision	Sheet Number	
11/13/2015	0	5	









Appendix C

Bolt Torque Calculations

The nominal diameter of the bolt

$$D_{\text{nom}} := 8\text{mm}$$

Number of Bolts

$$NB := 4$$

Input Gasket Parameters:

$$D_{\text{inner}} := 55\text{mm}$$

$$D_{\text{outer}} := 75\text{mm}$$

Sealing pressure on Gasket:

$$P_{\text{max}} := 10\text{MPa}$$

Determine gasket area:

$$A_{\text{outer}} := \frac{\pi \cdot D_{\text{outer}}^2}{4} = 4.418 \times 10^{-3} \text{ m}^2$$

$$A_{\text{inner}} := \frac{\pi \cdot D_{\text{inner}}^2}{4} = 2.376 \times 10^{-3} \text{ m}^2$$

$$A_{\text{gasket}} := A_{\text{outer}} - A_{\text{inner}} = 2.042 \times 10^{-3} \text{ m}^2$$

The total force required to induce the desired pressure;

$$F_{\text{tot}} := P_{\text{max}} \cdot A_{\text{gasket}}$$

$$F_{\text{tot}} = 20.42 \cdot \text{kN}$$

Force required by each bolt for 4 bolt design

$$F_{\text{ind}} := \frac{F_{\text{tot}}}{NB}$$

$$F_{\text{ind}} = 5.105 \cdot \text{kN} \quad \text{force per bolt}$$

The torque coefficient K

$$K := 0.2 \quad \text{http://euler9.tripod.com/fasteners/preload.html}$$

Finding the required torque

$$T_{\text{needed}} := F_{\text{ind}} \cdot K \cdot D_{\text{nom}}$$

$$T_{\text{needed}} = 8.168 \cdot \text{N} \cdot \text{m}$$

Appendix D

Determining the Effectiveness of Oleophobic Gaskets

Design for Manufacturing, Reliability, and Economics



Team Number: 1

Submission Date: 04-01-2016

Submitted To: Dr. Gupta, Dr. Shih

Faculty Advisor: Dr. Oates

Authors: Heather Davidson (hld12), David Dawson (dpd13), Aruoture Egoh (aje15f), Daniel Elliott (dse13), Norris McMahon (nfm11b), Erik Spilling (eds11b)

Table of Contents

Table of Figures	i
Table of Tables	ii
ACKNOWLEDGEMENTS	iii
ABSTRACT	iv
1. Introduction	1
2. Design for Manufacturing	2
2.1 Sub-Assembly Fabrication.....	2
2.2 Assembly of Test Rig.....	3
2.3 Manufacturing of Oleophobic Gaskets	4
2.4 Assembly Time	5
2.5 Design Optimization	5
3. Design for Reliability	7
4. Design for Economics	9
5. Conclusion	10
References	11
Appendix A	12
Appendix B	21
Biography	22

Table of Figures

Figure 1. Exploded view of the Top Assembly.	2
Figure 2. Exploded view of the final assembly of the test rig	3
Figure 3. FEA of the Pressure Distribution (10 MPa)	7
Figure 4. Pie chart showing distribution of funds.....	9

Table of Tables

Table 1. Assembly Time for Test Rig.....	5
Table 2. FMEA Table	7

ACKNOWLEDGEMENTS

Thank you to Parker Harwood, our Cummins Inc. liaison, for providing guidance and support throughout the project as well as gasket materials for the team to use for baseline testing. Additionally, the team would like to thank Dr. Gupta and Dr. Shih for their oversight of the project and providing instruction to the team. Finally, the team would like to thank many faculty members, including Dr. Oates, Dr. Kumar, Dr. Hollis, Dr. Hruda, and Dr. Van Sciver, for being a source of knowledge and expertise in their chosen disciplines. Their advice and contribution has immeasurably enhanced the team's experience and taught valuable skills to the team members.

ABSTRACT

The goal of this Cummins Inc. sponsored project was to determine the effectiveness of oleophobic gaskets compared to standard nonoleophobic gaskets. This objective was completed by utilizing on market oleophobic solutions with current gasket materials, as well as non-traditional gasket materials and then testing these products in an experimental test rig, which was designed and constructed by the team. The effectiveness of the oleophobic gaskets was assessed by comparing the respective leak rates of each gasket type under several conditions, including two variable temperatures and variable clamping pressures, to that of baseline nonoleophobic gasket leak rates. The test rig has been designed and built by the team so that it can test gaskets with oil at room temperature and at an elevated engine-like temperature while under a constant low internal pressure of 2.5 psi with variable gasket clamping pressure. The manufacturing steps required in the construction of the test rig and gaskets were documented by the team, as well as suggestions for how to improve the test rig. The test rig was also designed to be as reliable as possible through the use of FEA and other design tools. Finally, the economics of the project were analyzed and the team was able to complete the project under budget.

1 Introduction

Cummins Inc. has proposed a project to determine the effectiveness of oleophobic gaskets to reduce the measured leak rate at low pressure, large joints on engines compared to the current gaskets used on engines. Oleophobic items are items which repel oil by having a lower surface energy than the oil. A gasket is an item which is placed between two flanges to form a seal, which is meant to prevent oils from leaking to the opposite side of the flange. The theory behind the project is that if the gasket can repel the oil, it is less likely that oil will be capable of leaking past the gasket.

In order to determine the effectiveness of oleophobic gaskets, the design team determined what products on the market could be used to give a gasket oleophobic properties, created oleophobic gaskets using these products and nontraditional gasket materials, as well as designed and built a test rig which measures the leak rate of a gasket at various temperatures and pressures. The test rig must be capable of testing oils that range from 22 to 120° C and inducing a pressure on the oil ranging from 0 to 2.5 psi. Once the design and construction of the project was completed, tests were performed on oleophobic and standard gaskets using the test rig and results will be compared to determine the effectiveness.

2 Design for Manufacturing

For the fabrication of the test rig, machining occurred in two locations. The machining and fabrication of the steel components, such as the flanges, was completed at the FAMU-FSU College of Engineering Machine Shop because the use of the water jet was needed. The only component not fabricated at the FAMU-FSU College of Engineering Machine Shop was the strain gauge bolts. These bolts were machined at a Cummins Inc. facility in Columbus, Indiana. Cummins Inc. had the experience and capabilities to modify a standard M10 bolt in order to incorporate strain gauges; therefore, it was decided it would be best to allow Cummins Inc. to prepare the bolts. Full CAD drawings are shown in Appendix B, where details such as dimensions, materials, and tap sizes can be found. The drawings in Appendix B also state all the part names, as well as the quantity in which they are needed in the test rig.

2.1 Sub-Assembly Fabrication

Before assembly of the test rig could occur, the Top Assembly sub-assembly needed to be fabricated. The Top Assembly consists of the following parts: Top Flange, Top Tube, and Top Cap. These parts were welded together using stainless steel weld, and the welds were done as full beads in order to create an air tight joint between the parts. In Figure 1, the Top Assembly is shown in its exploded view in order to show how the components mate together prior to welding. After the welding was completed, the Oil Inlet Valve, Pressure Relief Valve, Air Inlet Valve, and the RTD sensor with its compression fitting were assembled to the Top Assembly. Each of these parts had NPT threads in order to create an air tight seal; therefore, it was required to apply significant torque to each part while installing in order to distort the threads as desired. As an additional form of sealing, PTFE Teflon tape was wrapped around the threads of the parts before they were installed into the Top

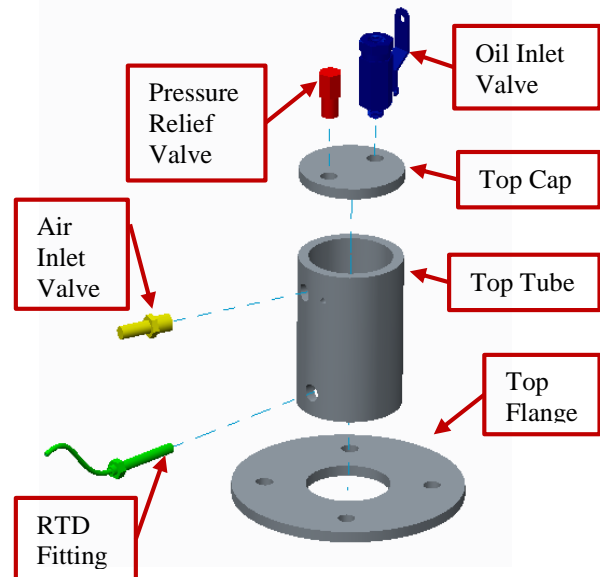


Figure 1. Exploded view of the Top Assembly

Assembly. This serves as an additional seal in order to ensure there is no gap between threads. The rest of the parts for the test rig do not require sub-assembly, and therefore are included in the final assembly stage.

2.2 Assembly of Test Rig

After completing the Top Assembly sub-assembly, the remaining components could be assembled to the test rig. This assembly process occurs before every use of the test rig, meaning that this assembly is done before every gasket test. Figure 2 shows the final assembly exploded view for the test rig.

The first step of the assembly is to place the Bottom Flange on top of the Spacer. If the test being performed is a high heat test, then the Spacer should be placed on top of the cool hot plate prior to placing the Bottom Flange onto it. Once the Bottom Flange is in position, the next step is to place the gasket onto the Bottom Flange. The tabs which were welded onto the Bottom Flange serve as a method of centering the gasket. So while assembling the gasket to the Bottom Flange, the tabs on the Bottom Flange were always placed within the inner diameter of the gasket.

With the gasket in position, the Top Assembly was then lowered onto the gasket. While lowering the Top Assembly, care was taken to ensure the bolt thru holes from the Top Assembly and the Bottom Flange were aligned along their

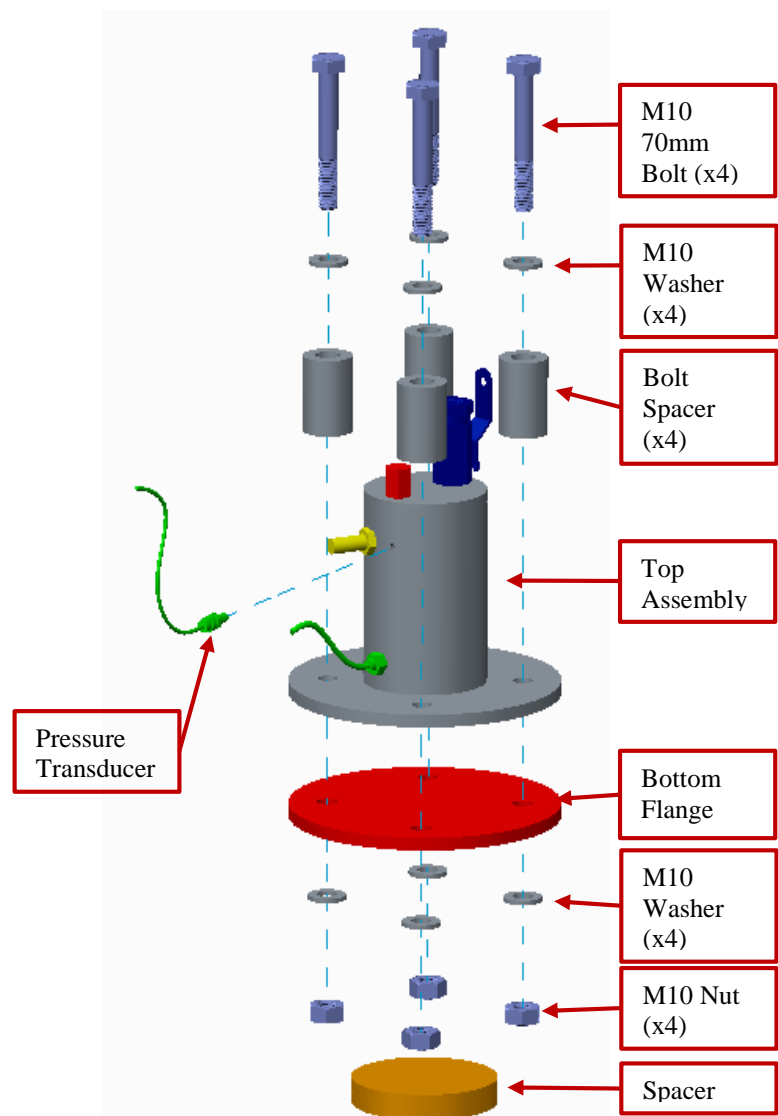


Figure 2. Exploded view of the final assembly for the test rig.

respective center axes. This removes the need to adjust the alignment after the Top Assembly is fully lowered, since adjustments after that point can cause damage to the gasket.

The next step in the assembly was to install the Bolt Spacers, Bolts, Washers, and Nuts. The arrangement of these parts can be found in Figure 2. For the purpose of conducting an experiment/test on a gasket, the nuts are not torqued down immediately. Since the bolts are strain gauged, it is important to collect the unstrained microstrain value. This is used to calibrate each bolt prior to applying a load. After the unstrained microstrain value was recorded, the bolts were tightened to the desired bolt load value. During the tightening process, the bolts were gradually loaded while alternating between sides of the test rig in order to ensure even loading on the gasket.

With the Bolts installed, the final step in the assembly of the Test Rig was to install the Pressure Transducer. This is done after oil is added to the test rig. That process is part of the testing procedure, and not the assembly of the test rig. The Pressure Transducer is installed into the Top Assembly section of the test rig using an 8 mm wrench.

2.3 Manufacturing of Oleophobic Gaskets

Oleophobic gaskets were also manufactured by the team. There were two different solutions chosen to make gaskets oleophobic; Staingaurd WB Impregnator and Ultra-EverDry Spray. For the Impregnator, the manufacturing process consists of dipping the gaskets into a bath of the solution and then allowing it to dry for 24 hours. For the Spray, the manufacturing process consists of applying two different coats via an aerosol spray. The first coat is an adhesive layer, which must be allowed to dry for 1 hour before application of the second coat. The second coat is the oleophobic solution, and it must be allowed to dry for 2 hours after application.

The gaskets which were manufactured were impregnated paper gaskets, sprayed Rubber Coated Metal (RCM) gaskets, and impregnated and sprayed combination felt gaskets. The oleophobic paper and RCM gaskets were made by applying the solutions to standard paper and RCM gaskets which were provided by Cummins Inc. The felt gasket was first cut to size from a sheet of high density felt and then had the oleophobic solutions applied. The total time to create the gaskets, including the 24 hour dry time, was 25 hours.

2.4 Assembly Time

The assembly of our test rig occurred over a period of about 2 months. However, this is not reflective of how long the actual assembly time is. The reason that the assembly process took a month to complete was because the strain gauged bolts provided by Cummins Inc. arrived much later than scheduled. Table 1 shows the timeline of the assembly process of the test rig in both the actual dates, as well as the physical number of hours to perform the task. The majority of the assembly time was from the fabrication process in the COE Machine Shop, where the cutting and welding of the Top Assembly was done. The rest of the assembly process was just installing threaded components, so the assembly time in terms of hours was relatively short.

Table 1. Assembly Time for Test Rig

Assembly Task	Time Span to complete	Duration (hours)
Fabrication in COE Machine Shop	1/11/2016 - 1/20/2016	5
Installation of Oil Inlet Valve, Air Inlet Valve, and Pressure Relief Valve	1/21/2016	1
Installation of RTD sensor	3/1/2015	0.25
Final Mock Up Assembly	3/1/2015	0.5
Total Assembly Time	1/11/2016 - 3/1/2016	6.75

2.5 Design Optimization

During the design process of the test rig, the team made a strong effort to keep the design as simple as possible. Therefore, it would be very difficult to reduce the number of components of the system. Every component on the system serves an important role. For example, all items on the Top Assembly, such as the Oil Inlet Valve, Air Valve, etc. were needed for the functionality of the test rig. Even items such as the Bolt Spacer were required for functional usage, since Cummins, Inc. required that the strain gauged bolts have at least two inches of length between the bolt head and the first engaged thread.

However, there could be an added component to the test rig which the team did not anticipate needing. This component is an additional RTD sensor in the air cavity. During testing, it was

discovered that the air temperature does not reach equilibrium as quickly as the oil, and thus the air temperature continued to increase even after the RTD sensor in the oil displayed a stabilized condition. With the addition of an RTD sensor in the air cavity, the air temperature could be measured as well to ensure that there isn't a temperature fluctuation in the air. The team discovered this air temperature fluctuation during testing, because a pressure increase was recorded instead of a pressure decrease. The only source of a pressure increase would be the air temperature changed.

3 Design for Reliability

In order to ensure consistent results when testing gaskets, various methods of design analysis were completed before the final prototype was constructed, including a Failure Modes and Effects Analysis (FMEA), a Finite Element Analysis (FEA) of the contact pressure, a surface roughness measurement, and a minimum material thickness analysis.

The first analysis conducted was FMEA on the test rig (Table 2). Each part of the test rig was analyzed to determine the most likely methods of failure. In order to reduce or eliminate the possibility of these failure modes, the last column of the table recommends an action.

Table 2. FMEA Table

Component	Mode Of Failure	Cause	Probability	Effect	Severity	Recommended Action
Flanges	Bending	Torque	4	Increase in leak rate	2	Monitor torque wrench
	Surface Roughness	Machining Flaw	2			Follow machining standards
Gasket	Blowout	Material selection	1	Safety hazard	5	Material testing
	Oil leak	Improper materials	4	Increase in leak rate	4	Material testing
		Leak paths	6		2	Design selection
Pressure Vessel	Crack/break	Material selection	1	Blowout	6	Factor of Safety
		Tolerances	2			
Sensors	Overload	Improper selection	1	Inaccurate results	6	Consult sensor data sheet
	Inaccuracy					

Ranking Scale: 1-6; 1 = Low 6 = High

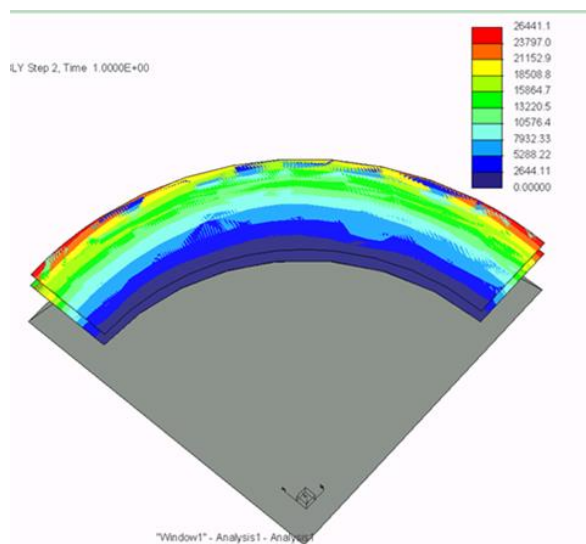


Figure 3. FEA of the Pressure Distribution (10 MPa)

The second analysis conducted on the prototype was FEA on the gasket pressure, shown in Figure 3. This shows the pressure distribution along the gasket face due to a 10MPa clamping pressure. The FEA results proved that the use of four bolts was sufficient because the gasket face had the desired clamping load and showed no leak paths as a result of the design.

Another analysis completed was the measurement of the flange surface roughness using a Coherix ShaPix S150 sensor. Initially, the average surface roughness values found were higher than the 3.2

micron RA maximum Cummins Inc. had set for the test rig; however, this was mitigated by sending the flanges back to the machine shop in order to decrease the surface roughness.

The final analysis conducted was to verify that the thickness of the material being used for the test rig was thick enough to prevent any yielding or failure under pressurized and loaded conditions. This analysis considered the maximum internal stress of the test rig of 2.5 psig and the maximum clamping bolt pressure of 10 MPa. The result of the analysis was that the minimum thickness of the test rig was 4.94 mm, and therefore the team selected 6.35 mm material to provide a factor of safety.

In addition to the above analyses, the reliability of the test rig could be improved with some additional long-term design problem mitigations. The provided raw strain gauge wires protruding from the bolts machined by Cummins Inc. would not be sustainable long-term because of their susceptibility to breakage with a small application of force to the connection. This weakness could be corrected through the use of a protective casing to ensure the protection of the connections.

This design could be reliable for hundreds of tests because of the careful analyses conducted on each aspect of the test rig, as well as the simplicity of the design. One source of reliability concern would be damage to the flange surfaces after repeated use, such as scratches. This damage could be easily remedied with a simple finishing pass or some other method of machining the flange to produce a surface roughness within the defined machining standards.

4 Design for Economics

The budget given for this project was \$2,000 through the Aero Propulsion, Mechatronics and Energy Center. This budget was used to acquire all of the materials that were needed for application and testing for determining the effectiveness of oleophobic gaskets. Even after calculating for the maximum prices, the total estimated cost only came out to \$1,850, which left a remainder of \$150 in case of an emergency.

The test rig sensors cost \$704.00 and the test rig materials cost \$218.41. The oleophobic solution cost \$70.00, whereas the teflon gaskets cost \$170.00. The rest of the money spent was used for anything needed for the testing process which totaled \$73.42. The pie chart in Figure 4 shows the percentage breakdown of the different budget categories.

After extensive research, a similar test rig made by the German company Amtec was found; however, this test rig is not for sale [1]. It measures bolt load and leak rate but does not measure temperature. Also, for the leak rate to be calculated correctly, the test rig must be placed in a vacuum chamber and the leak is measured using a helium mass spectrometer, which would be much more expensive than our test rig design.

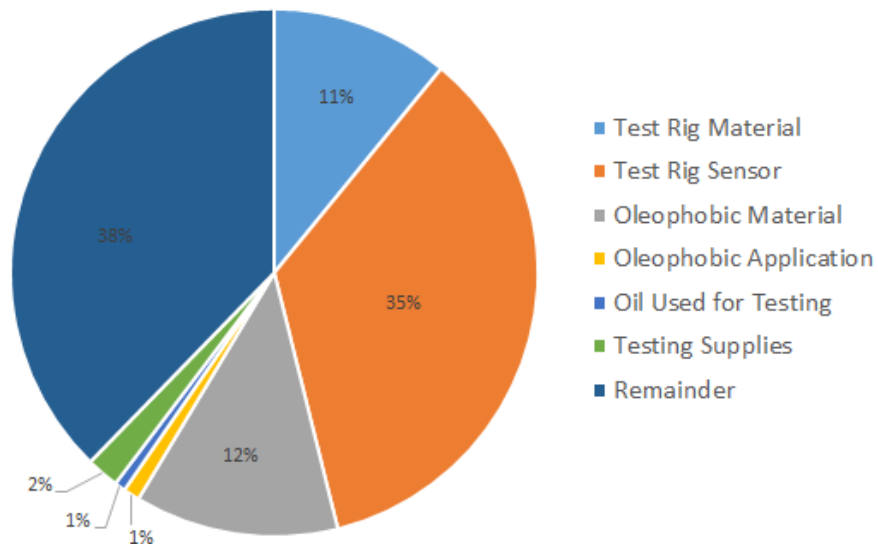


Figure 4. Pie chart showing distribution of funds

5 Conclusion

The team was tasked with designing and building a test rig which could test standard and non-standard gaskets, with and without oleophobic solutions. The test rig was also designed to handle an internal pressure of 2.5 psi, a temperature range between 22°C and 120°C, and variable clamping loads between 0.5 MPa and 10 MPa.

The estimated assembly time for the machine shop was listed at about 5 hours total to completely manufacture the test rig. The rest of the components assembly took about 2 hours to have a full functioning test rig that could provide adequate results. FMEA, minimum thickness analysis, and FEA were done to ensure the safety of the test rig and that the test rig would satisfy all required constraints. For example, the FEA confirmed that there were no significant leak paths as a result of the test rig design, and therefore any leak would be a result of the gaskets. Also, a Coherix ShaPix S150 sensor was used to ensure an acceptable surface roughness for the top and both interchangeable bottom flanges.

Lastly, the majority of the budget Cummins Inc. provided went to test rig sensor acquisition which amounted to 35% of the overall \$2,000 budget. The second and third largest went to purchasing the oleophobic material (12%) and purchasing the test rig A36 steel (11%). The rest of the items in the budget were a small percentage of the budget. At the end of item purchasing, the team ended up only spending 62% of the overall \$2,000 budget allocated for this project. Also, a leak rate testing device could not be found on the market which was capable of testing as many conditions as the test rig built by the team, so a price comparison could not be computed.

References

- [1] "Leakage Test Rig." Gasket Test Rig for Leakage Testing. Web. 01 Apr. 2016.
<<http://www.amtec-services.com/leakage-test-rig-TA-Luft.html>

Appendix E

Determining the Effectiveness of Oleophobic Gaskets

Operations Manual



Team Number: 1

Submission Date: 04-01-2016

Submitted To: Dr. Gupta, Dr. Shih

Faculty Advisor: Dr. Oates

Authors: Heather Davidson (hld12), David Dawson (dpd13), Aruoture Egoh (aje15f), Daniel Elliott (dse13), Norris McMahon (nfm11b), Erik Spilling (eds11b)

Table of Contents

Table of Figures.....	i
Table of Tables	ii
ACKNOWLEDGEMENTS	iii
ABSTRACT.....	iv
1. Introduction.....	1
2. Functional Analysis/Diagram.....	2
3. Project/Product Specifications.....	3
4. Product Assembly	4
5. Operation Instructions	5
6. Troubleshooting	7
7. Regular Maintenance.....	8
8. Spare Parts/Inventory Requirement	9
9. Conclusion.....	10
References	11
Appendix A	12
Appendix B	13
Appendix C.....	14
Biography.....	16

Table of Figures

Figure 1. Functional Diagram of Project.	2
Figure 2. Exploded view of the Top Assembly	4
Figure 3. Exploded view of the final assembly for the test	4

Table of Tables

Table 1. Test Rig Critical Dimensions.....	3
Table 2. Spare and Initial Inventory Items.....	9

ACKNOWLEDGEMENTS

Thank you to Parker Harwood, our Cummins Inc. liaison, for providing guidance and support throughout the project as well as gasket materials for the team to use for baseline testing. Additionally, the team would like to thank Dr. Gupta and Dr. Shih for their oversight of the project and providing instruction to the team. Finally, the team would like to thank many faculty members, including Dr. Oates, Dr. Kumar, Dr. Hollis, Dr. Hruda, and Dr. Van Sciver, for being a source of knowledge and expertise in their chosen disciplines. Their advice and contribution has immeasurably enhanced the team's experience and taught valuable skills to the team members.

ABSTRACT

The goal of this Cummins Inc. sponsored project was to determine the effectiveness of oleophobic gaskets compared to standard nonoleophobic gaskets. This objective was completed by utilizing on market oleophobic solutions with current gasket materials, as well as non-traditional gasket materials and then testing these products in an experimental test rig, which was designed and constructed by the team. The effectiveness of the oleophobic gaskets was assessed by comparing the respective leak rates of each gasket type under several conditions, including two variable temperatures and variable clamping pressures, to that of baseline nonoleophobic gasket leak rates. The test rig has been designed and built by the team so that it can test gaskets with oil at room temperature and at an elevated engine-like temperature while under a constant low internal pressure of 2.5 psi with variable gasket clamping pressure. A functional diagram was created to show the interactions between components, as well as a CAD model to show how the test rig components are assembled. An operations manual was created, which walks the user through all the steps for the use of the test rig in an experiment. Also, the team documented some common troubleshooting techniques and regular maintenance requirements for the test rig.

1 Introduction

Cummins Inc. has proposed a project to determine the effectiveness of oleophobic gaskets to reduce the measured leak rate at low pressure, large joints on engines compared to the current gaskets used on engines. Oleophobic items are items which repel oil by having a lower surface energy than the oil. A gasket is an item which is placed between two flanges to form a seal, which is meant to prevent oils from leaking to the opposite side of the flange. The theory behind the project is that if the gasket can repel the oil, it is less likely that oil will be capable of leaking past the gasket.

In order to determine the effectiveness of oleophobic gaskets, the design team determined what products on the market could be used to give a gasket oleophobic properties, created oleophobic gaskets using these products and nontraditional gasket materials, as well as designed and built a test rig which measures the leak rate of a gasket at various temperatures and pressures. The test rig must be capable of testing oils that range from 22 to 120° C and inducing a pressure on the oil ranging from 0 to 2.5 psi. Once the design and construction of the project was completed, tests were performed on oleophobic and standard gaskets using the test rig and results will be compared to determine the effectiveness.

2 Functional Analysis/Diagram

The test rig was designed to determine the effectiveness of various oleophobic gasket materials (both conventional and non-conventional). The various components that make up the experimental set-up include: strain gauged bolts, nuts, washers, spacers, flanges, a RTD sensor, a pressure transducer, an air inlet valve, an oil valve, and a pressure relief valve. The tests were carried out for both room temperature and an elevated temperature (120°C).

Figure 1 shows the functional diagram of the test set up. The gasket material to be tested was placed in between the flanges of the test rig, and then the strain gauged bolts were torqued down to the desired clamping load. The desired clamping load for the experimental set-up was obtained through the use of the strain gauges that were connected to the DAQ system.

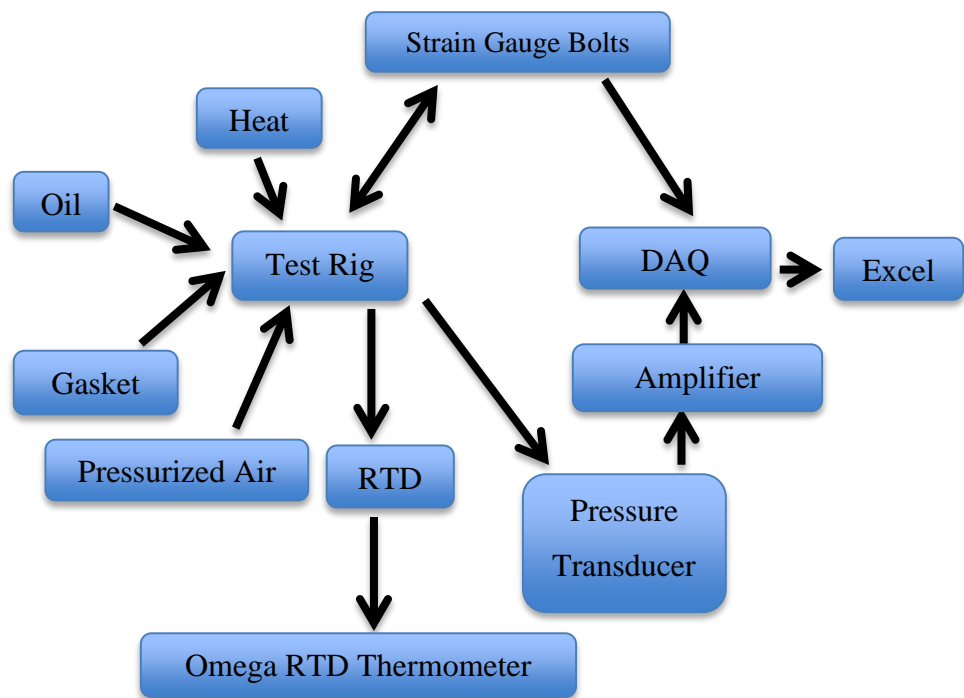


Figure 1. Functional Diagram of Project

Oil was poured into the test rig through the oil valve and pressurized air (2.5 psig) was induced into system. For elevated temperature testing, the test rig was heated to a desired temperature, which was monitored by the RTD sensor which was connected to the omega RTD thermometer.

The pressure transducer which was connected to the DAQ system through the amplifier to record the internal pressure during each test. The initial air volume (V_1) and pressure (P_1) were obtained at the start of the test, and the instantaneous air pressure (P_2) was recorded during the tests. Using the modified ideal gas law $P_1V_1=P_2V_2$, the final air volume (V_2) was calculated and was divided by the time duration of the test to give the leak rate.

3 Project/Product Specifications

The test rig fixture is of two main parts: the top assembly (made up of the Top Cap, Top Tube, Top Flange, Oil Inlet Valve, Air Inlet Valve, Pressure Relief Valve, and the RTD Compression Fitting), and the Bottom Flange. For the body of the test rig, A36 steel was chosen because of its machinability, ability to withstand heat, good welding properties, and price.

The crucial dimensions of the test rig as shown in Table 1. The Top Flange and Bottom Flange have a diameter of 140 mm to accommodate the four M10 bolts and the gasket size. The Top Flange required an inner diameter of less than 55 mm in order to accommodate the gaskets. The thickness of the flanges were selected to be 6.35 mm in order to prevent yielding when loaded, and the surface roughness was required to be 3.2 micron RA or smoother. The bolts and their respective hardware components were M10x1.5, which was the minimum size allowed to use with the strain gauges.

Other important components used in the test rig were the sensors. The Kulite pressure transducer was chosen because it met the requirement of reading pressures between 0-5 psig and was small in overall size, which was beneficial since the test rig is a small item. Appendix G contains the data sheet for the pressure transducer selected [1].

Another sensor which was used was an Omega RTD sensor. The data sheet for the chosen RTD sensor is shown in Appendix H [2]. This RTD sensor was chosen because it was capable of reading oil temperatures of 120°C, and was only 2 inches in length. Again, the small size was beneficial because of the size of the test rig.

Table 1. Test Rig Critical Dimensions

Product Specifications	Values
Top Flange Dimensions	Inner Diameter (ID): 55 mm Outer Diameter (OD): 140 mm
Bottom Flange Dimensions	Outer Diameter (OD): 140 mm
Flange thickness	6.35 mm
Bolts (strain gauges)	M10x1.5 70mm
Washers and nuts	M10x1.5
Flange Surface Roughness	Maximum 3.2 microns RA.

4 Product Assembly

The test rig was assembled in two main steps: Top Assembly sub assembly and final assembly. The Top Assembly consists of the Top Flange, Top Tube, Top Cap, Oil Inlet Valve, Pressure Relief Valve, Air Inlet Valve, and the RTD Compression Fitting. The welding of the Top Flange, Top Tube, and Top Cap was done first to create the air tight chamber required for the design. Then the other components were all threaded into their respective positions in the Top Assembly. Figure 2 shows the Top Assembly CAD model.

The rest of the assembly occurs before each test, and is outlined in detail in the Operation Instructions section of this document. The main assembly tasks in this process are the placing of the test gasket and the Top Assembly on the Bottom Flange, and the tightening of the stain gauged M10 bolts. In Figure 3, the final assembly of the test rig is shown. Appendix B contains the CAD drawing of the test rig assembly.

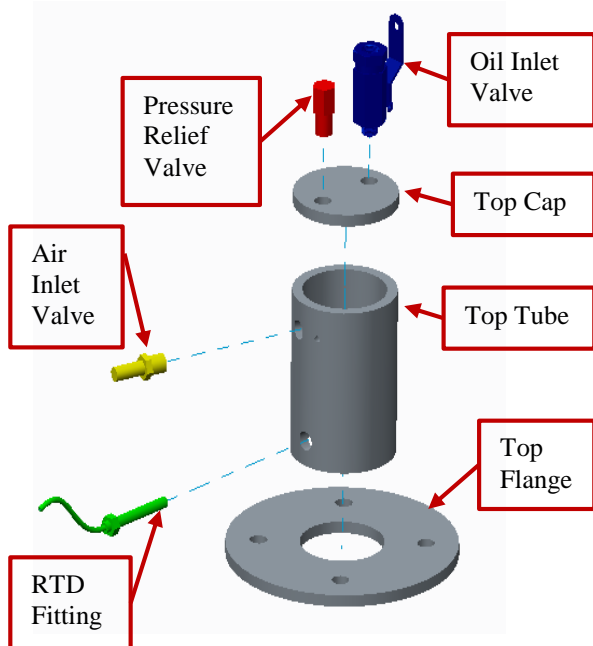


Figure 2. Exploded view of the Top Assembly

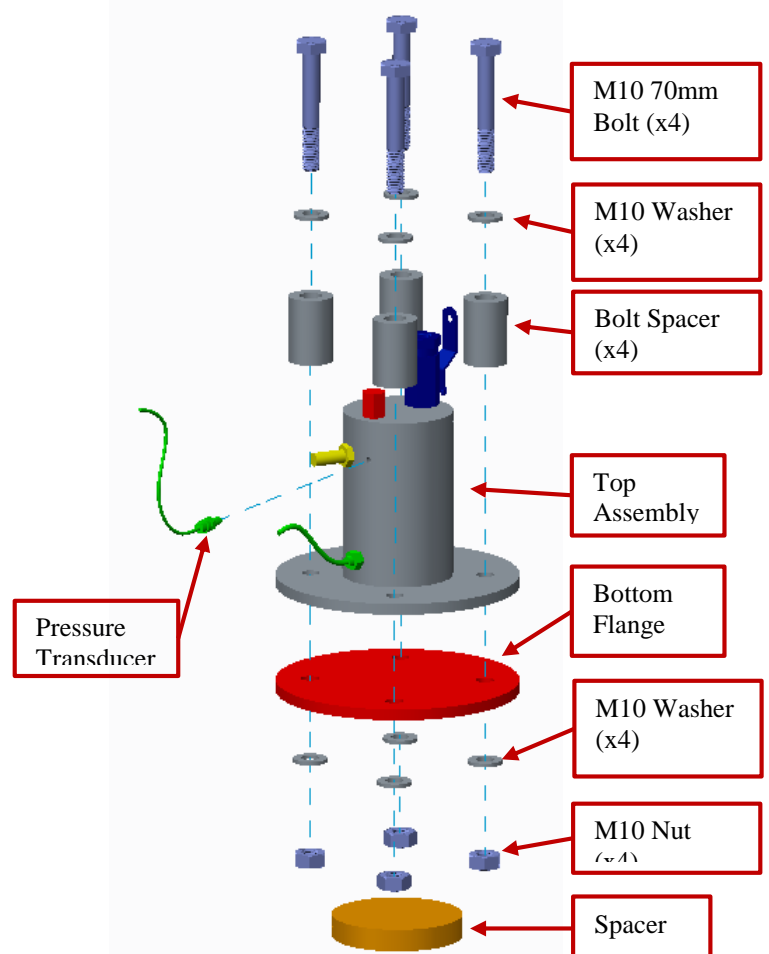


Figure 3. Exploded view of the final assembly for the test rig.

5 Operation Instructions

This test rig is designed to measure the leak rate of various circular gaskets with an inner diameter of 55 mm and an outer diameter of 75 mm. The internal pressure can only be set to 2.5 psi or less; however, the temperature is variable, as well as the bolt clamping loads. The following instructions refer to testing procedures:

39. Turn on power to the signal box for the pressure transducer. Let it warm up and stabilize while the test is being set up.
40. Place selected gasket in the center of the bottom flange. Four small weld marks have been placed radially out from the center of the flange. All four welds should be inside the gasket inner radius, which will ensure the gasket does not move out of place during set up.
41. Carefully set the top flange on top of the bottom flange. Make sure the four bolt holes in the top flange match with the bolt holes in the bottom flange.
42. Place a washer and spacer around each bolt and then place all of the bolts in the bolt holes. Write the number of each bolt with a permanent marker on its washer. This is important as each bolt has a different calibration curve provided by Cummins Inc.
43. Loosely tighten a washer and a nut onto the end of each bolt. Do not let the washer and nut touch the bottom flange.
44. Connect two bolts that are physically across from one another on the test rig to the DAQ system. Plug in their respective power sources. Be careful to not tangle or break any wires.
45. Open the DAQ two channel VI in Labview. Keep all inputs at their default values, except for the sampling rate which should be set to 20,000 Hz. Set the file path to the desired location and name the file accordingly.
46. Run the VI from the front panel. Locate and open the output file with Excel. There should be two columns of many data points which correspond to many samples of the unstrained voltage of each bolt.
47. For each bolt, take an average of all of its unstrained voltage data points. Record the two average unstrained voltage values in Excel. It is common for these values to differ.
48. Begin tightening down these two bolts to the specified clamping load either through two wrenches or a torque wrench, depending upon how much torque needs to be applied.
49. Run the VI from the front panel once again at the same conditions as step six. Repeat the process of accessing the file in Excel and finding one average value.
50. Using the respective Cummins Inc. calibration curves and standard formulas for strain gauges, an excel file was set up such that the only required values to calculate the bolt loads are the average unstrained and average strained voltage values from each bolt. Place the experimentally determined average values in this Excel sheet.
51. Adjust the tightness of the bolt until the desired bolt load is met.
52. Repeat steps 6-13 for the other two bolts.

53. Carefully measure 75 milliliters of Shell Rotella T 15W-40 diesel oil and pour into the test rig via the oil inlet valve on the top of the test rig (a small funnel is recommended).
54. Connect RTD to an instrument that will read out the temperature on a digital screen. This data does not need to be recorded.
55. For room temperature tests, skip steps 18-22.
56. For elevated temperature tests, set hot plate to 500°C. Place the test rig on the hot plate on top of a metal spacer. This spacer is to ensure the bolts are not touching the hot plate.
57. Continuously monitor the temperature of the oil from the instrument digital screen. When it reaches approximately 100°C, change hot plate to about 345°C.
58. Wait for the oil temperature to stabilize around 119°C-120°C. Carefully close oil inlet valve using proper heat protectant gloves.
59. Every few minutes, pop open oil inlet valve to relieve pressure and then close again.
60. After about 15 minutes at a steady temperature, relieve pressure one last time.
61. Close oil inlet valve.
62. Tighten pressure transducer into the appropriate hole in the test rig using an 8 mm wrench. Be careful to not tangle or break any wires.
63. Open the DAQ one channel VI in Labview. Change the sampling rate to 100 Hz, the timeout to 7,200 seconds, and samples per channel to 720,000. These are the settings for a two hour run time test. All tests are run for two hours. Set the file path to the desired location and name the file accordingly.
64. Connect the pressure transducer to the DAQ system.
65. Start running the VI from the front panel.
66. Unscrew cap off of air inlet valve and begin pumping air into the test rig via a bike pump. Stop pumping when the pressure safety valve pops open, which should occur at 2.5 psi. Replace cap back onto air inlet valve.
67. Let the test run for the entire two hours. Have at least one person present in the room at all times.
68. Access the output file as previously described.
69. Input experimental data into an Excel file that is already set up to convert the change in the pressure of the air to an oil leak rate.
70. For hot tests, allow entire test rig to cool down before handling.
71. Remove pressure transducer.
72. Carefully open the oil inlet valve and tilt the test rig to slowly drain most of the oil out making sure to not allow the oil to enter the pressure relief valve. Dispose of the oil.
73. Loosen the bolts and open the test rig up.
74. Document the state of the gasket and dispose of it.
75. Wipe down the bottom and the top flange with paper towels, as well as carefully cleaning inside of the test rig.
76. Return the test rig back to its original condition and begin testing again.

6 Trouble Shooting

Rarely do experiments ever happen without some error or unexpected occurrence. Thus, there were a few problems throughout the duration of the experimentation. The first and most common problem was the breaking of strain gauge bolt wires. The wires on the strain gauges are very thin and fragile. Making too fast or strong of movements with them would cause them to break connection. This was noticed either visually or when there was a zero voltage return on Labview. The wires could be repaired using a soldering iron and shrinkwrap.

Another noticeable occurrence throughout the experiment was having oil come out of the pressure relief valve. When the pressurized air was inserted into the test rig, remaining oil from previous experiments that had gotten into the valve would shoot out. This could possibly affect the internal pressure for the next experiments. The best way to mitigate this is to remove the oil very slowly from the test rig and to be very careful when cleaning the inside of the test rig for the next experiment.

Fluctuating internal temperature was also an issue. The hot plate heats the spacers, the spacers heat the test rig, and the test rig heats the oil. So we had to gauge the internal temperature by changing the external applied temperature from the hot plate. When the temperature is fluctuating, the best way to mitigate that was to allow the temperature to equalize for a longer time. Once the temperature remained constant for 30 minutes, then experimentation should begin.

The last noticeable occurrence was when we tested a sprayed rubber coated metal gasket with high heat. After the experiment, the RCM gasket had partially melted onto the flange. To fix the partially melted gasket, place the flange back on the hot plate so the gasket will warm up and be easier to remove. The melting was a result of the oleophobic solution, not the test rig. However, in the event that tested gaskets do melt, re-heating the flange allows the gasket to be removed.

7 Regular Maintenance

There was only minimal regular maintenance to be done throughout the course of this experimentation process because the test rig was designed to be as simple as possible. One part of the maintenance was using the RTV Silicone to ensure no air leaks were present so that the test rig would remain pressurized. While the RTV Silicone is not required since NPT threading was used to prevent air leaks, the RTV Silicone can be added as an additional safe guard to prevent air leakage.

The second part of the maintenance plan, and most common, was to remove residual oil that was in the test rig between each experiment. Once a majority of the oil was poured out of the test rig and it was disassembled, the inside of the upper cavity and the bottom flange had to be cleaned every time. Depending on the amount of leakage for the test, sometimes the bolts, spacers, washers, and nuts had to be cleaned off if oil ended up reaching them.

The last part of the routine maintenance was to check the integrity of all the components of the test rig and fix any issues. The only noticeable component that had to be repaired was the o-ring on the pressure transducer. Due to the continuous high heat in addition to repeated loading, the o-ring on the pressure transducer sheared and had to be replaced with the back-up o-ring that was supplied.

8 Spare Parts/Inventory Requirements

Table 2 lists spare parts which would be useful to have on hand while using the test rig for an extended period of experiments. The first two items listed are wear parts on the test rig. After repeated use, the washers and the pressure transducer o-ring tend to show signs of wear from the repeated loading due to removing the items between tests. The other spare items are for creating additional gaskets for testing. This also lists the inventory of parts which are required for the construction of the test rig and the testing of gaskets.

Table 2. Spare and Initial Inventory Items

Spare Items List	Initial Inventory Items List	
Item	Item	Quantity
M10 General Purpose steel washer	M10 General Purpose steel washer	4
Pressure Transducer O-Ring	M10 Class 8 Zinc Plated Steel Hex Nut	4
Teflon Gaskets	Zinc-Plated Steel Unthreaded Spacer	4
Rubber Coated Metal Gaskets	M10x1.5 70mm long class 8.8 cap screw	4
Paper Gaskets	Pressure Relief Valve	1
Ultra Everdry	Compact High-Pressure Brass Ball Valve	1
StainGuard-WB	Brass Air Fill Valve Straight	1
	1ft x 1ft x ¼ in Thick A36 Steel Plate	1
	1ftLong2-1/2 OD x 2 ID Round Steel Tube	1
	Short RTD Probe	1
	Compression Fitting	1
	Pressure Transducer	1
	Teflon Gaskets	6
	Rubber Coated Metal Gaskets	12
	Paper Gaskets	12
	Felt Gaskets	6
	Ultra Everdry	2 canisters
	StainGuard-WB	1 quart
	T Triple Protection CJ-4 15W-40 Motor Oil	1 gallon
	Hot Plate	1

9 Conclusion

A functional analysis was completed to demonstrate the relationship between the inputs and the outputs of the test rig. The inputs include a gasket, oil, heat, pressurized air, and strain gauged bolts. All of these interface with the test rig and produce useful outputs. The outputs of the test rig include raw data which was converted to bolt load, pressure, and temperature through the use of components such as an amplifier, DAQ system, RTD Omega Thermometer, and Excel.

The project and product specifications were outlined by the team. This includes the dimensions of critical components such as the diameter of the flanges, the thickness of the test rig, and the size of the bolts, nuts, washers, and bolt spacers. Additionally, the data sheets for both the pressure transducer and the RTD sensor were included.

A brief explanation was provided for assembling the test rig; however, due to the nature of the test rig, much of the assembly is repeated before every single test. Therefore, a much more in depth description of how to set it up is provided in the actual operation instructions. The operation instructions include a step by step process of how to properly perform a test by installing a gasket, sensors, oil, pressurized air, tightening the bolts to a desired value, and then extracting the raw data from the DAQ system.

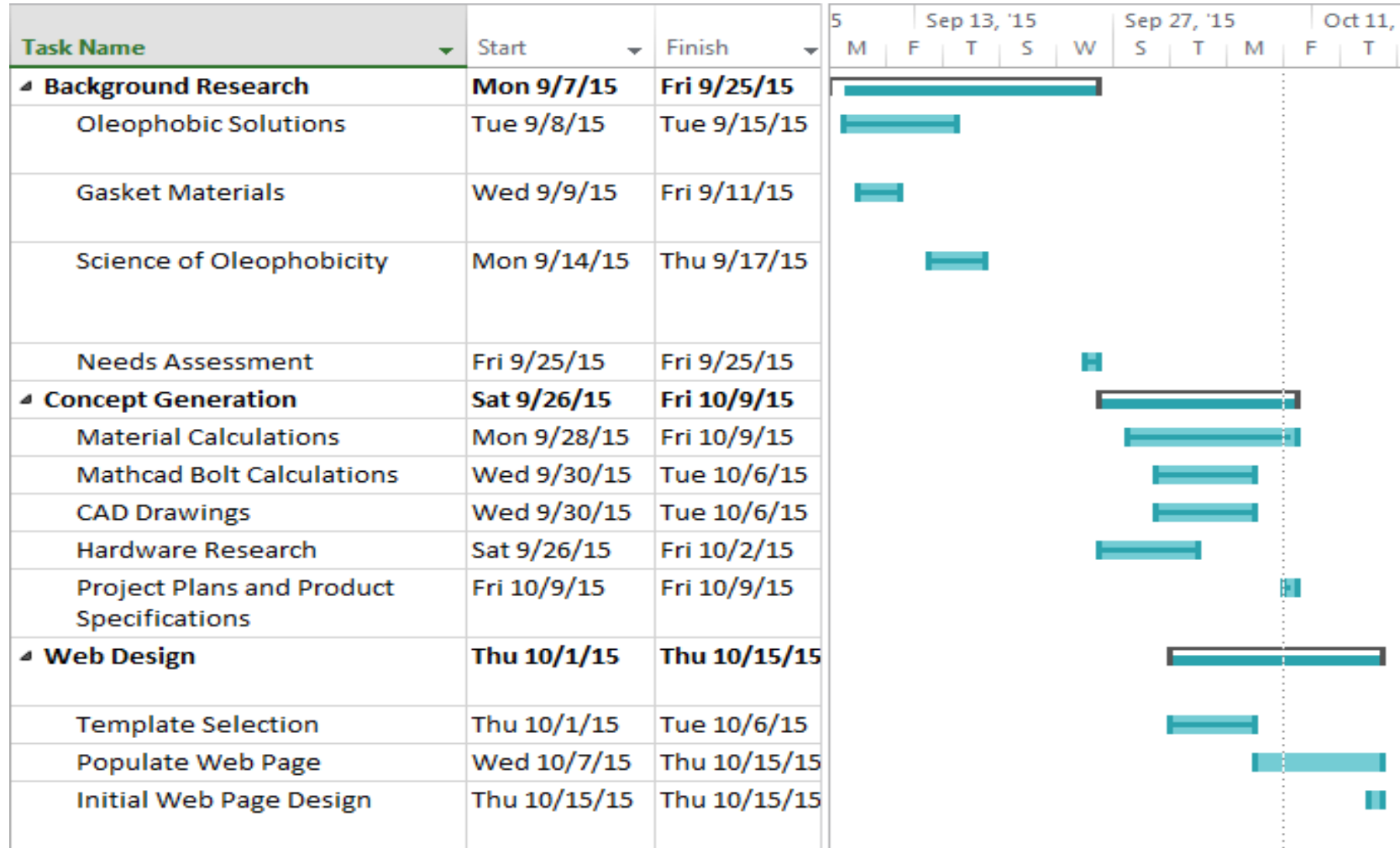
In addition to these previous items, troubleshooting help and regular maintenance was reported in hopes of shedding lights on common issues that may occur if the test was performed according to our procedure. Finally, a list of spare parts and an initial inventory was created to summarize what is required in order to accomplish this test.

References

[1] " Pressure Transducers XTL-123B-190." Kulite. Web. 30 Mar. 2016.

[2] "Short RTD Probe." Short RTD Probe. Web. 30 Mar. 2016.

Appendix F



Gantt chart displaying the projected schedule



Gantt chart displaying the projected schedule

Appendix H

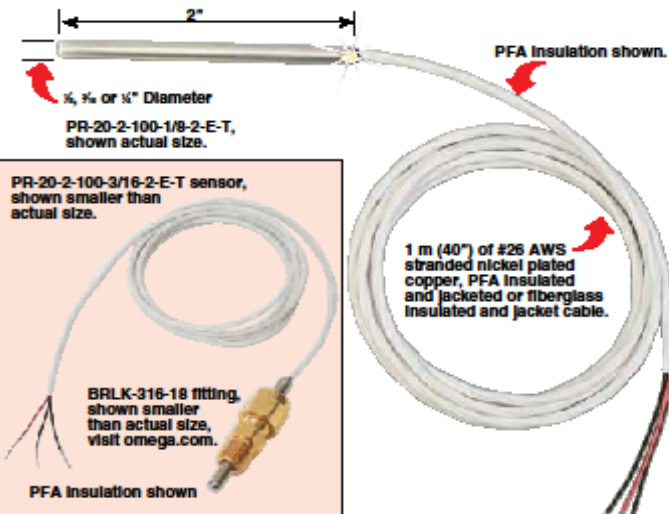
Short RTD Probe

PR-20 Series



- ✓ 2" Compact Design for Applications with Space Restrictions
- ✓ Transitions Directly to Lead Wires (No Transition Fitting)
- ✓ Temperature Range:
PFA: -50 to 260°C (-58 to 500°F)
Fiberglass: -50 to 450°C (-58 to 842°F)
Depending on Cable Selection
- ✓ High-Accuracy, 100 Ω, Class "A" DIN Platinum Elements per IEC751 (alpha = 0.00385 Ω/Ω°C)
- ✓ 2-, 3-, 4-Wire Constructions Available

These general purpose 2" long sensors can be used in most liquid and air applications. When used in liquid environments, the epoxy-sealed end should not be immersed



directly into the liquid. Compression fittings are also available for installation. These probes can be used as stand-alone sensors, or they can be configured with a

variety of termination options, and combined with controllers, indicators, or precision thermometers to create complete measurement systems.

To Order Visit omega.com/pr-20 for Pricing and Details

Model Number	Probe Diameter (inch)	Lead Wire Style*	Max Temp Range °C (°F)
PR-20-2-100-1/8-2-E-T	1/8	3-wire/PFA insulation	260 (500)
PR-20-2-100-3/16-2-E-T	3/16	3-wire/PFA insulation*	260 (500)
PR-20-2-100-1/4-2-E-T	1/4	3-wire/PFA insulation*	260 (500)
PR-20-2-100-1/8-2-E-G	1/8	3-wire/fiberglass insulation	450 (842)
PR-20-2-100-3/16-2-E-G	3/16	3-wire/fiberglass insulation*	450 (842)
PR-20-2-100-1/4-2-E-G	1/4	3-wire/fiberglass insulation*	450 (842)

Note: For leads longer than 40", add "(desired length in inches)" to the model number for additional price.
 * For 4 wire configurations change the "2" to a "3" in the model number for additional price.
 4-wire constructions are not available in 1/8" diameters.
 Terminations Available: for "LUG", for "OTP" and "MTP" connectors. Visit omega.com for additional price.
 Ordering Example: PR-20-2-100-3/16-2-E-T, 2", 3/16" diameter, 3-wire 100 Ω RTD probe with 40" PFA Insulated lead wire.

Accessories

Model Number	Description
MTP-U-M	Miniature male 3-prong flat pin connector
OTP-U-M	Heavy-duty male 3-prong round pin connector
DPI32	1/8" DIN panel meter
SSLK-18-18	Compression fitting for 1/8" probe with 1/8" male NPT
SSLK-14-14	Compression fitting for 1/4" probe with 1/4" male NPT
SSLK-316-14	Compression fitting for 3/16" probe with 1/4" male NPT
SSLK-316-18	Compression fitting for 3/16" probe with 1/8" male NPT

Biography

Erik Spilling: Project Leader

Erik is a Florida State University Mechanical Engineering student from Saint Augustine, Florida. Erik has completed three internships at Cummins Inc., with two of those internships having been spent in High Horse Power Design Engineering. After graduation, Erik will join Cummins Inc. full time as a High Horse Power Design Engineer.

Heather Davidson: Lead ME and Web Designer

Heather is a Florida State University Mechanical Engineering student graduating in May of 2016. Heather was born in Deland, Florida. She has completed two summer internships with ExxonMobil at an oil refinery in Torrance, California. After graduation, she will be working at Southern Company in Birmingham, Alabama.

David Dawson: Financial Advisor

David is a Florida State University mechanical engineering student with a focus on Thermal Fluids and Energy. David was born in South Africa and raised in Jacksonville, Florida. Following graduation, David plans to pursue a job in either energy sustainability or work for the armed forces as a mechanical engineering officer.

Aruoture Egoh: Lead Materials Engineer

Aruoture is an exchange student of Florida Agricultural and Mechanical University from Federal University of Technology, Akure, Ondo state, Nigeria. He plans to complete his bachelor's degree in Materials Engineering, attend graduate school to pursue a master's degree and PhD in materials engineering focusing on Polymeric Materials.

Daniel Elliott: Research Coordinator

Daniel is a Senior Mechanical Engineering student with a minor in Psychology and a mixed focus in Materials and Energy Systems. After graduation, he plans to move to Austin, Texas as his first step in his professional career and in order to be closer to his family.

Norris McMahon: Chronicler

Norris is a student at Florida State University originally from Pensacola, Florida. His area of focus is Mechanics and Materials. He has experienced an internship with Blattner Energy Inc. Following graduation, Norris plans to pursue a Masters in Sports Engineering and would like to end up in the Research and Development of sports products field.